CAPITAL UNIVERSITY OF SCIENCE AND TECHNOLOGY, ISLAMABAD

Viscous Dissipation and Thermal Radiation of Squeezing Hybrid Nanofluid Flow with Bioconvection

by

Hajra Batool

A thesis submitted in partial fulfillment for the degree of Master of Philosophy

in the

Faculty of Computing

Department of Mathematics

2024

Dedicated to my beloved parents, whose unending love, everlasting support, and unfailing faith in my skills have been a driving force for my academic work are honored in my thesis. They installed in me rules and guidance that have defined my character and objectives, and I will always be thankful for that. I am fortunate to have such amazing parents and respected teacher Mam Dur-e-Shehwar for helping and guiding me to make a final output. With deep gratitude and affection, I dedicated my achievement to my beloved parents and teachers.

CERTIFICATE OF APPROVAL

Viscous Dissipation and Thermal Radiation of Squeezing Hybrid Nanofluid Flow with Bioconvection

by

Hajra Batool

(MMT213024)

THESIS EXAMINING COMMITTEE

S. No.	Examiner	Name	Organization
(a)	External Examiner	Dr. Bilal Ahmed	University of Wah, Rawalpindi
(b)	Internal Examiner	Dr. Rashid Ali	CUST, Islamabad
(c)	Supervisor	Dr. Dur-e-Shehwar Sagheer	CUST, Islamabad

Dr. Dur-e-Shehwar Sagheer
Thesis Supervisor
May, 2024

Dr. Muhammad Sagheer
Head
Dept. of Mathematics
May, 2024

Dr. M. Abdul Qadir
Dean
Faculty of Computing
May, 2024

Author's Declaration

I, **Hajra Batool** hereby state that my MPhil thesis titled "**Viscous Dissipation and Thermal Radiation of Squeezing Hybrid Nanofluid Flow with Bio-convection** " is my own work and has not been submitted previously by me for taking any degree from Capital University of Science and Technology, Islamabad or anywhere else in the country/abroad.

At any time if my statement is found to be incorrect even after my graduation, the University has the right to withdraw my MPhil Degree.

(Hajra Batool)

Registration No: MMT213024

Plagiarism Undertaking

I solemnly declare that research work presented in this thesis titled "**Viscous Dissipation and Thermal Radiation of Squeezing Hybrid Nanofluid Flow with Bioconvection**" is solely my research work with no significant contribution from any other person. Small contribution/help wherever taken has been duly acknowledged and that complete thesis has been written by me.

I understand the zero tolerance policy of the HEC and Capital University of Science and Technology towards plagiarism. Therefore, I as an author of the above titled thesis declare that no portion of my thesis has been plagiarized and any material used as reference is properly referred/cited.

I undertake that if I am found guilty of any formal plagiarism in the above titled thesis even after award of MPhil Degree, the University reserves the right to withdraw/revoke my MPhil degree and that HEC and the University have the right to publish my name on the HEC/University website on which names of students are placed who submitted plagiarized work.

(Hajra Batool)

Registration No: MMT213024

Acknowledgement

In the name of Allah, the Creator of all things, the Most Generous, the Most Merciful. His numerous blessings have provided us with the ability to study and employ other abilities in order to complete this thesis.

I am really thankful to my respected supervisor and mentor, Dr. Dur-e-Shehwar Sagheer, for her assistance throughout this thesis. I'd want to convey mydeep appreciation to her for the advice she gave to improve the quality of this thesis. Working underher supervision has taught me not just my technical expertise but also how to be a nice human being. I would also want to thank her for always being willing to have discussions concerning this thesis, despite ofher highly hectic schedule. I am eternally grateful to Dr. Muhammed Sagheer for his excellent advice and never-ending inspiration during this thesis. I would not have been able to begin my present research endeavor without her relentless assistance. I am grateful to all of my professors at Capital University of Science and Technology. I learned a lot from them during my M.Phil study as they are great teachers. My heartfelt and warmest greetings to my friends, especially my university fellows, who were always a source of support for me. I am eternally thankful to my dear parents, sisters, and brothers for their love and prayers, for providing with bothspiritual and moral support whenever I need it. The appreciation would undoubtedly be incomplete until I convey my heartfelt gratitude and heartfelt thanks to my friends for their excellent advice and assistance during my thesis.

Hajra Batool

Registration No: MMT213024

Abstract

The current research has yielded a comprehensive insights into the predominant characteristics of hybrid nanofluids, notably their heightened thermal and electrical conductivity, leading to the heat transfer rate. Numerous researchers have consistently substantiated these effects through various methodologies, thereby enhancing the thermal performance of the base fluid. This study is focused on the analysis of impact of viscous dissipation and heat radiation on two dimensional unsteady incompressible squeezing flow of hybrid nanoparticles between two parallel plates with variable viscosity are investigated in this work. By incorporating the appropriate similarity transformations, these partial differential equations are converted into a system of coupled nonlinear ordinary differential equations. The mathematical simulation is performed using the shooting technique. The analysis involves the examination of two distinct nanoparticles: copper oxide and aluminum oxide. The numerical results are presented in tables and graphs for variation in parameters, for example, Radiation parameter, Squeezing parameter, Suction/injection parameter, Magnetic parameter and nanoparticle volume fraction parameter. The impact of physical parameters on the velocity profile, temperature distribution, skin friction coefficient, Nusselt number are discussed. The findings indicate that elevated values of variable viscosity and squeezing parameters contribute significantly to the enhancement of both velocity and motile microorganism profiles. Meanwhile, raising the viscous dissipation and thermal radiation parameters reduces the temperature distribution while having no effect on fluid velocity.

Contents

List of Figures

List of Tables

Abbreviations

BCs	Boundary Conditions
BVP	Boundary Value Problem
HNF	Hybrid Nano Fluid
IVPs	Initial value problems
NF	Nano Fluid
ODEs	Ordinary Differential Equations
PDEs	Partial Differential Equations
RK-4	Runge-Kutta order 4

Symbols

$\tilde{u}$	x-component of fluid velocity
$\tilde{v}$	y-component of fluid velocity
R	Radiation parameter
M	Magnetic parameter
Pr	Prandtle number
m	Viscosity variation parameter
Sq	Squeezing fluid parameter
S	Suction parameter
Ec	Eckert number
$\tilde{C}$	Concentration
$\tilde{C}_2$	Ambient concentration of hybrid nanofluid
$\tilde{\mu}$	Dynamic viscosity
η	Similarity variable
$f(\eta)$	Dimensionless velocity
$\theta(\eta)$	Dimensionless temperature
$\phi(\eta)$	Dimensionless concentration
$\chi(\eta)$	Dimensionless Motile Micro-organism
$\tilde{T}$	Temperature of the hybrid nanofluid
$\tilde{T}_2$	Ambient temperature of nanofluid
U_w	Stretching velocity
B_o	Magnetic field constant
λ	Stretching parameter
$\tilde{\rho}\tilde{c}_p$	Heat capacity
Le	Lewis number

Sr	Soret number
Nb	Brownian motion parameter
Nt	Thermophoresis parameter
We	Weissenberg number
Pe	Peclet number
Cf_1, Cf_2	Skin friction of lower and upper plates, respectively.
Nux_1, Nux_2	Local Nusselt number of lower and upper plates, respectively.
Sh	Sherwood number
Sh_x	Local Sherwood number
Re	Reynolds number
Re_x	Local Reynolds number
Sc	Schmidt number
$\tilde{\rho}_{hnf}$	Density of the hybrid nanofluid
$\tilde{\rho}_f$	Density of the pure fluid
$\tilde{\rho}_{p_1}$	Density of $\mathtt{Cu}$
$\tilde{\rho}_{p_2}$	Density of $\mathtt{Al_2O_3}$
$\tilde{\mu}_{hnf}$	Viscosity of the hybrid nanofluid
$\tilde{\mu}_f$	Viscosity of the base fluid
$(\rho\tilde{C}_p)_{hnf}$	Heat capacitance of hybrid nanofluid
$(\rho\tilde{C}_p)_f$	Heat capacitance of base fluid
$\tilde{\sigma}_{hnf}$	Electrical conductivity of the hybrid nanofluid
$\tilde{\sigma}_f$	Electrical conductivity of the base fluid
$\tilde{\kappa}_{hnf}$	Thermal conductivity of the hybrid nanofluid
$\tilde{\kappa}_{nf}$	Thermal conductivity of the nanofluid
$\tilde{\kappa}_f$	Thermal conductivity of the base fluid
$\tilde{D}_{hnf}$	Mass diffusion of the hybrid nanofluid
$\tilde{D}_f$	Diffusivity of the base fluid
k	Thermal Conductivity
t	Time
μ_{nf}	Viscosity of the nanofluid
B	Time depended magnetic field
$\tilde{\rho}_f$	Density of the fluid

$\tilde{\mu}_f$	Viscosity of the fluid
ν_f	Kinematic viscosity of the base fluid
ρ_{nf}	Density of the nanofluid

Chapter 1

Introduction

1.1 Background

The enhancement of thermo-physical properties in conventional fluids through ultrafine particle dispersion (1-100 nm), known as nanofluid, was introduced by Choi [1]. Renowned for exceptional heat transfer capabilities, nanofluids have diverse applications. Recently, hybrid nanofluids, a novel class with various nanoparticles in regular base fluids, gained attention for superior characteristics. Atif et al. [2] numerically explored tangent hyperbolic nanofluid flow past a wedge, considering heat modes and thermal radiation. Sreedevi et al. [3] analyzed heat and mass transfer in hybrid nanofluid flow over a stretching surface, considering chemical reaction, suction, slip and thermal radiation effects. Jawad et al. [4] studied the behavior of stagnation point flow towards a stretched surface, incorporating melting heat transfer, second-order slip, electric field, and magnetic field effects using the Homotopy Analysis Method (HAM). Alhowaity et al. [5] used the parametric continuation method for numerical heat transfer analysis of hybrid nanofluid flow with thermal radiation. Sen et al. [6] studied the entropy and heat transfer rate of hybrid nanofluid flow over a pervious stretchable cylinder influenced by nonlinear radiation and magnetic field effects, employing the bvp4c tool in MATLAB. Ongoing research explores diverse applications and behaviors of hybrid nanofluids [7–9].

Magnetohydrodynamics (MHD) is a specialized field in physics exploring the interaction between electrically conducting fluids and magnetic fields. Its applications span fusion reactors, plasma physics, astrophysics, and aerospace engineering. The introduction of a magnetic field in an electrically conductive fluid induces electric currents, dynamically interacting and giving rise to additional forces, profoundly influencing fluid motion. The investigation of Asad et al. [10] about Brownian motion and thermophoresis diffusion in non-Newtonian fluid flow over a stretching sheet with thermal radiation. Raje et al. [11] conducted a numerical analysis of Jeffrey fluid flow through an inclined pipe with a circular cross-section in a uniform porous medium, subjected to a constant pressure gradient and a uniform magnetic field.

Despite the complexities of non-Newtonian fluids, researchers actively explore their mechanics due to their crucial roles in systems like biotechnology, pharmaceuticals, and chemical engineering. The Casson fluid model, introduced by Robert Casson in 1959 [12], mathematically describes the rheological behavior of shear-thinning and yield-stress non-Newtonian fluids. Widely applied in diverse fields, including biofluids and food processing, the Casson model effectively captures the flow dynamics of materials like honey and soups. Bejawada et al. [13] numerically studied thermal radiation, chemical reaction, and heat source effects on MHD Casson fluid flow over a nonlinear inclined stretching surface. Alqahtani et al. [14] analytically explored energy and mass transition in Casson hybrid nanofluid flow across an extended stretching sheet, considering Darcy effects, heat absorption, viscous dissipation, and thermal radiation using the Homotopy Analysis method. A study on optimized MHD ternary hybrid nanofluid using Casson fluid over a porous shrinking sheet with thermal radiation effect by Zeeshan et al. [15] can also be referred to for deep insight.

Flow occurring when a fluid passes through a constricted channel, called Squeeze flow, is prevalent in various applications, including biological systems, industrial processes, and environmental phenomena. Li et al. [16] analyzed the squeezing flow of Newtonian nonconducting fluid through a porous system, applying Darcy's law and solving the resulting problem with the DaftardarJarfari Method to obtain

a series solution. Umavathi et al. [17] numerically investigated Casson liquid flow between two convectively heated disks using the Buongiorno model.

Chemical reactions are crucial in industrial processes, influencing energy production, material synthesis and environmental remediation. Venkateswarlu et al. [18] used perturbation techniques to study slip's impact on heat and mass transfer in hydromagnetic pulsatile flow through a porous medium-filled parallel plate channel. Tarakaramu and Narayana [19] numerically analyzed nanoparticle concentration effects using Brownian motion and thermophoresis diffusion. Raghunath [20] examined the flow of an incompressible water-based nanofluid over a stretching sheet with a transverse magnetic field, incorporating thermal radiation and Soret effects, using a regular perturbation technique.

When microorganisms aggregate in the upper region of a fluid, the initiation of bioconvection occurs due to the unstable density stratification of these microorganisms. Bioconvection plumes develop during this process, facilitating the movement of microorganisms from the upper fluid region to the lower fluid regions, driven by density differences. The term Bioconvection was introduced in 1961 by James Henry Platt [21], in his report aiming to draw attention to the physics of streaming patterns observed in dense cultures of free-swimming organisms. According to Platt [21], the moving polygonal patterns in dense cultures of Tetrahymena (ciliate and flagellate) resemble Benard cells but are not a result of thermal convection. Considering the susceptibility of many bacteria to high temperatures, it is essential to explore their behavior under various conditions. Patil et al. [22] delved into the bioconvection flow along a sphere, considering the influence of a periodic magnetic field. These works contribute to the expanding body of knowledge in understanding and manipulating bioconvection phenomena for diverse applications.

In 2022 Famakinwa et al. [23] investigated the impact of viscous dissipation and thermal radiation on time-dependent, incompressible squeezing flow of $\mathtt{CuO}$-$\mathtt{Al_2O_3}$ between parallel plates with variable viscosity regulation. The study addresses key research inquiries, including the influence of volumetric fractions (ϕ_1,ϕ_2) of

nanoparticles, viscous dissipation parameter, thermal radiation parameter R, viscosity modification factor m, and other pertinent parameters on heat transfer rates at the plates. Additionally, the significance of varying squeezing fluid parameter Sq on velocity and temperature distribution is analyzed both in the presence and absence of the viscous parameter. Furthermore, the study explores the effects of the stretching sheet parameter λ on velocities and temperature distribution, considering the presence or absence of thermal radiation.

In addressing the research gap identified in existing literature, this study presents a novel two-dimensional unsteady squeezing Casson water-based hybrid nanofluid model between parallel plates, incorporating the synergistic effects of Casson rheology, squeezing dynamics, magnetic field influence, bioconversion, chemical reactions, Brownian and thermophoresis motions, and boundary layer flow. The literature survey reveals that no model has so far been proposed addressing the viscous dissipation and thermal radiation on time-dependent squeezing flow along with the presence of concentration and motile gyrotactic micro-organisms phenomenon. The integration of these intricate factors offers an understanding of the complex fluid dynamics within the system. The numerical solution of the system of ordinary differential equations is achieved through shooting techniques, ensuring accuracy in capturing the velocity, temperature, concentration, and motile behavior. The model's applications extend to diverse fields, including biomedical engineering, where it can enhance the understanding of bioconversion processes, as well as in materials science for optimizing nanofluid-based technologies. Moreover, the results contribute to advancements in thermal management systems, with implications for designing efficient cooling systems in various engineering applications. This work is guided by the following research questions:

- How do volumetric fractions (ϕ_1, ϕ_2) of nanoparticles, viscous dissipation parameter (Ec), thermal radiation parameter (R), viscosity modification factor (m), Brownian motion parameter (Nb), thermophoresis parameter (Nt), and other emerging parameters influence the rates of heat transfer, the

rate of mass transfer, and the density distribution of motile microorganisms at either plate?

- What is the significance of the Casson fluid parameter (β) on the velocity, temperature, concentration, and motile microorganisms distribution of CuO-Al_2O_3 water hybrid nanofluid in the presence/absence of viscous parameter?

- What is the significance of varying Brownian motion (Nb) and thermophoresis motion (Nt) on the concentration and motile microorganisms distribution of CuO-Al_2O_3 water hybrid nanofluid in the presence/absence of viscous parameter?

- How does the bioconvection Schmidt number (Lb) influence the motile microorganism's distribution with or without thermal radiation?

- What is the effect of Schmidt number Sc and microorganisms constant ω on the motile microorganism of Casson hybrid nanofluid in the presence and absence of viscous parameter?

1.1.1 Layout of Thesis

The following is a concise overview of the thesis's content.

In **Chapter 2**, the basic definitions and terminologies are presented, which are vital to interpreting the ideas covered in the subsequent chapters. The purpose of this chapter is to provide a fundamental grasp of the crucial terminologies and concepts that will be utilized throughout the thesis.

Chapter 3 provides a detailed review of the work conducted by Famakinwa et al. [23]. The demonstrated numerical model accounts for heat and mass transport between the two parallel plates in the Cartesian coordinate system. The shooting approach is used to acquire the numerical results of the governing flow equations. This chapter explores the flow characteristics and performance of thermal radiation are investigated in this chapter.

Chapter 4 extends the suggested model flow outlined in Chapter 3 by incorporating the Casson effect in the momentum equation and energy equation. Furthermore, concentration equation and motile density equation is considered to observe the mass transfer within the fluid model. The similarity transformation is used to turn the partial differential equations into a system of ordinary differential equations, which are then solved numerically.

Chapter 5 contains the conclusion and emphasizes the main findings from the study performed in this thesis.

The **Bibliography** portion contains a full list of all references and sources utilized in the thesis.

Chapter 2

Basic Terminologies

This chapter contains the fundamental definitions, rules, terminologies, and critical ideas required for the analysis of the flow discussed in the next chapters. These core aspects are critical for understanding the succeeding chapters of this thesis and will give a strong framework for developing a thorough knowledge.

2.1 Foundational Concepts

This section examines, few basic definitions, laws and essential fluid features that are critical for understanding fluid dynamics, an area that scientists from numerous disciplines study. **Definition 2.1.1 (Fluid)**
"A substance exists in three primary phases: solid, liquid, and gas. (At very high temperatures, it also exists as plasma.) A substance in the liquid or gas phase is referred to as a fluid. Distinction between a solid and a fluid is made on the basis of the substances ability to resist an applied shear (or tangential) stress that tends to change its shape. A solid can resist an applied shear stress by deforming, whereas a fluid deforms continuously under the influence of shear stress, no matter how small. In solids stress is proportional to strain, but in fluids stress is proportional to strain rate. When a constant shear force is applied, a solid eventually stops deforming, at some fixed strain angle, whereas a fluid never stops deforming and approaches a certain rate of strain." [24]

Definition 2.1.2 (Fluid Mechanics)

"Fluid mechanics is that branch of science which deals with the behavior of the fluid (liquids or gases) at rest as well as in motion." [25]

Definition 2.1.3 (Fluid Dynamics)

"The study of fluid if the pressure forces are also considered for the fluids in motion, the branch of science is called fluid dynamics." [25]

Definition 2.1.4 (Viscosity)

"Viscosity is defined as the property of a fluid which offers resistance to the movement of one layers of fluid over another adjacent layer of the fluid. When two layers of a fluid, a distance 'dy' apart, move one over the other at different velocities, say u and $u + du$ as shown in the viscosity together with relative velocity causes a shear stress acting between the fluid layers.

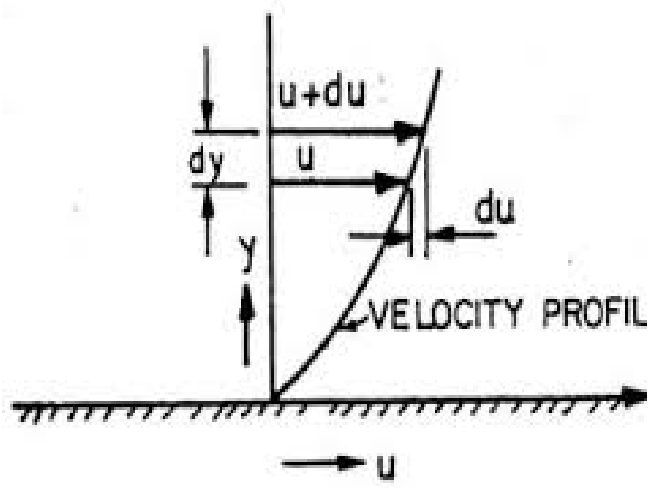

FIGURE 2.1: Velocity variation near a solid surface.

The top layer causes a shear stress on the adjacent lower layer while the lower layer causes a shear stress on the adjacent top layer. This shear stress is proportional to the rate of change of velocity with respect to y. it is denoted by symbol τ called Tau.

Mathematically,

$$\tau \propto \frac{du}{dy},$$

$$\Rightarrow \quad \tau = \mu \frac{du}{dy},$$

$$\Rightarrow \quad \mu = \frac{\tau}{\frac{\partial u}{\partial y}}, \tag{2.1}$$

where μ is viscosity coefficient, τ is shear stress and $\frac{\partial u}{\partial y}$ represents the velocity gradient or rate of shear strain. The unit of viscosity is newton-second per square metre, which is usually expressed as pascal-second in SI units." [26]

Definition 2.1.5 (Kinematic Viscosity)

"Kinematic viscosity is defined as the ratio between the dynamic viscosity and density of fluid. It is denoted by the Greek symbol ν, thus mathematically,

$$\nu = \frac{\text{Viscosity}}{\text{Density}} = \frac{\mu}{\rho}$$

where the unit of kinematic viscosity is square meters per second." [26]

Definition 2.1.6 (Magnetohydrodynamics)

"Magnetohydrodynamics (MHD) is concerned with the flow of electrically conducting fluids in the presence of magnetic fields, either externally applied or generated within the fluid by inductive action." [27]

Definition 2.1.7 (Thermal Conductivity)

"The Fourier heat conduction law states that the heat flow is proportional to the Temperature gradient. The coefficient of proportionality is a material parameter known as the thermal conductivity, which may be a function of several variables."[28]

Definition 2.1.8 (Thermal Diffusivity)

"It is the ratio of the thermal conductivity of fluid or material to the specific heat capacity of fluid or material. It is represented by α.

$$\alpha = \frac{k}{\rho C_p},$$

where α is the thermal diffusivity, k is the thermal conductivity, ρ is the density and C_p is the specific heat at constant pressure."[28]

Definition 2.1.9 (Porous Material)

"A solid containing holes or voids, either connected or non-connected, dispersed

within it in either a regular or random manner known as porous material provided that holes occur relatively frequently within the solid. Pores are either interconnected or non-interconnected. A fluid can flow through a porous material only if at least some of the pores are interconnected."[29]

Definition 2.1.10 (Nanofluid)

"Nanofluids are engineered colloids made of a base fluid and nanoparticles. Nanofluids have higher thermal conductivity and single phase heat transfer coefficients than their base fluids metals, oxides, carbides, or carbon nanotubes are the typical nanoparticles which are used in nanofluids and oil, ethylene glycol and water are examples of common base fluids."[25]

Definition 2.1.11 (Hybrid Nanofluid)

"Hybrid nanofluids are advanced forms of nanofluids that have reportedly even better thermal properties than basic nanofluids. These special nanofluids are made of nanoparticles of two or more different materials of same or different size mixed in a traditional fluid."[30]

2.2 Classifications of different Fluid Flow

In this section, we have discussed some crucial forms of fluid flow.

Definition 2.2.1 (Steady and Unsteady Flows)

"Steady flow is defined as that type of flow in which the fluid characteristics like velocity, pressure, density, etc., at a point do not change with time. Thus for steady flow, mathematically, we have

$$\left(\frac{\partial V}{\partial t}\right)_{x_0,y_0,z_0} = 0, \quad \left(\frac{\partial p}{\partial t}\right)_{x_0,y_0,z_0} = 0, \quad \left(\frac{\partial \rho}{\partial t}\right)_{x_0,y_0,z_0} = 0,$$

where (x_0, y_0, z_0) is fixed point in fluid field." [26]

" Unsteady flow is that type of flow, in which the velocity, pressure or density at

a point changes with respect to time. thus, mathematically, for unsteady flow

$$\left(\frac{\partial V}{\partial t}\right)_{x_0,y_0,z_0} \neq 0, \quad \left(\frac{\partial p}{\partial t}\right)_{x_0,y_0,z_0} \neq 0 \text{ etc.}" \text{ [26]}$$

Definition 2.2.2 (Uniform and Non-uniform Flows)

"Uniform flow is defined as the type of flow in which the velocity at any given time does not change with respect to space (i.e., length of direction of the flow). Mathematically, for uniform flow

$$\left(\frac{\partial V}{\partial s}\right)_{t=\text{constant}} = 0,$$

where $\partial V =$ Change of velocity

$\partial s =$ Length of flow in the direction S.

Non-uniform flow is the type of flow in which the velocity at any given time changes with respect to space. Thus, mathematically, for non-uniform flow

$$\left(\frac{\partial V}{\partial s}\right)_{r=\text{constant}} \neq 0." \text{ [26]}$$

Definition 2.2.3 (Laminar and Turbulent Flows)

"Laminar flow is defined as that type of flow in which the fluid particles move along well-defined paths or stream line and all the stream-lines are straight and parallel. Thus the particles move in lamines or layers gliding smoothly over the adjacent layer. This type of flow is also called stream-line flow or viscus flow." [26]

"Turbulent flow is that type of flow in which the fluid particles move in a zig-zag way. due to the movement of fluid particles in a zig-zag way, the eddies formulation takes place which are responsible for high energy loss." [26]

Definition 2.2.4 (Compressible and Incompressible Flows)

"Compressible flow is that type of flow in which the density for the fluid changes from point to point or in other words the density (ρ) is not constant for the fluid. Thus, mathematically, for compressible flow

$$\rho \neq \text{constant}$$

Incompressible flow is that type of flow in which the density is constant for the fluid flow. Liquids are generally incompressible while gases are compressible. Mathematically, for incompressible flow

$$\rho = \text{constant.}" \text{ [26]}$$

Definition 2.2.5 (Rotational and Irrotational Flows)

"Rotational flow is that type of flow in which the fluid particles while flowing along stream-lines, also rotate about their own axis. And if the fluid particles while flowing along stream-lines, do not rotate about their own axis then that type of flow is called irrotational flow." [26]

Definition 2.2.6 (Inviscous Flow)

"A flow in which viscosity of the fluid is equal to zero is known as inviscous (inviscid) flow."

2.3 Classification of Fluid

Fluids are categorized into the following five types.

Definition 2.3.1 (Ideal Fluid)

"A fluid which is incompressible and is having no viscosity, is known as an ideal fluid. Ideal fluid is only an imaginary fluid as all the fluids, which exist, have some viscosity." [26]

Definition 2.3.2 (Real Fluid)

"A fluid, which possesses viscosity, is known as a real fluid. All the fluids, in actual practice, are real fluids." [26]

Examples are water, petrol, oil, alcohol are real fluids.

Definition 2.3.3 (Newtonian Fluid)

"A real fluid, in which shear stress is directly, proportional to the rate of shear strain (or velocity gradient), is known as a Newtonian fluid". [26]

Some examples of Newtonian fluids are water, air, alcohol, glycerol and thin motor oil over a wide range of shear stresses and shear rates observed in everyday life.

Definition 2.3.4 (Non-Newtonian Fluid)

"A real fluid, in which the shear stress is not proportional to the rate of shear strain (or velocity gradient), is known as a Non-Newtonian fluid". [26]

Non-Newtonian fluid are most typically encountered in our daily lives, including ketchup, toothpaste, paint and shampoo."

Definition 2.3.5 (Ideal Plastic Fluid)

"A fluid, in which shear stress is more than the yield value and shear stress is proportional to the rate of shear strain (or velocity gradient), is known as ideal plastic fluid." [26]

Examples are blood and saliva.

Definition 2.3.6 (Casson Fluid)

"Casson fluid can be defined as a shear thinning liquid which is assumed to have an infinite viscosity at zero rate of shear, a yield stress below which no flow occurs, and a zero viscosity at an infinite rate of shear."[31]

Examples of casson fluids are blood, melted chocolate and shakes.

2.4 Modes of Heat Transfer

Heat transfer refers to the transfer of energy and entropy from one location to another. In this section, first the formal definition of heat transfer is given and then different forms of heat transfer are elaborated.

Definition 2.4.1 (Heat Transfer)

"Heat transfer is a branch of engineering that deals with the transfer of thermal energy from one point to another within a medium or from one medium to another due to the occurrence of a temperature difference."[28]

For example, the heat from the burner is transmitted to the cooking pan. Heat

transfer may take place in one or more of its three basic forms: conduction, convection, and radiation.

Definition 2.4.2 (Conduction)

"The mechanism of heat transfer due to a temperature gradient in a stationary medium is called conduction. The medium may be a solid or a fluid. A very popular example of conduction heat transfer is that when one end of metallic spoon is dipped into a cup of hot tea, the other end becomes gradually hot. In solids, the conduction of heat is attributed to two effects:

(i) the flow of free electrons and

(ii) the lattice vibrational waves caused by the vibrational motions of the molecules at relatively fixed positions called a lattice."[32]

Examples are a concrete or asphalt sidewalk may become exceedingly hot on a sunny day. When you walk barefoot on it, heat is carried from the heated surface to the soles of your feet, and you can feel it and in addition, when heat from the campfire is transferred to your hands when you keep your hands close to it. You experience warmth because the air in close proximity to your skin is being heated by the fire through conduction.

Definition 2.4.3 (Convection)

"The mode by which heat is transferred between a solid surface and the adjacent fluid in motion when there is a temperature difference between the two is known as convection heat transfer. The temperature of the fluid stream refers either to its bulk or free stream temperature."[32]

Examples are heating water on the stove and using an air conditioner.

Convection is further classified into following three types.

Definition 2.4.4 (Forced Convection)

"In forced convection, the fluid is forced to flow over a solid surface by external means such as fan, pump or atmospheric wind." [32]

Definition 2.4.5 (Free Convection)

"When the fluid motion is caused by the buoyancy forces that are induced by density differences due to the variation in temperature or species concentration

(in case of multicomponent systems) in the fluid, the convection is called natural (or free) convection." [32]

Definition 2.4.6 (Mixed Convection)

"Mixed convection occurs when both natural convection and forced convection play significant roles in the transfer of heat. Mixed convection occurs when the heat transfer is significantly different from that for either pure natural convection or pure forced convection."[33]

Definition 2.4.7 (Radiation)

"Any substance at a finite temperature emits energy in the form of electromagnetic waves in all directions and at all wavelengths (from a very low one to a very high one). The energy emitted within a specific band of wavelength (0.1100 μm) is termed thermal radiation. The exchange of such radiant energy between two bodies at different temperatures is defined as heat transfer between the bodies by radiation. We have seen earlier that the heat transfer by conduction or convection requires the presence of a medium. But the radiation heat transfer does not necessarily require a medium, rather it occurs most efficiently in a vacuum." [32] Examples are microwaves from an oven, X-rays from an X-ray tube, and UV light from the sun.

Definition 2.4.8 (Mass Transfer)

"Mass transfer is the flow of molecules from one body to another when these bodies are in contact or within a system consisting of two components when the distribution of materials is not uniform. When a copper plate is placed on a steel plate, some molecules from either side will diffuse into the other side. When salt is placed in a glass and water poured over it, after sufficient time the salt molecules will diffuse into the water body. A more common example is drying of clothes or the evaporation of water spilled on the floor when water molecules diffuse into the air surrounding it. Usually mass transfer takes place from a location where the particular component is proportionately high to a location where the component is proportionately low. Mass transfer may also take place due to potentials other than concentration difference."[34]

2.5 Dimensionless Parameters

The discussion in the next chapter will reference the dimensionless numbers listed below.

Definition 2.5.1 (Reynold Number)

"It is the most significant dimensionless number which is used to identify the different flow behaviors like laminar or turbulent flow. Mathematically, it is expressed as

$$Re = \frac{LU}{\nu},$$

where U denotes the free stream velocity, L is the characteristic length and ν stands for kinematic viscosity." [25]

Definition 2.5.2 (Nusselt Number)

"It is the relationship between the convective to the conductive heat transfer through the boundary of the surface. Mathematically, it is defined as

$$Nu = \frac{hL}{k},$$

where h stands for convective heat transfer, L stands for characteristic length and k stands for thermal conductivity." [35]

Definition 2.5.3 (Prandtl Number)

"The ratio of kinematic diffusivity to heat the diffusivity is said to be Prandtl number. It is denoted by Pr. Mathematically, it can be written as

$$\begin{aligned} Pr &= \frac{\nu}{\alpha} \\ \Rightarrow \quad Pr &= \frac{\mu c_p}{\rho k}, \end{aligned}$$

where μ and α denote the momentum diffusivity or kinetic diffusivity and thermal diffusivity respectively. The relative thickness of thermal and momentum boundary layer is controlled by Prandtl number. For small Pr, heat distributed rapidly corresponds to the momentum." [36]

Definition 2.5.4 (Schmidt Number)

"It is the ratio between kinematic viscosity ν and molecular diffusion D. It is denoted by Sc and mathematically we can write it as:

$$Sc = \frac{\nu}{D},$$

where ν is the kinematic viscosity and D is the mass diffusivity".[28]

Definition 2.5.5 (Skin Friction Number)

"The skin friction coefficient is typically defined as

$$Cf = \frac{2\tau_w}{\rho U_w^2},$$

where τ_w is the local wall shear stress, ρ is the fluid density and U_w is the free stream velocity (usually taken outside the boundary layer or at the inlet)." [37]

Definition 2.5.6 (Sherwood Number)

"It is a non-dimensional quantity which describes the ratio of the mass transport by convection to the transfer of mass by diffusion. Mathematically,

$$Sh = \frac{kL}{D},$$

here L is characteristics length, D is the mass diffusivity and k is the mass transfer coefficient." [38]

Definition 2.5.7 (Eckert Number)

"It is a dimensionless number used in continuum mechanics. It describes the relation between flows and the boundary layer enthalpy difference and it is used for characterized heat dissipation. Mathematically,

$$Ec = \frac{u^2}{c_p \delta T}$$

, where, u $(\mathtt{ms}^1)$ is fluid flow velocity far from body, Cp denotes the specific heat capacity and δT is the temperature difference. [39]

2.6 Conservation Laws

Three laws of conservation, which may be expressed in integral or differential form, are used to represent the model problems of fluid dynamics. These law's integral formulations take into account changes in mass, momentum, or energy throughout the control volume. We cover several essential conservation laws in this section.

Definition 2.6.1 (Law of Conservation of Mass)

"The principle of conservation of mass can be stated as the time rate of change of mass in a fixed volume is equal to the net rate of mass across the surface. The mathematical statement of the principle results in the following equation, known as the continuity (of mass) equation

$$\frac{\partial \rho}{\partial t} + \delta.\left(\rho \mathbf{V}\right), \tag{2.2}$$

where ρ is the density $(\mathtt{kg/m^3})$ of the medium, $\mathbf{V}$ the velocity vector $(\mathtt{ms^{-1}})$, and δ is the nabla or del operator. The continuity equation in (2.2) is in conservation (or divergence) form since it can be derived directly from an integral statement of mass conservation. By introducing the material derivative or Eulerian derivative operator $\frac{D}{Dt}$

$$\frac{D}{Dt} = \frac{\partial}{\partial t} + \mathbf{V}.\delta, \tag{2.3}$$

the continuity equation (2.2) can be expressed in the alternate, non-conservation (or advective) form

$$\frac{\partial \rho}{\partial t} + \mathbf{V}.\delta\rho + \rho\delta.\mathbf{V} = \frac{D\rho}{Dt} + \rho\delta.\mathbf{V}. \tag{2.4}$$

For steady-state conditions the continuity equation becomes

$$\delta.\left(\rho \mathbf{V}\right) = 0. \tag{2.5}$$

When the density changes following a fluid particle are negligible, the continuum is termed incompressible and we have $\frac{D\rho}{Dt} = 0$. The continuity equation (2.4) the becomes

$$\delta.\mathbf{V} = 0, \tag{2.6}$$

which is often referred to as the incompressibility condition or incompressibility constraint" [28].

Definition 2.6.2 (Law of conservation of Momentum)

"The principle of conservation of linear momentum (or Newton's second law of motion) states that the time rate of change of linear momentum of a given set of particles is equal to the vector sum of all the external forces acting on the particles of the set, provided Newton's Third Law of action and reaction governs the internal forces. Newton's Second Law can be written as

$$\frac{\partial}{\partial t}(\rho \mathbf{V}) + \delta.(\rho \mathbf{V} \otimes \mathbf{V}) = \delta.\sigma + \rho f, \tag{2.7}$$

where $\otimes$ is the tensor (or dyadic) product of two vectors, σ is the Cauchy stress tensor $(\mathtt{N/m^2})$ and f is the body force vector, measured per unit mass and normally taken to be the gravity vector. Equation (2.7) describes the motion of a continuous medium, and in fluid mechanics they are also known as the Navier equations. The form of the momentum equation shown in (2.7) is the conservation (divergence) form that is most often utilized for compressible flows. This equation may be simplified to a form more commonly used with incompressible flows. Expanding the first two derivatives and collecting terms:

$$\rho\left(\frac{\partial \mathbf{V}}{\partial t} + \mathbf{V}\delta.\mathbf{V}\right) + \mathbf{V}\left(\frac{\partial \rho}{\partial t} + \delta.\rho\mathbf{V}\right) = \delta.\sigma + \rho f. \tag{2.8}$$

The second term in parentheses is the continuity equation (2.2) and neglecting this term allows (2.8) to reduce to the non-conservation (advective) form

$$\rho\left(\frac{D\mathbf{V}}{Dt}\right) = \delta.\sigma + \rho f. \tag{2.9}$$

where the material derivative (2.3) has been employed."[28]

Definition 2.6.3 (Law of Conservation of Energy)

"The law of conservation of energy (or the first law of thermodynamics) states that the time rate of change of the total energy is equal to the sum of the rate of work done by applied forces and the change of heat content per unit time. In

the general case, the first law of thermodynamics can be expressed in conservation form as

$$\frac{\partial \rho e^t}{\partial t} + \delta.\rho v e^t = -\delta.q + \delta.(\sigma.v) + Q + \rho f.v, \tag{2.10}$$

where $e^t = e + 1/2v.v$ is the total energy $(\mathtt{J/m^3})$, e is the internal energy, q is he heat flux vector $(\mathtt{W/m^2})$ and Q is the internal heat generation $(\mathtt{W/m^3})$." [28]

Definition 2.6.1 (Newtons Law of Viscosity)
"It states that the shear stress (τ) on a fluid element layer is proportional to the rate of shear strain. The constant of proportionally is called coefficient of viscosity. Mathematically, it is expressed as

$$\tau = \mu \frac{\partial u}{\partial y}."$$

2.7 Shooting Method

The shooting method is developed with the aim of converting the boundary value problem into an initial value problem. Finding the solution of initial value porob-lem is easy. Many simple methods are available for this purpose. The most famous methods are Runge - Kutta, Euler method and predictor corrector method.
To elaborate the shooting method, more precisely consider the following nonlinear boundary value problem:

$$\left.\begin{aligned} f''(\eta) - f(\eta) + f^2(\eta) = 0, \\ f'(0) = 0, \quad f(b) = 0. \end{aligned}\right\} \tag{2.11}$$

Introduce the following notations to simplify the order of the aforementioned BVP and then to convert it into initial value problem.

$$f(\eta) = U_1, \quad f'(\eta) = U_1' = U_2. \tag{2.12}$$

Incorporating the above notations following initial value problem is obtained.

$$U_1' = U_2, \qquad U_1(0) = 0. \tag{2.13}$$

$$U_2' = U_1^2 - U_1, \qquad U_2(0) = k. \tag{2.14}$$

where k is the initial condition to be estimated. To solve the above IVP numerically, the Runge - Kutta method of order four will be utilized. Choose missing condition k in such a way that

$$U_1(b, k) = 0. \tag{2.15}$$

To solve the non-linear algebraic equation (2.15) Newton's method is used with the following iterative scheme:

$$k^{(m+1)} = k^{(m)} - \frac{U_1(b,k)^{(m)}}{\left(\frac{\partial\ U_1(b,k)}{\partial k}\right)^{(m)}}. \tag{2.16}$$

To find $\left(\frac{\partial\ U_1(b,k)}{\partial k}\right)^{(m)}$, introduced the following notations:

$$\frac{\partial U_1}{\partial k} = U_3, \quad \frac{\partial U_2}{\partial k} = U_4. \tag{2.17}$$

Hence (2.17) implies

$$k^{(m+1)} = k^{(m)} - \frac{U_1(b,k)^{(m)}}{U_3(b,k)^{(m)}}. \tag{2.18}$$

Differentiating the system of two first order ODEs ((2.14))and (2.15) with respect to k, the following system of ODEs is obtained:

$$U_3' = U_4, \qquad U_3(0) = 0. \tag{2.19}$$

$$U_4' = 2U_1U_3 - U_3, \qquad U_4(0) = 1. \tag{2.20}$$

Writing all the four ODEs (2.14), (2.15), (2.19) and (2.20) together, following IVP is achieved.

$$U_1' = U_2, \qquad U_1(0) = 0.$$

$$U_2' = U_1^2 - U_1, \qquad U_2(0) = k.$$

$$U_3' = U_4, \qquad U_3(0) = 0.$$

$$U_4' = 2U_1U_3 - U_3, \qquad U_4(0) = 1.$$

The aforementioned system will be numerically solved using the $RK-4$ technique. The missing condition will be obtained by Newton's method and stopping criteria for the technique is

$$|U_1(b,k)| < \epsilon,$$

where $\epsilon > 0$ is an arbitrary small positive number.

Chapter 3

Effects of Viscous Dissipation and Thermal Radiation on Hybrid Nanofluid between two Parallel Plates with Variable Viscosity

3.1 Introduction

This chapter provides a comprehensive survey of the work of Famakinwa et al. [23]. This article provides the detailed examination of the effects of viscous dissipation and thermal radiation on time dependent incompressible squeezing flow of hybrid nanofluid between two parallel plates with variable viscosity. In this survey, hybrid nanofluids are made by adding copper and alumina nanoparticles to water. The model formed by those assumption results in a system of partial differential equations. The obtained BVP is numerically solved by shooting method. Furthermore, the results are validated by inbuilt command BVP4c of the MATLAB. At the end of this chapter, the impact of physical parameters over velocity profile $f'(\eta)$ and temperature profile $\theta(\eta)$ are presented through tables and graphs.

3.2 Mathematical Modeling

Consider a time-dependent incompressible squeezing flow of CuO-Al_2O_3/water hybrid nanofluid confined between two parallel plates that is subject to viscous dissipation and thermal radiation effects. The lower plate is kept fixed, while the upper plate is placed at a distance

$$y = h(t) = \sqrt{\frac{\tilde{v}_f(1-\delta t)}{\tilde{c}}}.$$

Furthermore, the distance of the upper plate to $(\delta > 0)$ or from $(\delta < 0)$ the lower plate is represented by

$$v(\tilde{t}) = \frac{dh}{dt} = -\frac{\delta}{2}\sqrt{\frac{\tilde{v}_f}{\tilde{c}(1-\delta t)}}.$$

In addition, $\tilde{T}_1$ and $\tilde{T}_2$ represent the steady temperature of the lower and upper plates, respectively. The lower plate is porous with velocity

$$\tilde{U}_w = \frac{\tilde{c}x}{(1-\delta t)}.$$

$(\tilde{v}_o > 0)$ represent the suction and $(\tilde{v}_o < 0)$ is for injection. Figure 3.1 depicts the geometrical description of the flow.

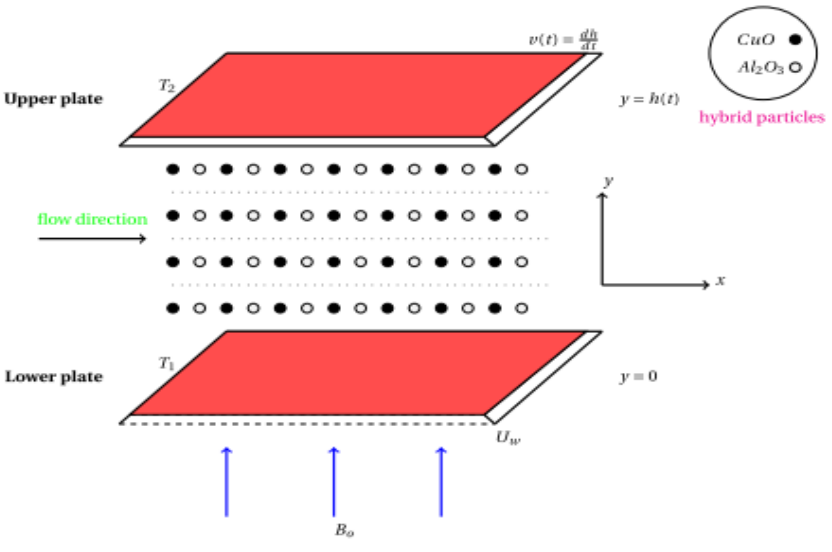

FIGURE 3.1: Flow model.

3.3 Governing Equations

By considering the all assumption discussed in above section along with hybrid nanofluid and using nanfluid model proposed by [40, 41], the following three field equations embody the conservation of mass, momentum and thermal energy respectively.

Mass conservation equation:

$$\tilde{u}_x + \tilde{v}_y = 0, \tag{3.1}$$

Momentum equation:

$$\tilde{V}_t + \tilde{u}\tilde{V}_x + \tilde{v}\tilde{V}_y = \frac{1}{\tilde{\rho}_{hnf}}\left(\tilde{\mu}_{hnf}(T)\tilde{V}_y\right)_y - \frac{\tilde{\sigma}_{hnf}B(t)\tilde{V}}{\tilde{\rho}_{hnf}}, \tag{3.2}$$

Energy equation:

$$\tilde{T}_t + \tilde{u}\tilde{T}_x + \tilde{v}\tilde{T}_y = \frac{\tilde{k}_{hnf}}{(\tilde{\rho}\tilde{c}_p)_{hnf}}\tilde{T}_{yy} + \frac{\tilde{\mu}_{hnf}(T)}{(\tilde{\rho}\tilde{c}_p)_{hnf}}(\tilde{u}_y)^2 - \frac{1}{(\tilde{\rho}\tilde{c}_p)_{hnf}}(\tilde{q}_r)_y, \tag{3.3}$$

subject to the following boundary conditions:

$$\left.\begin{aligned} &\tilde{u} = \lambda.\frac{\tilde{c}x}{1-\delta t}, \quad \tilde{v} = -\frac{\tilde{V}_o}{1-\delta t}, \quad \tilde{T} = \tilde{T}_1, \quad at \quad y = 0, && \text{(lower plate)} \\ &\tilde{u} = 0, \quad \tilde{v} = \frac{dh(t)}{dt}, \ \tilde{T} = \tilde{T}_2, \quad at \ y = h(t), && \text{(upper plate)} \end{aligned}\right\} \tag{3.4}$$

where

$$\tilde{V} = \frac{\partial\tilde{v}}{\partial\tilde{x}} - \frac{\partial\tilde{u}}{\partial\tilde{y}}.$$

Here $\tilde{u}$ and $\tilde{v}$ are the velocities along x and y directions respectively and $\tilde{T}$ denotes the temperature of hybrid nanofluid. The exponential expression of fluid viscosity is considered, which is presented by Massoudi and Christie as follows: [42]

$$\tilde{\mu}_{hnf}\tilde{T} = \tilde{\mu}_f \exp\left[-a\left(\tilde{T} - \tilde{T}_2\right)\right]. \tag{3.5}$$

The medium is considered optically thin with relatively low density, and consequently, the radiative heat flux $\tilde{q}_r$ follows the expression proposed by [43]

$$(\tilde{q_r})_y = 4\tilde{\sigma}^{*2}(\tilde{T} - \tilde{T_o}), \tag{3.6}$$

where $\tilde{\sigma}^{*2}$ denotes the mean absorption coefficient.

3.4 Thermal Physical Characteristics

The basic thermo-physical properties of nanofluids are used from the above literature review. Table 3.1 displays the thermophysical relations.

TABLE 3.1: Thermo-physical properties of water base fluid and nanoparticles. [44]

Nanofluid	**Hybrid Nanofluid**
$\tilde{\mu}_{nf} = \frac{\tilde{\mu}_f}{(1-\Phi)^{2.5}}$	$\tilde{\mu}_{hnf} = \frac{\tilde{\mu}_f}{(1-\Phi_1)^{2.5}(1-\Phi_2)^{2.5}}$
$\tilde{\rho}_{nf} = \tilde{\rho}_f(1-\Phi) + \Phi(\frac{\tilde{\rho}_s}{\tilde{\rho}_f})$	$\tilde{\rho}_{hnf} = \tilde{\rho}_f(1-\Phi_2)\big((1-\Phi_1) + \Phi_1(\frac{\tilde{\rho}_{s_1}}{\tilde{\rho}_f})\big) + \Phi_2\tilde{\rho}_{s_2}$
$(\tilde{\rho}\tilde{c}_p)_{nf} = (\tilde{\rho}\tilde{c}_p)_f(1-\Phi) + \Phi\frac{(\tilde{\rho}\tilde{c}_p)_s}{(\tilde{\rho}\tilde{c}_p)_f}$	$\frac{(\tilde{\rho}\tilde{c}_p)_{hnf}}{(\tilde{\rho}\tilde{c}_p)_f} = (1-\Phi_2)\big((1-\Phi_1) + \Phi_1\frac{(\tilde{\rho}\tilde{c}_p)_{s_1}}{(\tilde{\rho}\tilde{c}_p)_f}\big) + \Phi_2\frac{(\tilde{\rho}\tilde{c}_p)_{s_2}}{(\tilde{\rho}\tilde{c}_p)_f}$
$\frac{\tilde{K}_{nf}}{\tilde{K}_f} = \frac{\tilde{K}_s+(s_f-1)\tilde{K}_f-(s_f-1)\Phi(\tilde{K}_f-K_s)}{\tilde{K}_s+(s_f-1)\tilde{K}_f+\Phi(\tilde{K}_f-\tilde{K}_s)}$	$\frac{\tilde{K}_{hnf}}{\tilde{K}_{bf}} = \frac{\tilde{K}_{s_2}+(s_f-1)\tilde{K}_{bf}-(s_f-1)\Phi_2(\tilde{K}_{bf}-\tilde{K}_{s_2})}{\tilde{K}_{s_2}+(s_f-1)\tilde{K}_{nf}+\Phi_2(\tilde{K}_{bf}-\tilde{K}_{s_2})}$
	$\frac{\tilde{K}_{nf}}{\tilde{K}_f} = \frac{\tilde{K}_{s_1}+(s_f-1)\tilde{K}_f-(s_f-1)\Phi_1(\tilde{K}_f-\tilde{K}_{s_1})}{\tilde{K}_{s_1}+(s_f-1)\tilde{K}_f+\Phi_1(\tilde{K}_f-\tilde{K}_{s_1})}$

For purposes of simplicity, the following notations are used:

$$\widetilde{B}_1 = (1-\phi_1)^{-2.5}(1-\phi_2)^{-2.5}. \tag{3.7}$$

$$\widetilde{B}_2 = (1-\phi_2)\left\{(1-\phi_1) + \phi_1\frac{\widetilde{\rho}_{s1}}{\widetilde{\rho}_f}\right\} + \phi_2\frac{\widetilde{\rho}_{s2}}{\widetilde{\rho}_f}, \tag{3.8}$$

$$\widetilde{B}_3 = \left[1 + \frac{3\left(\frac{\widetilde{\sigma}_s}{\widetilde{\sigma}_f} - 1\right)\Phi}{\left(\frac{\widetilde{\sigma}_s}{\widetilde{\sigma}_f} + 2\right) - \left(\frac{\widetilde{\sigma}_s}{\widetilde{\sigma}_f} - 1\right)\Phi}\right], \tag{3.9}$$

$$\widetilde{B}_4 = \frac{\widetilde{K}_s + (s_f-1)\widetilde{K}_f - (s_f-1)\Phi(\widetilde{K}_f - K_s)}{\tilde{K}_s + (s_f-1)\tilde{K}_f + \Phi(\tilde{K}_f - \tilde{K}_s)}, \tag{3.10}$$

$$\widetilde{B}_5 = (1-\phi_2)\left\{(1-\phi_1) + \frac{\left(\widetilde{\rho}\widetilde{C}_p\right)_{s1}}{\left(\widetilde{\rho}\widetilde{C}_p\right)_f}\phi_1\right\} + \frac{\left(\widetilde{\rho}\widetilde{C}_p\right)_{s2}}{\left(\widetilde{\rho}\widetilde{C}_p\right)_f}\phi_2. \tag{3.11}$$

In order to facilitate a clear comparison, this study presents a detailed analysis of the essential thermo-physical characteristics inherent in both the hybrid nanofluid and nanofluid in Table 3.2.

TABLE 3.2: Thermo-physical characteristics related to present model [45–47]

.

Physical Properties	H_2o	CuO	Al_2O_3
$\widetilde{\rho}\left(kg.m^{-3}\right)$	997.1	6320	3970
$\widetilde{c_p}\left(J(kg.^ok)\right)$	4179	531	765
$\widetilde{k}\left(W(m.^ok)\right)$	0.6130	76.1	40
$\widetilde{\sigma}\left(\Omega.m\right)$	0.05	2.7×10^{-8}	3.69×10^{7}

The relations of different thermo-physical properties for both nanofluid and hybrid nanofluid are used in Table 3.1.

3.5 Similarity Transformation

In this section, we describe the non-dimensionalization for the mathematical model that governs the behavior of the hybrid nanofluid under discussion. For the transformation of the mathematical model into a non-dimensionless form, the following dimensionless quantities are used which are taken from [48].

$$\left.\begin{aligned} &\tilde{u} = \frac{\tilde{c}x}{1-\delta t}\frac{\partial f}{\partial \eta}, \quad \tilde{v} = -\sqrt{\frac{\tilde{c}\tilde{v}_f}{(1-\delta t)}}f(\eta), \quad \eta = y\sqrt{\frac{\tilde{c}}{\tilde{v}_f(1-\delta t)}}, \\ &\psi = \sqrt{\frac{\tilde{c}}{\tilde{v}_f(1-\delta t)}}xf(\eta), \quad \theta = \frac{\tilde{T}-\tilde{T}_o}{\tilde{T}_2-\tilde{T}_o}. \end{aligned}\right\} \tag{3.12}$$

The step-by-step process for transforming (3.1)-(3.3) into the dimensionless form is described below.

Continuity Equation:

For the continuity equation (3.1), following derivatives are needed:

$$\tilde{u}_x = \frac{\partial \tilde{u}}{\partial x},$$

$$\tilde{u}_x = \frac{\partial}{\partial x}\left(\frac{\tilde{c}x}{(1-\delta t)}f^{'}(\eta)\right),$$

$$\Rightarrow \tilde{u}_x = \left(\frac{\tilde{c}}{(1-\delta t)}\right)f^{'}(\eta), \tag{3.13}$$

$$\tilde{v}_y = \frac{\partial v}{\partial y},$$

$$= \frac{\partial}{\partial y}\left(-\sqrt{\frac{\tilde{c}\tilde{v}_f}{(1-\delta t)}}f(\eta)\right),$$

$$= -\sqrt{\frac{\tilde{c}\tilde{v}_f}{(1-\delta t)}}f^{'}(\eta)\frac{\partial \eta}{\partial x},$$

$$= -\sqrt{\frac{\tilde{c}\tilde{v}_f}{(1-\delta t)}}f^{'}(\eta)\sqrt{\frac{\tilde{c}}{\tilde{v}_f(1-\delta t)}},$$

$$\Rightarrow \tilde{v}_y = -\left(\frac{\tilde{c}}{(1-\delta t)}\right)f^{'}(\eta), \tag{3.14}$$

substituting values of (3.13) and (3.14) in (3.1) we get:

$$\tilde{u}_x + \tilde{v}_y = \left(\frac{\tilde{c}x}{(1-\delta t)}\right)f^{'}(\eta) - \left(\frac{\tilde{c}}{(1-\delta t)}\right)f^{'}(\eta) = 0, \tag{3.15}$$

The above result shows that the transformations satisfy the continuity equation.

Momentum Equation:

Now, for the conversion of momentum equation (3.2) the following derivatives are required.

$$\tilde{u} = \frac{\tilde{c}x}{1-\delta t}\frac{\partial f}{\partial \eta},$$

$$\frac{\partial \tilde{u}}{\partial y} = \frac{\tilde{c}x}{1-\delta t}f^{''}\frac{\partial \eta}{\partial x},$$

$$= \frac{\tilde{c}x}{1-\delta t}\sqrt{\frac{\tilde{c}}{\tilde{v}_f(1-\delta t)}}f^{''}(\eta), \tag{3.16}$$

$$\Rightarrow \tilde{v} = -\sqrt{\frac{\tilde{c}\tilde{v}_f}{(1-\delta t)}}f(\eta),$$

$$\frac{\partial \tilde{v}}{\partial x} = 0, \tag{3.17}$$

$$\tilde{V} = \frac{\partial \tilde{v}}{\partial x} - \frac{\partial \tilde{u}}{\partial y},$$

$$\tilde{V} = -\frac{\tilde{c}x}{1-\delta t}\sqrt{\frac{\tilde{c}}{\tilde{v}_f(1-\delta t)}}f^{''}(\eta), \tag{3.18}$$

$$\Rightarrow \tilde{V}_t = \frac{\partial}{\partial t}\left(-\tilde{c}x\sqrt{\frac{\tilde{c}}{\tilde{v}_f}}\frac{1}{(1-\delta t)^{\frac{3}{2}}}f^{''}(\eta)\right),$$

$$= -\tilde{c}x\sqrt{\frac{\tilde{c}}{\tilde{v}_f}}\frac{\partial}{\partial t}(1-\delta t)^{-\frac{3}{2}}f^{''}(\eta),$$

$$= -\tilde{c}x\sqrt{\frac{\tilde{c}}{\tilde{v}_f}}\left[\frac{3}{2}(1-\delta t)^{\frac{-3}{2}-1}(\delta)f^{''}(\eta) + (1-\delta t)^{-\frac{3}{2}}f^{''}\frac{\partial \eta}{\partial t}\right],$$

$$= -\tilde{c}x\sqrt{\frac{\tilde{c}}{\tilde{v}_f}}\left[\frac{3}{2}(1-\delta t)^{\frac{-5}{2}}(\delta)f^{''} + (1-\delta t)^{-\frac{3}{2}}f^{''}\frac{\eta\delta}{2(1-\delta t)}\right],$$

$$= -\tilde{c}x\sqrt{\frac{\tilde{c}}{\tilde{v}_f}}\left[\frac{3}{2}(1-\delta t)^{\frac{-5}{2}}(\delta)f^{''} + \frac{f^{'''}(\eta)\eta\delta}{2(1-\delta t)^{\frac{5}{2}}}\right],$$

$$\Rightarrow \tilde{V}_t = \frac{-3}{2}\tilde{c}x\delta\sqrt{\frac{\tilde{c}}{\tilde{v}_f(1-\delta t)}}\frac{1}{(1-\delta t)^2}f^{''}(\eta) - \frac{\tilde{c}x}{2(1-\delta t)^2}\sqrt{\frac{\tilde{c}}{\tilde{v}_f(1-\delta t)}}f^{'''}(\eta)\eta\delta, \tag{3.19}$$

$$\tilde{V}_x = \frac{\partial}{\partial x}\left(\frac{-\tilde{c}x}{(1-\delta t)}\sqrt{\frac{\tilde{c}}{\tilde{v}_f(1-\delta t)}}f^{''}(\eta)\right),$$

$$= \frac{-\tilde{c}}{(1-\delta t)}\sqrt{\frac{\tilde{c}}{\tilde{v}_f(1-\delta t)}}f^{''}, \tag{3.20}$$

$$\Rightarrow \tilde{u}\tilde{V}_x = \frac{-\tilde{c}x}{(1-\delta t)}\frac{\tilde{c}}{(1-\delta t)}\sqrt{\frac{\tilde{c}}{\tilde{v}_f(1-\delta t)}}f'(\eta)f^{''}(\eta),$$

$$= \frac{-\tilde{c}^2x}{(1-\delta t)^2}\sqrt{\frac{\tilde{c}}{\tilde{v}_f(1-\delta t)}}f'(\eta)f^{''}(\eta), \tag{3.21}$$

$$\tilde{V}_y = \frac{\partial}{\partial y}\left(\frac{-\tilde{c}x}{(1-\delta t)^2}\sqrt{\frac{\tilde{c}}{\tilde{v}_f(1-\delta t)}}\right)f^{''}(\eta),$$

$$= \left(\frac{-\tilde{c}x}{(1-\delta t)}\sqrt{\frac{\tilde{c}}{\tilde{v}_f(1-\delta t)}}\right)f^{'''}\frac{\partial \eta}{\partial y},$$

$$\tilde{V}_y = \frac{-\tilde{c}x}{(1-\delta t)}\sqrt{\frac{\tilde{c}}{v_f(1-\delta t)}}f^{'''}(\eta)\sqrt{\frac{\tilde{c}}{\tilde{v}_f(1-\delta t)}},$$

$$\tilde{V}_y = \frac{-\tilde{c}^2 x}{(1-\delta t)^2} f''', \tag{3.22}$$

$$\Rightarrow \tilde{v}\tilde{V}_y = \sqrt{-\frac{\tilde{c}}{\tilde{v}_f(1-\delta t)}} f \frac{-\tilde{c}^2 x}{(1-\delta t)^2} f''',$$

$$= \frac{\tilde{c}^2 x}{\tilde{v}_f(1-\delta t)^2} \sqrt{\frac{\tilde{c}}{\tilde{v}_f(1-\delta t)}} \frac{-\tilde{c}^2 x}{(1-\delta t)^2} f(\eta) f'''(\eta), \tag{3.23}$$

$$\frac{\tilde{\sigma}_{hnf}}{\tilde{\rho}_{hnf}} B(t)\tilde{V} = \frac{\tilde{\sigma}_{hnf}}{\tilde{\rho}_{hnf}} \frac{B_o}{(1-\delta t)} \frac{-\tilde{c}x}{(1-\delta t)} \sqrt{\frac{\tilde{c}}{\tilde{v}_f(1-\delta t)}} f''(\eta),$$

$$= -\frac{\tilde{\sigma}_{hnf}}{\tilde{\rho}_{hnf}} \frac{B_o}{(1-\delta t)} \sqrt{\frac{\tilde{c}}{\tilde{v}_f(1-\delta t)}} f'', \tag{3.24}$$

$$\frac{1}{\tilde{\rho}_{hnf}} \left(\tilde{\mu}_{hnf}(T)\tilde{V}_y\right)_y = -\frac{1}{\tilde{\rho}_{hnf}} \left(\frac{\mu_f \tilde{c}^2 x}{(1-\delta t)^2}\right) \frac{\partial}{\partial y} \left(e^{-m\theta} f'''(\eta)\right)$$

$$= -\frac{1}{\tilde{\rho}_{hnf}} \left(\frac{\mu_f \tilde{c}^2 x}{(1-\delta t)^2}\right) \left[e^{-m\theta} f^{iv} \frac{\partial \eta}{\partial y} - m e^{-m\theta} \theta' \frac{\partial \eta}{\partial y} f'''(\eta)\right],$$

$$= -\frac{1}{\tilde{\rho}_{hnf}} \left(\frac{\mu_f \tilde{c}^2 x}{(1-\delta t)^2}\right) e^{-m\theta} f^{iv} \sqrt{\frac{\tilde{c}}{\tilde{v}_f(1-\delta t)}}$$
$$+ \frac{1}{\tilde{\rho}_{hnf}} \left(\frac{\mu_f \tilde{c}^2 x}{(1-\delta t)^2}\right) m e^{-m\theta} \sqrt{\frac{\tilde{c}}{\tilde{v}_f(1-\delta t)}} f'''\theta',$$

$$= -\frac{\tilde{\mu}_f}{\tilde{\rho}_{hnf}\tilde{v}_f} \frac{\mu_{hnf}}{\mu_f} \left(\frac{\tilde{c}^2 x}{(1-\delta t)^2}\right) \sqrt{\frac{\tilde{c}}{\tilde{v}_f(1-\delta t)}} f^{iv}$$
$$+ \frac{\tilde{\mu}}{\tilde{\rho}_{hnf}\tilde{v}_f} \left(\frac{\tilde{c}^2 x}{(1-\delta t)^2}\right) \sqrt{\frac{\tilde{c}}{\tilde{v}_f(1-\delta t)}} m e^{-m\theta} f'''\theta'.$$

Combining all the above terms and substituting in (3.2), the following form is obtained:

$$\frac{-3}{2} \frac{\tilde{c}x\delta}{(1-\delta t)^2} \sqrt{\frac{\tilde{c}}{\tilde{v}_f(1-\delta t)}} f''(\eta) - \frac{\tilde{c}x}{2(1-\delta t)^2} \sqrt{\frac{\tilde{c}}{\tilde{v}_f(1-\delta t)}} f'''(\eta)\eta\delta$$
$$- \frac{-\tilde{c}^2 x}{(1-\delta t^2)} \sqrt{\frac{\tilde{c}}{\tilde{v}_f(1-\delta t)}} f'(\eta) f''(\eta) + \frac{\tilde{c}^2 x}{\tilde{v}_f(1-\delta t)^2} \sqrt{\frac{\tilde{c}}{\tilde{v}_f(1-\delta t)}} f(\eta) f'''(\eta)$$

$$= -\frac{\tilde{\mu}_f}{\tilde{\rho}_{hnf}\upsilon_f}\frac{\mu_{hnf}}{\mu_f}\left(\frac{\tilde{c}^2 x}{(1-\delta t)^2}\right)\cdot\sqrt{\frac{\tilde{c}}{\tilde{\upsilon}_f(1-\delta t)}}f^{iv}$$
$$+\frac{\tilde{\mu}_f}{\tilde{\rho}_{hnf}\upsilon_f}\left(\frac{\tilde{c}^2 x}{(1-\delta t)^2}\right)\sqrt{\frac{\tilde{c}}{\tilde{\upsilon}_f(1-\delta t)}}me^{-m\theta}f'''\theta'$$
$$+\frac{\tilde{\sigma}_{hnf}}{\tilde{\rho}_{hnf}}\frac{B_o}{(1-\delta t)}\frac{-\tilde{c}x}{(1-\delta t)}\sqrt{\frac{\tilde{c}}{\tilde{\upsilon}_f(1-\delta t)}}f''(\eta),$$

$$\Rightarrow \left(\frac{B_1}{B_2}\right)f^{iv}-\left(\frac{m}{B_2}\right)f'''\theta'e^{-m\theta}+ff'''-f'f''-\frac{Sq}{2}(3f''+\eta f''')-\left(\frac{\tilde{\sigma}_{hnf}}{\tilde{\rho}_{hnf}}\right)B_o f''=0,$$

$$\Rightarrow \left(\frac{B_1}{B_2}\right)f^{iv}-\left(\frac{m}{B_2}\right)f'''\theta'e^{-m\theta}+f(\eta)f'''-f'f''-\frac{Sq}{2}(3f''+\eta f''')-\left(\frac{B_3}{B_2}\right)Mf''=0.$$

Therefore, the dimensionless form of the momentum equation is

$$\Rightarrow \left(\frac{B_1}{B_2}\right)f^{iv}-\left(\frac{m}{B_2}\right)f'''\theta'e^{-m\theta}+f(\eta)f'''-f'f''-\frac{Sq}{2}(3f''+\eta f''')$$
$$-\left(\frac{B_3}{B_2}\right)Mf''=0. \tag{3.25}$$

The following dimensionless parameters are used in (3.25) are:

$$B_1=\frac{\tilde{\mu}_{hnf}}{\tilde{\mu}_f},\quad B_2=\frac{\tilde{\rho}_{hnf}}{\tilde{\rho}_f},\quad B_3=\frac{\tilde{\sigma}_{hnf}}{\tilde{\sigma}_f},\quad M=\frac{\tilde{\sigma}_f(\tilde{\rho}\tilde{c}_p)_f}{\tilde{k}_f},\quad Sq=\frac{\delta}{\tilde{c}},\quad m=a(\tilde{T}_1-\tilde{T}_2).$$

Energy Equation:

Now dimensional energy equation is converted into non-dimensional form by using following derivatives. So, the transformation of energy equation (3.3),re required following derivatives.

$$\theta=\frac{\tilde{T}-\tilde{T}_o}{\tilde{T}_2-\tilde{T}_o},$$
$$\tilde{T}=\theta(\eta)(\tilde{T}_2-\tilde{T}_o)+\tilde{T}_o, \tag{3.26}$$

$$\tilde{T}_x=0, \tag{3.27}$$

$$\tilde{T}_y=\frac{\partial}{\partial y}\left(\theta(\tilde{T}_2-\tilde{T}_o)\right),$$
$$=(\tilde{T}_2-\tilde{T}_o)\theta'\frac{\partial\eta}{\partial y},$$
$$=(\tilde{T}_2-\tilde{T}_o)\sqrt{\frac{\tilde{c}}{\tilde{\upsilon}_f(1-\delta t)}}\theta'(\eta), \tag{3.28}$$

$$\tilde{T}_{yy} = (\tilde{T}_2 - \tilde{T}_o)\sqrt{\frac{\tilde{c}}{\tilde{v}_f(1-\delta t)}}\theta''(\eta)\frac{\partial \eta}{\partial y},$$

$$= (\tilde{T}_2 - \tilde{T}_o)\left(\frac{\tilde{c}}{\tilde{v}_f(1-\delta t)}\right)\theta''(\eta), \tag{3.29}$$

$$\eta = y\sqrt{\frac{\tilde{c}}{\tilde{v}_f(1-\delta t)}},$$

$$\frac{\partial \eta}{\partial t} = y\sqrt{\frac{\tilde{c}}{\tilde{v}_f}}(1-\delta t)^{\frac{-1}{2}},$$

$$= y\sqrt{\frac{\tilde{c}}{v_f}}(1-\delta t)^{\frac{-1}{2}-1}\frac{-1}{2}(-\delta),$$

$$\frac{\partial \eta}{\partial t} = y\sqrt{\frac{\tilde{c}}{v_f}}(1-\delta t)^{\frac{-3}{2}}(-\delta),$$

$$= \frac{1}{2}y\sqrt{\frac{\tilde{c}}{v_f(1-\delta t)}}\frac{\delta}{(1-\delta t)},$$

$$= \frac{\delta \eta}{2(1-\delta t)}, \tag{3.30}$$

$$\tilde{T}_t = \frac{1}{2}(\tilde{T}_2 - \tilde{T}_o)\theta'\frac{\delta \eta}{(1-\delta t)} \tag{3.31}$$

$$(\tilde{q}_r)_y = 4\tilde{\sigma^*}2(\tilde{T} - \tilde{T}_o),$$

$$= 4\tilde{\sigma}^{*2}(\tilde{T}_2 - \tilde{T}_o)\theta, \tag{3.32}$$

$$\frac{\tilde{\mu}_{hnf}(T)}{(\tilde{\rho}\tilde{c}_p)_{hnf}}(\tilde{u}_y)^2 = \frac{\tilde{\mu}_f e^{-m\theta}}{(\tilde{\rho}\tilde{c}_p)_{hnf}}\left(\frac{\tilde{c}x}{1-\delta t}f''\frac{\partial \eta}{\partial y}\right)^2$$

$$= \frac{\tilde{\mu}_f e^{-m\theta}}{(\tilde{\rho}\tilde{c}_p)_{hnf}}\frac{\tilde{c}\tilde{U}_w^2 f''^2}{\tilde{v}_f(1-\delta t)}, \tag{3.33}$$

Using (3.5) into (3.3)

$$\tilde{T}_t + u\tilde{T}_x + v\tilde{T}_y = \frac{\tilde{k}_{hnf}}{(\tilde{\rho}\tilde{c}_p)_{hnf}}\tilde{T}_{yy} + \frac{\tilde{\mu}_{hnf}(T)}{(\tilde{\rho}\tilde{c}_p)_{hnf}}(\tilde{u}_y)^2 - \frac{4\tilde{\sigma}^{*2}}{(\tilde{\rho}\tilde{c}_p)_{hnf}}(\tilde{T} - \tilde{T}_o). \tag{3.34}$$

Using all the above derivatives in (3.34), to get:

$$\theta'\frac{\delta\eta}{2(1-\delta t)}(\tilde{T}_1-\tilde{T}_2)-\frac{\tilde{c}f(\tilde{T}_1)-\tilde{T}_2)}{(1-\delta t)}=\frac{\tilde{k}_{hnf}}{(\tilde{\rho}\tilde{c}_p)_{hnf}}(\tilde{T}_1-\tilde{T}_2)\frac{\tilde{c}\theta'}{v_f(1-\delta t)}$$
$$+\frac{\tilde{\mu}_f e^{-m\theta}}{(\tilde{\rho}\tilde{c}_p)_{hnf}}\frac{\tilde{c}\tilde{U}_w^2 f''^2}{v_f(1-\delta t)}-\frac{1}{\tilde{\rho}\tilde{c}_{p\,hnf}}4\tilde{\sigma}^{*2}(\tilde{T}-\tilde{T}_o),$$

$$\Rightarrow\ \frac{\delta\eta}{2\tilde{c}}\theta'-\theta' f=\frac{\tilde{k}_{hnf}}{(\tilde{\rho}\tilde{c}_p)_{hnf}\,v_f}\theta''+\frac{\tilde{\mu}_f e^{-m\theta}}{(\tilde{\rho}\tilde{c}_p)_{hnf}}\frac{\tilde{U}_w^2 f''^2}{v_f(\tilde{T}_1-\tilde{T}_2)}-\frac{1}{\tilde{c}(\tilde{\rho}\tilde{c}_p)_{hnf}}4\tilde{\sigma}^{*2}(1-\delta t)\theta,$$

$$\Rightarrow\ \frac{\tilde{k}_{hnf}}{(\tilde{\rho}\tilde{c}_p)_{hnf}}\frac{\tilde{k}_f}{\tilde{k}_f\frac{\tilde{\mu}_f}{\tilde{\rho}_f}}\frac{(\tilde{\rho}\tilde{c}_p)_f}{(\tilde{\rho}\tilde{c}_p)_f}+\frac{\tilde{\mu}_f e^{-m\theta}}{(\tilde{\rho}\tilde{c}_p)_{hnf}}\frac{\tilde{U}_w^2 f''^2}{v_f(1-\delta t)}-\frac{1}{\tilde{c}(\tilde{\rho}\tilde{c}_p)_{hnf}}\frac{(\tilde{\rho}\tilde{c}_p)_f}{(\tilde{\rho}\tilde{c}_p)_f}4\tilde{\sigma}^{*2}(1-\delta t)\theta$$
$$+f\theta'-\frac{1}{2}\theta' S_q\eta,$$

$$\Rightarrow\left(\frac{B_4}{P_r B_5}\right)\theta''+\left(\frac{E_c}{B_5}\right)e^{-m\theta}f''^2+f\theta'-\frac{S_q}{2}\eta\theta'-\frac{R}{B_5}\theta=0. \tag{3.35}$$

Following parameters are used in the above equations:

$$B_4=\frac{\tilde{k}_{hnf}}{\tilde{k}_f},\quad B_5=\frac{(\tilde{\rho}\tilde{c}_p)_{hnf}}{(\tilde{\rho}\tilde{c}_p)_f},\quad P_r=\frac{v_f(\tilde{\rho}\tilde{c}_p)_f}{\tilde{k}_f},\quad R=\frac{4\tilde{\sigma}^{*2}(1-\delta t)}{\tilde{c}(\tilde{\rho}\tilde{c}_p)_f},$$
$$E_c=\frac{\tilde{U}_w^2}{(\tilde{c}_p)_f(\tilde{T}_1-\tilde{T}_2)},\quad S_q=\frac{\delta}{\tilde{c}},\quad m=a(\tilde{T}_1-\tilde{T}_2).$$

3.6 Dimensionless form of the BCs

The following BCs are converted into the dimensionless form by the following procedure. Firstly when y=0 which implies η=0.

- $\tilde{u}=\lambda\frac{\tilde{c}x}{(1-\delta t)}$,

$\Rightarrow\quad \frac{\tilde{c}x}{(1-\delta t)}f'(\eta)=\lambda\frac{\tilde{c}x}{(1-\delta t)}$,

$\Rightarrow\quad f'(0)=\lambda.$

- $\tilde{v}=-\frac{\tilde{V}_o}{(1-\delta t)}$,

$\Rightarrow\quad -\sqrt{\frac{\tilde{c}v_f}{(1-\delta t)}}f(\eta)=-\frac{\tilde{V}_o}{(1-\delta t)}$,

$\Rightarrow\quad f(\eta)=\frac{\tilde{V}_o}{(1-\delta t)}\left(\frac{1-\delta t}{\tilde{c}v_f}\right)^{\frac{1}{2}}$,

$$\Rightarrow \quad f(\eta) = \frac{\tilde{V}_o}{\sqrt{v_f(1-\delta t)\tilde{c} \times \frac{\tilde{c}}{\tilde{c}}}},$$

$$\Rightarrow \quad f(\eta) = \frac{\tilde{V}_o}{\sqrt{\frac{v_f(1-\delta t)\tilde{c}^2}{\tilde{c}}}},$$

$$\Rightarrow \quad f(0) = \frac{\tilde{V}_o}{\tilde{c}h}$$

$$\Rightarrow \quad f(0) = S.$$

- $\tilde{T} = \tilde{T}_1,$

$$\Rightarrow \quad \theta(\eta)(\tilde{T}_2 - \tilde{T}_o) + \tilde{T}_o = \tilde{T}_1,$$

$$\Rightarrow \quad \theta(\eta)(\tilde{T}_2 - \tilde{T}_o) = \tilde{T}_1 - \tilde{T}_o$$

$$\Rightarrow \theta(0) = \frac{\tilde{T}_1 - \tilde{T}_o}{\tilde{T}_2 - \tilde{T}_o},$$

$$\Rightarrow \quad \theta(0) = \gamma.$$

Now choose at $y = h(t) \Rightarrow \ \eta = 1$

- $\tilde{u} = 0,$

$$\Rightarrow \quad \frac{\tilde{c}x}{(1-\delta t)} f^{'}(\eta) = 0,$$

$$\Rightarrow \quad f^{'}(\eta) = 0.$$

$$\Rightarrow \quad f^{'}(1) = 0.$$

- $\tilde{V} = \frac{dh(t)}{dt},$

$$\Rightarrow \quad -\sqrt{\frac{\tilde{c}\tilde{v}_f}{(1-\delta t)}} f(\eta) = -\frac{\delta}{2}\sqrt{\frac{\tilde{v}_f}{\tilde{c}(1-\delta t)}}$$

$$\Rightarrow \quad f(\eta) = \frac{\delta}{2\tilde{c}}$$

$$\Rightarrow \quad f(1) = \frac{S_q}{2}.$$

- $\tilde{T} = \tilde{T}_2,$

$$\Rightarrow \theta(\eta)(\tilde{T}_2 - \tilde{T}_o) + \tilde{T}_o = \tilde{T}_2$$

$$\Rightarrow \theta(\eta)(\tilde{T}_2 - \tilde{T}_o) = \tilde{T}_2 - \tilde{T}_o$$

$$\Rightarrow \theta(1) = \frac{\tilde{T}_2 - \tilde{T}_o}{\tilde{T}_2 - \tilde{T}_o},$$

$$\Rightarrow \theta(\eta) = 1.$$

Finally the dimensionless form of the fluid model along with the converted boundary conditions is:

$$\left(\frac{B_1}{B_2}\right) f^{iv} - \left(\frac{m}{B_2}\right) f'''\theta' e^{-m\theta} + ff''' - f'f'' - \frac{Sq}{2}(3f'' + \eta f''') - \left(\frac{B_3}{B_2}\right) Mf'' = 0, \tag{3.36}$$

$$\left(\frac{B_4}{P_r B_5}\right)\theta'' + \left(\frac{E_c}{B_5}\right) e^{-m\theta} f''^2 + f\theta' - \frac{S_q}{2}\eta\theta - \frac{R}{B_5}\theta = 0. \tag{3.37}$$

$$\left.\begin{aligned} f = S, \quad f' = \lambda, \quad \theta = \gamma, \quad \text{at} \quad \eta = 0, \\ f = \frac{Sq}{2}, \quad f' = 0, \quad \theta = 1, \quad \text{at} \quad \eta = 1. \end{aligned}\right\} \tag{3.38}$$

3.7 Dimensionless Physical Quantities

Skin friction or drag force is drag caused by the function of the fluid against the surface is denoted by C_{fx}. The conversion of this force into dimensionless form is explained below [49].

$$C_{fx} = \frac{\tilde{\tau}_w}{\tilde{\rho}_f U_w^2}, \tag{3.39}$$

where the expression for the surface shear stress is specified by

$$\tilde{\tau}_w = \tilde{\mu}_{hnf} \left.\frac{\partial \tilde{u}}{\partial y}\right|_{y=0}. \tag{3.40}$$

Therefore, the dimensionless form of C_{fx} is obtained by using (3.40) in (3.39), we get

$$\begin{aligned} C_{fx} &= \frac{\tilde{\mu_{hnf}} \frac{\tilde{c}x}{(1-\delta t)} f'' \sqrt{\frac{\tilde{c}}{\tilde{\nu}_f(1-\delta t)}}}{\tilde{\rho}_f \frac{\tilde{c}^2 x^2}{(1-\delta t)^2}}, \\ &= \frac{\frac{\mu_{\tilde{hnf}}\tilde{\nu}_f}{\tilde{\mu}_f} \frac{\tilde{c}x}{(1-\delta t)} f''(0) \sqrt{\frac{\tilde{c}}{\tilde{\nu}_f(1-\delta t)}}}{\frac{\tilde{c}^2 x^2}{(1-\delta)^2}}, \\ &= B_1 f''(0) \sqrt{\frac{1-\delta t}{\tilde{c}x}} \sqrt{\frac{\tilde{\nu}_f}{x}}, \\ &= B_1 f''(0) \frac{1}{\sqrt{Re_x}}, \\ Re_x^{\frac{1}{2}} C_{fx} &= B_1 f''(0). \end{aligned}$$

Here, $Re_x{=}\frac{\tilde{U}_w x}{\tilde{\nu}_f}$ denotes the local Reynolds number.

The Nusselt number is ratio of convective to conductive heat transfer at boundary in fluid. Nusselt number is an important parameter that can contribute to a better rate of heat exchange [49].

$$Nu_x = \frac{\tilde{q}_w x}{\tilde{k}_f \Delta \tilde{T}}, \tag{3.41}$$

where the expression for the wall heat flux is specified by

$$\tilde{q}_w = -\tilde{k}_{hnf} \frac{\partial \tilde{T}}{\partial y}\bigg|_{y=o}. \tag{3.42}$$

Therefore, putting $\tilde{q}_w$ in (3.41), we get

$$\begin{aligned}
Nu_x =& \frac{-x\tilde{k}_{hnf}(\tilde{T}_2 - \tilde{T}_o)\theta' \sqrt{\frac{\tilde{c}}{\tilde{\nu}_f(1-\delta t)}}}{\tilde{k}_f \Delta \tilde{T}}, \\
=& - xB_4\theta' \sqrt{\frac{\tilde{c}}{\tilde{\nu}_f(1-\delta t)}}, \\
=& B_4\theta'(0) \sqrt{\frac{\tilde{c}}{\tilde{\nu}_f(1-\delta t)}} x, \\
=& - B_4\theta'(0) \sqrt{U_w} \sqrt{\frac{x}{\tilde{\nu}_f}}, \\
=& - B_4\theta'(0) Re_x^{\frac{1}{2}}, \\
Nu_x Re_x^{-\frac{1}{2}} =& - B_4\theta'(0),
\end{aligned} \tag{3.43}$$

where $Re_x{=}\frac{\tilde{U}_w x}{\tilde{\nu}_f}$ denotes the local Reynolds number.

3.8 Solution Methodology

Shooting numerical technique is used to solve the system of ordinary differential equations (3.36)-(3.37), subject to the boundary conditions (3.38). To incorporate shooting method the BVP is converted into the initial value problem by using the

following notations.

$$f(\eta) = \tilde{U}_1, \quad f'(\eta) = \tilde{U}_1' = \tilde{U}_2, \quad f''(\eta) = \tilde{U}_2' = \tilde{U}_3,$$

$$f'''(\eta) = \tilde{U}_3' = \tilde{U}_4, \quad \theta(\eta) = \tilde{U}_5, \quad \theta'(\eta) = \tilde{U}_5' = \tilde{U}_6.$$

The following system of first order ODE's are formed by using the momentum and energy equations.

$$\begin{aligned}
&\tilde{U}_1' = \tilde{U}_2, && \tilde{U}_1(0) = S.\\
&\tilde{U}_2' = \tilde{U}_3, && \tilde{U}_2(0) = \lambda.\\
&\tilde{U}_3' = \tilde{U}_4, && \tilde{U}_3(0) = E1.\\
&\tilde{U}_4' = \frac{B_2}{B_1}\Bigg[\left(\frac{m}{B_2}\right)\tilde{U}_4\tilde{U}_6 e^{-m\tilde{U}_5} - \tilde{U}_1\tilde{U}_4 + \tilde{U}_2\tilde{U}_3 + \frac{Sq}{2}(3\tilde{U}_3 + \eta\tilde{U}_4)\\
&\quad + \frac{B_3}{B_2}M\tilde{U}_3\Bigg], && \tilde{U}_4(0) = E2.\\
&\tilde{U}_5' = \tilde{U}_6, && \tilde{U}_5(0) = \gamma.\\
&\tilde{U}_6' = Pr\left(\frac{B_5}{B_4}\right)\left[\left(\frac{Sq}{2}\right)\eta\tilde{U}_6 + \frac{R}{B_5}\tilde{U}_5 - \left(\frac{Ec}{B_5}\right)\tilde{U}_3^2 e^{-m\tilde{U}_5} - \tilde{U}_1\tilde{U}_6\right], && \tilde{U}_6(0) = E3,
\end{aligned}$$

where the missing initial conditions are E1, E2 and E3. Now, the Runge-Kutta method is used to solve the above mentioned first order initial value problem. It is necessary to choose the missing conditions, such as:

$$\left.\begin{aligned}
&\tilde{U}_1(\eta_1, E1, E2, E3) - \frac{Sq}{2} = 0,\\
&\tilde{U}_2(\eta_1, E1, E2, E3) = 0,\\
&\tilde{U}_5(\eta_1, E1, E2, E3) - 1 = 0.
\end{aligned}\right\} \tag{3.44}$$

Newton's method is used to solve the algebraic equation (3.44) numerically. This formula has the following iterative form:

$$\begin{bmatrix} E1 \\ E2 \\ E3 \end{bmatrix}_{(n+1)} = \begin{bmatrix} E1 \\ E2 \\ E3 \end{bmatrix}_{(n)} - \begin{bmatrix} \frac{\partial\tilde{U}_1}{\partial E1} & \frac{\partial\tilde{U}_1}{\partial E2} & \frac{\partial\tilde{U}_1}{\partial E3} \\ \frac{\partial\tilde{U}_3}{\partial E1} & \frac{\partial\tilde{U}_3}{\partial E2} & \frac{\partial\tilde{U}_3}{\partial E3} \\ \frac{\partial\tilde{U}_5}{\partial E1} & \frac{\partial\tilde{U}_5}{\partial E2} & \frac{\partial\tilde{U}_5}{\partial E3} \end{bmatrix}^{-1} \begin{bmatrix} \tilde{U}_1 - \frac{Sq}{2} \\ \tilde{U}_2 \\ \tilde{U}_5 - 1 \end{bmatrix}_{(n)}$$

To successfully iterate the above formula we need the following derivative

$$\frac{\partial \tilde{U}_1}{\partial E_1} = \tilde{U}_7, \quad \frac{\partial \tilde{U}_2}{\partial E_1} = \tilde{U}_8, \quad \frac{\partial \tilde{U}_3}{\partial E_1} = \tilde{U}_9, \quad \frac{\partial \tilde{U}_4}{\partial E_1} = \tilde{U}_{10}, \quad \frac{\partial \tilde{U}_5}{\partial E_1} = \tilde{U}_{11}, \quad \frac{\partial \tilde{U}_6}{\partial E_1} = \tilde{U}_{12},$$
$$\frac{\partial \tilde{U}_1}{\partial E_2} = \tilde{U}_{13}, \quad \frac{\partial \tilde{U}_2}{\partial E_2} = \tilde{U}_{14}, \quad \frac{\partial \tilde{U}_3}{\partial E_2} = \tilde{U}_{15}, \quad \frac{\partial \tilde{U}_4}{\partial E_2} = \tilde{U}_{16}, \quad \frac{\partial \tilde{U}_5}{\partial E_2} = \tilde{U}_{17}, \quad \frac{\partial \tilde{U}_6}{\partial E_2} = \tilde{U}_{18},$$
$$\frac{\partial \tilde{U}_1}{\partial E_3} = \tilde{U}_{19}, \quad \frac{\partial \tilde{U}_2}{\partial E_3} = \tilde{U}_{20}, \quad \frac{\partial \tilde{U}_3}{\partial E_3} = \tilde{U}_{21}, \quad \frac{\partial \tilde{U}_4}{\partial E_3} = \tilde{U}_{22}, \quad \frac{\partial \tilde{U}_5}{\partial E_3} = \tilde{U}_{23}, \quad \frac{\partial \tilde{U}_6}{\partial E_3} = \tilde{U}_{24},$$

The Newton's iterative technique takes on the following transform as a result of these additional notations:

$$\begin{bmatrix} E1 \\ E2 \\ E3 \end{bmatrix}_{(n+1)} = \begin{bmatrix} E1 \\ E2 \\ E3 \end{bmatrix}_{(n)} - \begin{bmatrix} \tilde{U}_7 & \tilde{U}_{13} & \tilde{U}_{19} \\ \tilde{U}_9 & \tilde{U}_{15} & \tilde{U}_{21} \\ \tilde{U}_{11} & \tilde{U}_{17} & \tilde{U}_{23} \end{bmatrix}^{-1} \begin{bmatrix} \tilde{U}_1 - \frac{Sq}{2} \\ \tilde{U}_2 \\ \tilde{U}_5 - 1 \end{bmatrix}_{(n)}$$

To find the missing derivative present in the Newton formula the following equation will add up in the above initial value problem.

$$\tilde{U}_7' = \tilde{U}_8, \qquad \tilde{U}_7(0) = 0.$$
$$\tilde{U}_8' = \tilde{U}_9, \qquad \tilde{U}_8(0) = 0.$$
$$\tilde{U}_9' = \tilde{U}_{10}, \qquad \tilde{U}_9(0) = 1.$$

$$\tilde{U}_{10}' = \frac{B_2}{B_1}\Bigg[\left(\frac{m}{B_2}\right)\left(\tilde{U}_4\tilde{U}_6 e^{-m\tilde{U}_5}(-m\tilde{U}_{11}) + \tilde{U}_{10}\tilde{U}_6 e^{-m\tilde{U}_5} + \tilde{U}_4\tilde{U}_{12}e^{-m\tilde{U}_5}\right)$$
$$- \tilde{U}_1\tilde{U}_{10} - \tilde{U}_7\tilde{U}_4 + \tilde{U}_2\tilde{U}_9 + \tilde{U}_8\tilde{U}_3 + \frac{Sq}{2}(3\tilde{U}_9 + \eta\tilde{U}_{10}) + \frac{B_3}{B_2}M\tilde{U}_9\Bigg], \ \tilde{U}_{10}(0) = 0.$$

$$\tilde{U}_{11}' = \tilde{U}_{12}, \qquad \tilde{U}_{11}(0) = 0.$$
$$\tilde{U}_{12}' = Pr\left(\frac{B_5}{B_4}\right)\Bigg[\left(\frac{Sq}{2}\right)\eta\tilde{U}_{12} + \frac{R}{B_5}\tilde{U}_{11} - \left(\frac{Ec}{B_5}\right)(2\tilde{U}_3\tilde{U}_9 e^{-m\tilde{U}_5}$$
$$+ \tilde{U}_3^2 e^{-m\tilde{U}_5}(-m\tilde{U}_{11})) - \tilde{U}_1\tilde{U}_{12} - \tilde{U}_7\tilde{U}_6\Bigg] \qquad \tilde{U}_{12}(0) = 0.$$

$$\tilde{U}_{13}' = \tilde{U}_{14}, \qquad \tilde{U}_{13}(0) = 0.$$
$$\tilde{U}_{14}' = \tilde{U}_{15}, \qquad \tilde{U}_{14}(0) = 0.$$

$$\tilde{U}'_{15} = \tilde{U}_{16}, \qquad \tilde{U}_{15}(0) = 0.$$

$$\tilde{U}'_{16} = \frac{B_2}{B_1}\Bigg[\left(\frac{m}{B_2}\right)(\tilde{U}_4\tilde{U}_6 e^{-m\tilde{U}_5}(-m\tilde{U}_{17}) + \tilde{U}_{16}\tilde{U}_6 e^{-m\tilde{U}_5} + \tilde{U}_4\tilde{U}_{18}e^{-m\tilde{U}_5}) - \tilde{U}_1\tilde{U}_{16} - \tilde{U}_{13}\tilde{U}_4 + \tilde{U}_2\tilde{U}_{15} + \tilde{U}_{14}\tilde{U}_3 + \frac{Sq}{2}(3\tilde{U}_{15} + \eta\tilde{U}_{16} + \frac{B_3}{B_2}M\tilde{U}_{15}\Bigg], \qquad \tilde{U}_{16}(0) = 1.$$

$$\tilde{U}'_{17} = \tilde{U}_{18}, \qquad \tilde{U}_{17}(0) = 0.$$

$$\tilde{U}'_{18} = Pr\left(\frac{B_5}{B_4}\right)\Bigg[\left(\frac{Sq}{2}\right)\eta\tilde{U}_{18} + \frac{R}{B_5}\tilde{U}_{17} - \left(\frac{Ec}{B_5}\right)(2\tilde{U}_3\tilde{U}_{15}e^{-m\tilde{U}_5} + \tilde{U}_3^2 e^{-m\tilde{U}_5}(-m\tilde{U}_{17})) - \tilde{U}_1\tilde{U}_{18} - \tilde{U}_{13}\tilde{U}_6\Bigg] \qquad \tilde{U}_{18}(0) = 0.$$

$$\tilde{U}'_{19} = \tilde{U}_{20}, \qquad \tilde{U}_{19}(0) = 0.$$

$$\tilde{U}'_{20} = \tilde{U}_{21}, \qquad \tilde{U}_{20}(0) = 0,$$

$$\tilde{U}'_{21} = \tilde{U}_{22}, \qquad \tilde{U}_{21}(0) = 0.$$

$$\tilde{U}'_{22} = \frac{B_2}{B_1}\Bigg[\left(\frac{m}{B_2}\right)\left(\tilde{U}_4\tilde{U}_6 e^{-m\tilde{U}_5}(-m\tilde{U}_{23}) + \tilde{U}_{22}\tilde{U}_6 e^{-m\tilde{U}_5} + \tilde{U}_4\tilde{U}_{24}e^{-m\tilde{U}_5}\right) - \tilde{U}_1\tilde{U}_{22} - \tilde{U}_{19}\tilde{U}_4 + \tilde{U}_2\tilde{U}_{21} + \tilde{U}_{20}\tilde{U}_3 + \frac{Sq}{2}(3\tilde{U}_{21} + \eta\tilde{U}_{22}) + \frac{B_3}{B_2}M\tilde{U}_{21}\Bigg], \qquad \tilde{U}_{22}(0) = 1.$$

$$\tilde{U}'_{23} = \tilde{U}_{24}, \qquad \tilde{U}_{23}(0) = 0.$$

$$\tilde{U}'_{24} = Pr\left(\frac{B_5}{B_4}\right)\Bigg[\left(\frac{Sq}{2}\right)\eta\tilde{U}_{24} + \frac{R}{B_5}\tilde{U}_{23} - \left(\frac{Ec}{B_5}\right)(2\tilde{U}_3\tilde{U}_{21}e^{-m\tilde{U}_5} + \tilde{U}_3^2 e^{-m\tilde{U}_5}(-m\tilde{U}_{23})) - \tilde{U}_1\tilde{U}_{24} - \tilde{U}_{19}\tilde{U}_6\Bigg] \qquad \tilde{U}_{24}(0) = 1.$$

Following stopping criteria is used for Newton's method

$$\max\left\{\left|\tilde{U}_1(\eta_1, E1, E2, E3) - \frac{Sq}{2}\right|, \left|\tilde{U}_2(\eta_1, E1, E2, E3)\right|, \left|\tilde{U}_5(\eta_1, E1, E2, E3) - 1\right|\right\} < \epsilon,$$

where $\epsilon = 10^{-6}$.

3.9 Analysis of Results and its Interpretation

Shooting method is incorporated on MATLAB to obtain the numerical solutions. Furthermore, the inbuilt function bp4c of MATLAB is used to validate the numerical result. Table 3.3 and 3.4 reveals the effects of different parameter on the skin friction $Re_x^{\frac{1}{2}} C_{fx}$ and Nusselt number $Re_x^{\frac{-1}{2}} Nu_x$. Table 3.3 and 3.4 explain the effects of magnetic parameter M, Squeezing fluid parameter Sq, suction/injection parameter S, nanoparticle volume friction parameter ϕ_1 and ϕ_2 and stretching sheet λ with fixed prandtle number $Pr = 1$ and $m = 0$ on the fluid motion and $M = 0.25$ on temperature variation of hybrid nanofluid. For M=0.25, 0.5, 1 and 2, computation is carried out with nanoparticle volume fraction of $\phi_1 = 0.2$. The values show a decreasing trend of skin friction on lower plate which reduces the heat transfer rate and shows an increasing behavior on upper plate but very small change is observed on upper plate. For increasing values of Sq, the skin friction increases on lower plate and upper plate. Table 3.4 depicts that increasing values of squeezing parameter results an increase in Nusselt number both for lower and upper plate. Table 3.3 that by increasing positive values of suction parameter skin friction on lower plate decreases and on upper plate it increases. Table 3.4 depicts that by increasing the value of suction parameter the Nusselt number increases slightly on lower plate but decreases on upper plate.

Table 3.5 and 3.6, shows the skin friction and Nusselt number corresponding to different parameters for non-zero values of viscosity variable parameter m.

Table 3.5 and 3.6, disclose the results of skin friction and Nusselt number for the enhancing values of viscosity variation parameter m, Ec and thermal radiation parameter R. For the increasing values of m, the skin friction for both the upper and lower plate increases slightly and Nusselt number shows an increasing behavior for the upper plate while opposite trend is seen for the lower plate. For increasing values of R, skin friction increases both for lower and upper plate but Nusselt number decreases. The increasing values of Ec have no effect on the skin friction but Nusselt number is reduced both for upper and lower plate.

TABLE 3.3: Results of $Re_x^{\frac{1}{2}} C_{fx}$ for various values of M, Sq and S when $m = 0$.

M	Sq	S	ϕ_1	ϕ_2	λ	$Re_{x1}^{\frac{1}{2}} C_{fx1}$ (Shooting)	$Re_{x2}^{\frac{1}{2}} C_{fx2}$ (Shooting)	$Re_{x1}^{\frac{1}{2}} C_{fx1}$ (bvp4)	$Re_{x2}^{\frac{1}{2}} C_{fx2}$ (bvp4)
0.25	0.1	0.2	0.2	0	0.3	-2.1691	1.4639	-2.1691	1.4639
0.5			0.2	0		-2.1748	1.4645	-2.1748	1.4645
1			0.2	0		-2.1861	1.4658	-2.1861	1.4658
2			0.2	0		-2.2086	1.4685	-2.2086	1.4685
	-0.2		0	0.2		-3.0443	2.3502	-3.0443	2.3502
	-0.1		0	0.2		-2.7963	2.0710	-2.7493	2.0592
	0.4		0	0.2		-1.2498	0.5791	-1.2498	0.5791
		0.8	0.2	0.2		-6.0753	4.8413	-6.0753	4.8413
		1	0.2	0.2		-7.4676	5.9048	-7.4676	5.9048
		1.5	0.2	0.2		-11.1471	8.4315	-11.1471	8.4351
			0.2	0.5	0.5	-2.9263	1.8848	-2.9263	1.8848
			0.2	0.5	0.7	-3.7381	2.2781	-3.7381	2.2780

TABLE 3.4: Results of $Re_x^{\frac{1}{2}} C_{fx}$ for various values of M, Sq and S when $m = 0$.

M	Sq	S	λ	ϕ_1	ϕ_2	$Re_{x1}^{\frac{-1}{2}} Nu_{x1}$ (Shooting)	$Re_{x2}^{\frac{-1}{2}} Nu_{x2}$ (Shooting)	$Re_{x1}^{\frac{-1}{2}} Nu_{x1}$ (bvp4)	$Re_{x2}^{\frac{-1}{2}} Nu_{x2}$ (bvp4)
0.25	0.1	0.2	0.3	0.2	0	0.9281	1.2518	0.9279	1.2526
0.5				0.2	0	0.9281	1.2518	0.9278	1.2526
1				0.2	0	0.9280	1.2518	0.9278	1.2526
2				0.2	0	0.9280	1.2518	0.9277	1.2526
	-0.2			0	0.2	0.9731	1.0950	0.9722	1.0979
	-0.1			0	0.2	0.9728	1.0947	0.9720	1.0977
	0.4			0	0.2	0.9717	1.0933	0.9708	1.0962
		0.8		0.2	0.2	1.0289	1.0626	1.0210	1.0648
		1		0.2	0.2	1.0475	1.0554	1.0492	1.0573
		1.5		0.2	0.2	1.0946	1.0375	1.0980	1.0389
			0.5	0.2	0.5	0.9933	1.0226	0.9927	1.0244
			0.7	0.2	0.5	0.9939	1.0222	0.9435	1.0240

TABLE 3.5: Results of $Re_x^{\frac{1}{2}} C_{fx}$ for various values of m, Sq and Ec when $M = 0.25$ and $Pr = 1$.

m	Sq	Ec	R	ϕ_1	ϕ_2	$Re_{x1}^{\frac{1}{2}} C_{fx1}$ (Shooting)	$Re_{x2}^{\frac{1}{2}} C_{fx2}$ (Shooting)	$Re_{x1}^{\frac{1}{2}} C_{fx2}$ (bvp4)	$Re_{x2}^{\frac{1}{2}} C_{fx2}$ (bvp4)
0	0.1	0	1	0.2	0	-1.5368	0.8831	-1.5367	0.8831
0.5				0.2	0	-1.5368	0.8831	-1.5367	0.8831
1				0.2	0	-1.4625	0.9502	-1.4625	0.9503
1.5				0.2	0	-1.4439	0.9604	-1.4439	0.9604
	-0.2			0	0.2	-2.4165	1.7763	-2.4165	1.7763
	0.2			0	0.2	-1.2304	0.5870	-1.2304	0.5870
	0.4			0	0.2	-0.6276	-0.0174	-0.6276	-0.0174
		0.1		0.2	0.2	-1.5237	0.8886	-1.5237	0.8886
		0.3		0.2	0.2	-1.5237	0.8886	-1.5237	0.8886
		0.6		0.2	0.2	-1.5237	0.8886	-1.5236	0.8886
			0.3	0.5	0.2	-1.5105	0.8946	-1.5105	0.8947
			0.6	0.5	0.2	-1.5106	0.8947	-1.5105	0.8946

TABLE 3.6: Results of $Re_x^{\frac{-1}{2}} Nu_x$ for various values of m, Sq and Ec when $M = 0.25$ and $Pr = 1$.

m	Sq	Ec	R	ϕ_1	ϕ_2	$Re_{x1}^{\frac{-1}{2}} Nu_{x1}$ (Shooting)	$Re_{x2}^{\frac{-1}{2}} Nu_{x2}$ (Shooting)	$Re_{x1}^{\frac{-1}{2}} Nu_{x1}$ (bvp4)	$Re_{x2}^{\frac{-1}{2}} Nu_{x2}$ (bvp4)
0	0.1	0	1	0.2	0	0.9015	1.2627	0.9011	1.2635
0.5				0.2	0	0.9017	1.2624	0.9014	1.2632
1				0	0.2	0.9019	1.2623	0.9016	1.2631
1.5				0.2	0	0.9020	1.2621	0.9017	1.2630
	-0.2			0	0.2	0.9629	1.0993	0.9617	1.1024
	0.2			0	0.2	0.9619	1.0982	0.9607	1.101
	0.4			0	0.2	0.9614	1.0976	0.9602	1.1007
		0.1		0.2	0.2	0.9773	1.0840	0.9765	1.0868
		0.3		0.2	0.2	1.0360	1.0609	1.0373	1.0631
		0.6		0.2	0.2	0.9982	1.0185	0.9981	1.0194
			0.3	0.5	0.2	0.9982	1.0185	0.9981	1.0194
			0.6	0.5	0.2	0.9864	1.0422	0.9864	1.0423

TABLE 3.7: Comparison of skin friction coefficient of the lower and upper plate for various values of M, S, when Sq=0, λ=B_1=B_2=B_3=B_4=B_5=1.

M	S	[40]	[41]	Present	[40]	[41]	Present
0	0.5	7.411153	7.4111525	7.41116301	4.713303	4.713303	4.713309
1	0.5	7.591618	7.5916177	7.59161947	4.739017	4.739017	4.739016
4	0.5	8.110334	8.1103342	8.11031645	4.820251	4.820251	4.820230
9	0.5	8.910096	8.9100956	8.91005974	4.964870	4.964870	4.964835
4	0	4.587891	4.5878911	4.58787791	1.842447	1.842445	1.842427
4	0.3	6.665662	6.6656620	6.66564661	3.653695	3.653695	3.653675
4	0.6	8.851444	8.8514442	8.85142537	5.391248	5.391248	5.391227
4	1.0	11.948584	11.9485843	11.94856162	7.593426	7.593426	7.593415

Comparative study reveals an excellent agreement as evident in Table 3.7

3.10 Representation of Graphs

The graphical representation of the numerical results is presented in this section. The graphical representation of velocity profiles and temperature profiles give a visual inside view into the system's behavior.

3.11 Velocity Profile

In this section, we examine the impact of several physical parameters on the velocity distribution of hybrid nanofluid.

- The graphical representation of the impact of the squeezing parameter on velocity distribution is depicted in Figure 3.2. It is observed that when the values of the

squeezing fluid parameter Sq are increased from -0.2 to 0.2 with and without the viscosity variation parameter m, the velocity profile increases.

- Figure 3.3 illustrates the influence of the suction parameter on the velocity profile. Velocity field reduces for larger suction parameter. The raising values of parameter S, drop the velocity profile in either situation of m and hence reduce the flow speed. The incorporation of the lower porous plate reduces the velocity profile. This means that a greater magnitude of suction reduces the velocity distribution.

- Figure 3.4 , depicts the fact that a very minor rise appears in velocity by increasing the value of radiation parameter.

- Figures 3.5 and 3.6 show the impact of the stretching parameter on the velocity distributions. It is visible that increasing the values of λ accelerates both respective axial and radial velocities. While the radial velocity undergoes a reversal around $\eta = 0.3$, it is crucial to emphasize that both velocities are influenced by the presence of the parameter of R.

- Figure 3.7 reflects that, when ϕ_1 is increased, the velocity increases in the lower half but decreases in the upper half. Same behaviors can be seen in the velocity profile by increasing the magnetic parameter M in Figure 3.8.

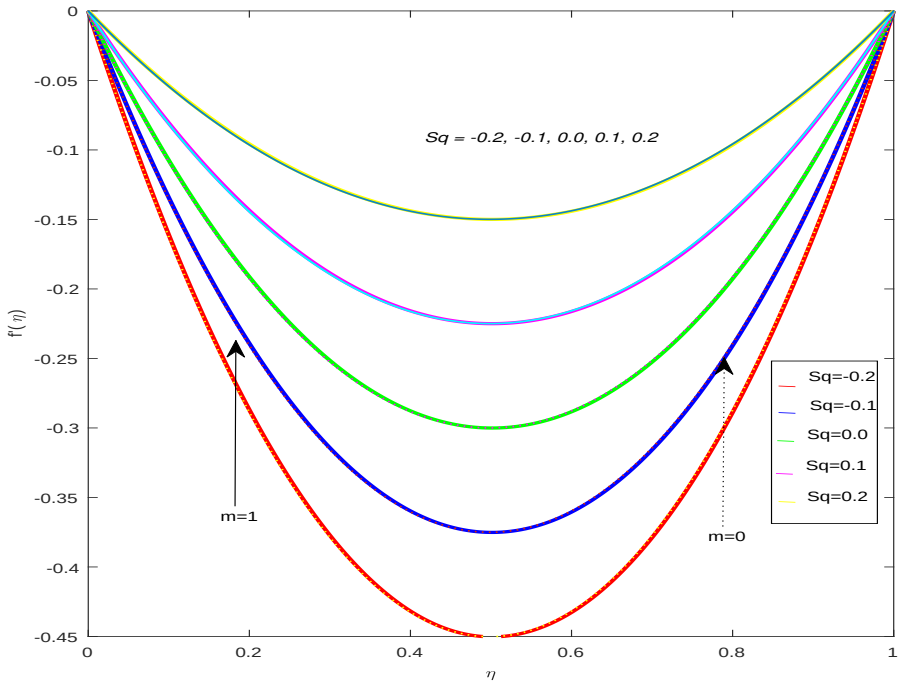

FIGURE 3.2: Influence of m and Sq on velocity profile when $Ec = R = 1$, $S = 0.2$, and $\lambda = 0$.

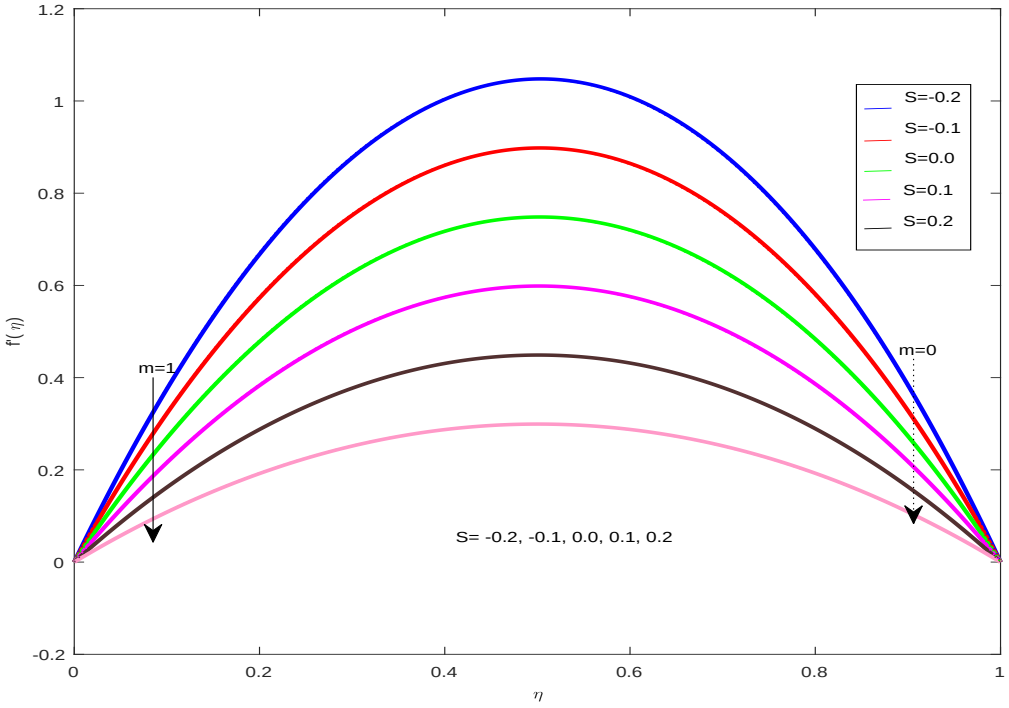

FIGURE 3.3: Influence of m and S on velocity profile when $Sq = Ec = R = 1$, $S = 0.2$, and $\lambda = 0$.

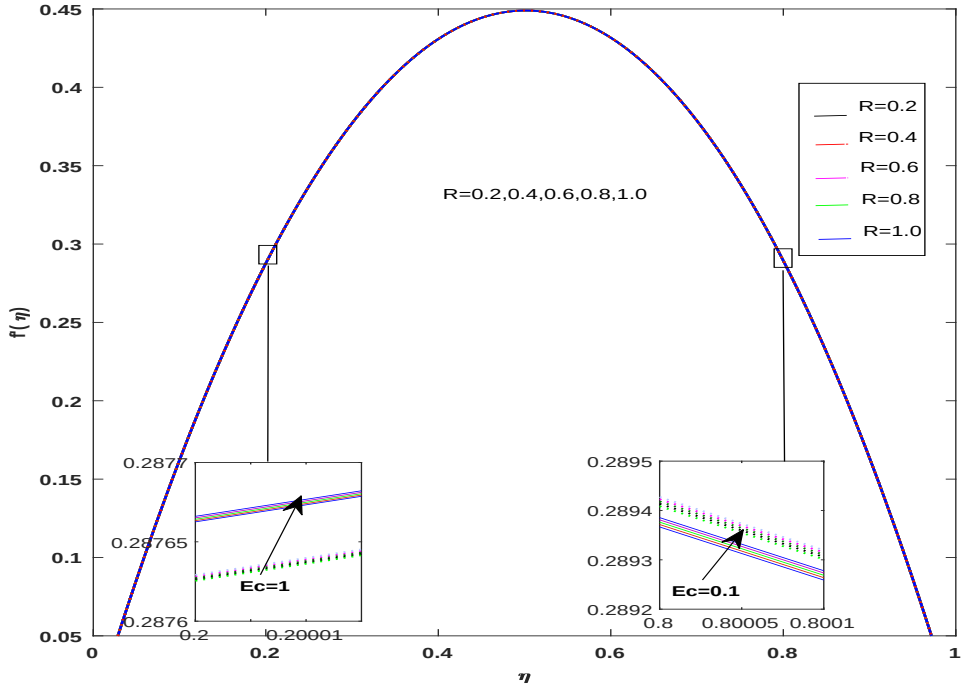

FIGURE 3.4: Influence of R and Ec on velocity profile when $Sq = m = 1$, $S = 0.2$, and $\lambda = 0$.

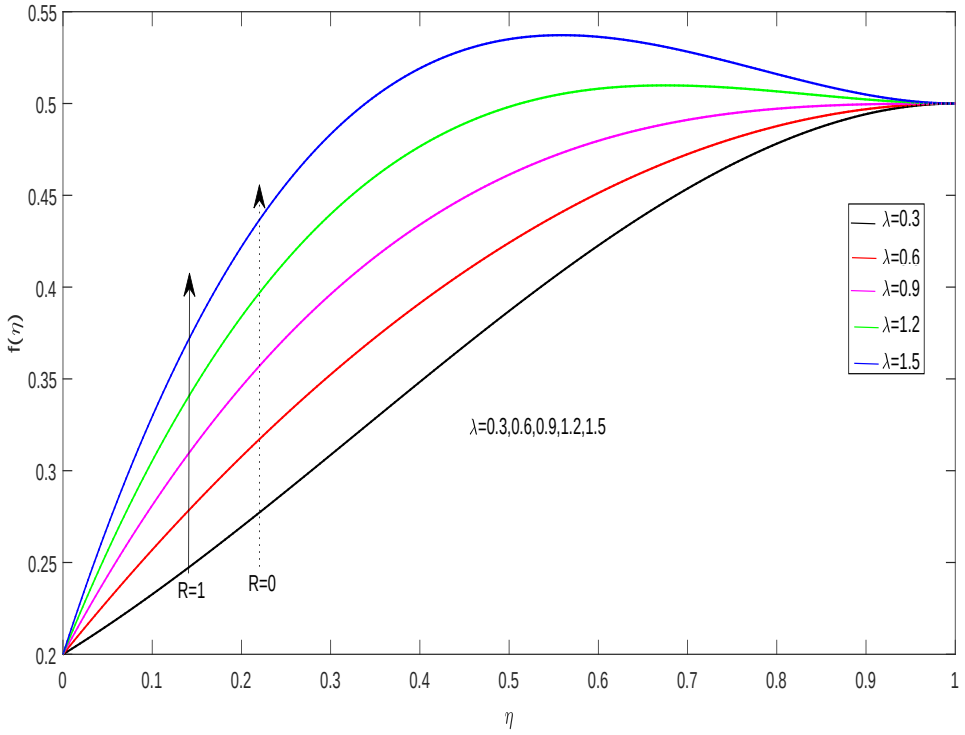

FIGURE 3.5: Influence of λ and R on radial velocity when $Sq = m = R = 1$, $S = 0.2$,

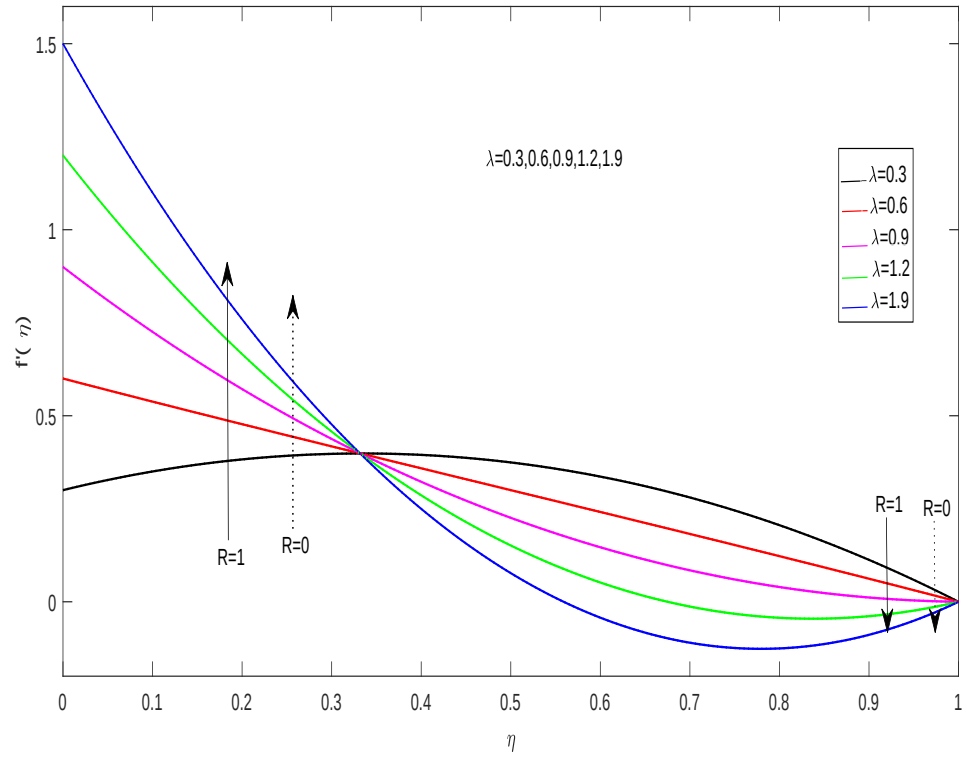

FIGURE 3.6: Influence of λ and R on axial velocity when $Sq = Ec = m = 1$, $S = 0.2$,

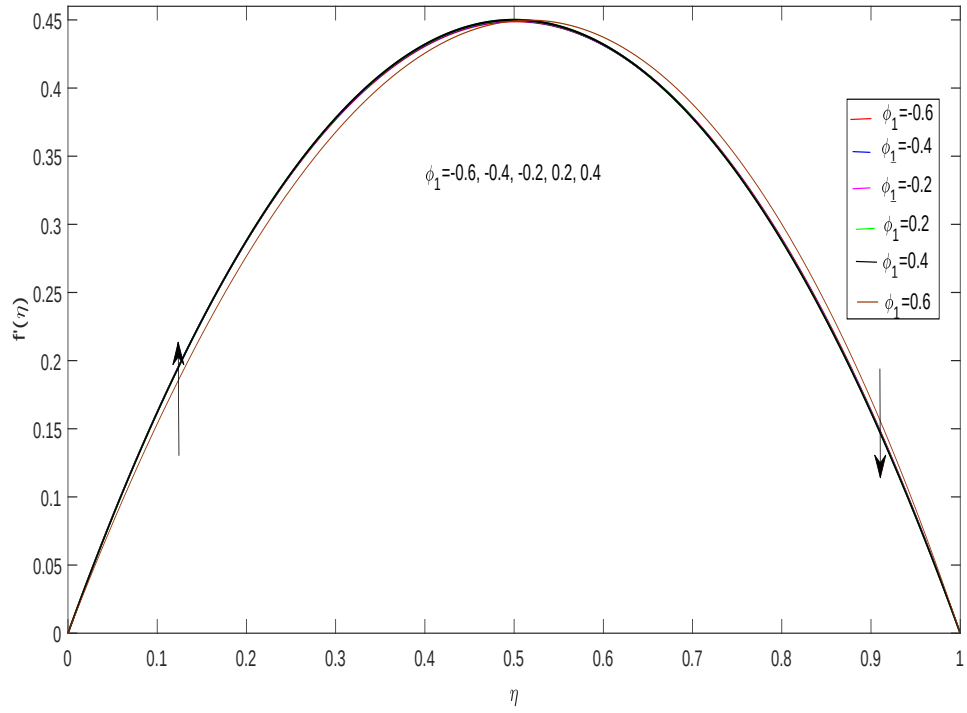

FIGURE 3.7: Influence of ϕ_1 on velocity profile when $Sq = Ec = m = 1$, $S = 0.2$,$M = 0.25$

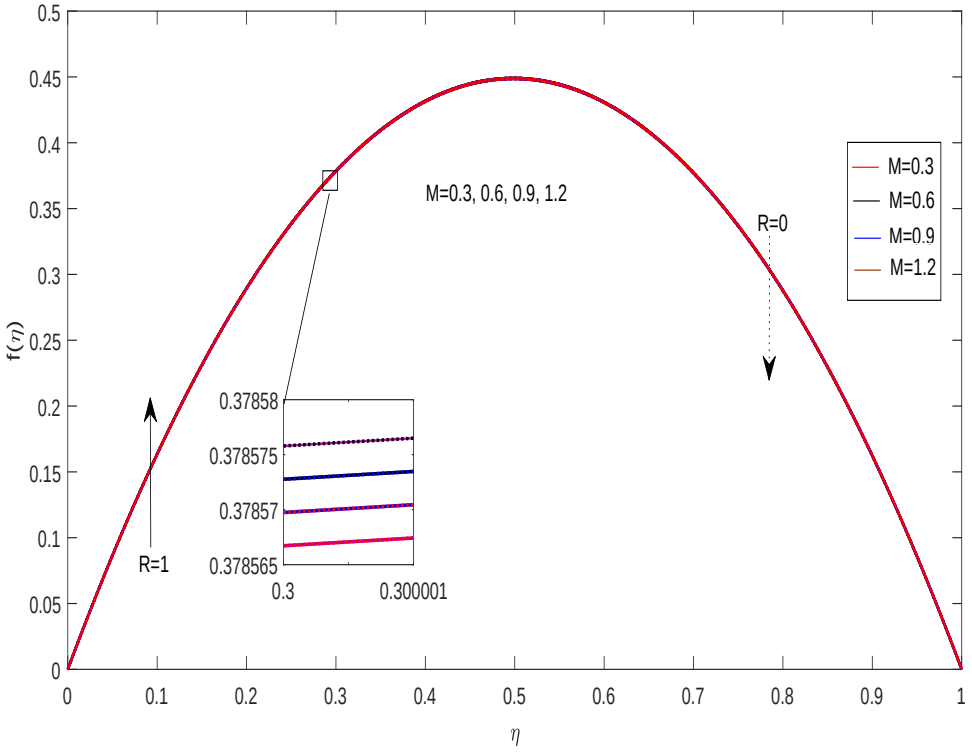

FIGURE 3.8: Influence of M and R on velocity profile when $Sq = Ec = m = 1$, $S = 0.2$, $\lambda = 0.3$

3.12 Temperature Profile

The impact of several physical parameters on the temperature distribution $\theta(\eta)$ is described below:

- Figure 3.9 describe the influence of the squeezing parameter Sq on the temperature profile $\theta(\eta)$. Elevated values of Sq yield a noticeable reduction in the temperature profile $\theta(\eta)$. This reduction is particularly perceivable when $m = 0$, indicating that an increased squeezing parameter decreases the temperature profile.

- In Figure 3.10, scrutiny of the injection/suction parameter S reveals that augmenting the value of S results in a small reduction of temperature profiles for both values of viscosity variation parameter m. This reduction is accentuated in the presence of a lower porous plate, particularly as it approaches the fixed lower plate. The practical implication is that modulating suction strength, especially in conjunction with a porous plate, can be a potent strategy for actively controlling and diminishing temperature profiles in scenarios involving water-based copper oxide and aluminum oxide hybrid nanofluids.

- Figure 3.11 demonstrates that an increase in the radiation parameter R correlates with a consistent decrease in temperature for any given Eckert number Ec. This observation underscores the potential utility of a radiating fluid material in actively reducing temperatures. In practical applications, this could inform the design of systems where radiative properties play a pivotal role in temperature management, such as certain industrial processes.

- Figure 3.12 depicts the impact of the stretching parameter λ on the temperature profile. An elevation in λ, both in the presence and absence of R, manifests as a discernible enhancement in the temperature profile. This implies that adjusting the stretching parameter can actively influence heat transfer within the fluids, stimulating their thermal behavior. In practical terms, higher values of λ could be strategically employed to enhance heat transfer efficiency in specific applications.

- Figure 3.13 sketched for the volume fraction parameter of copper oxide, ϕ_1. It is observed that an increase in fluid temperature with larger values of ϕ_1 suggests that the introduction of copper oxide nanoparticles induces a heating effect on

the fluid. This enhances the temperature distribution monotonically for $\eta = 0$ to $\eta = 1$. This finding is pivotal for applications requiring precise control over the addition of copper oxide nanoparticles to effectively manage temperature levels.

- In Figure 3.14, the influence of the magnetic parameter M on the temperature profile θ is examined in the absence and presence of thermal radiation R. In the presence of thermal radiation, an increase in M leads to an augmentation in the temperature profile, while in the absence of thermal radiation, the effect is inverse, signifying a reduction in temperature with an increase in M. This observation underscores the potential of magnetic fields to actively influence temperature profiles, with implications for magnetic-based temperature control strategies in practical applications.

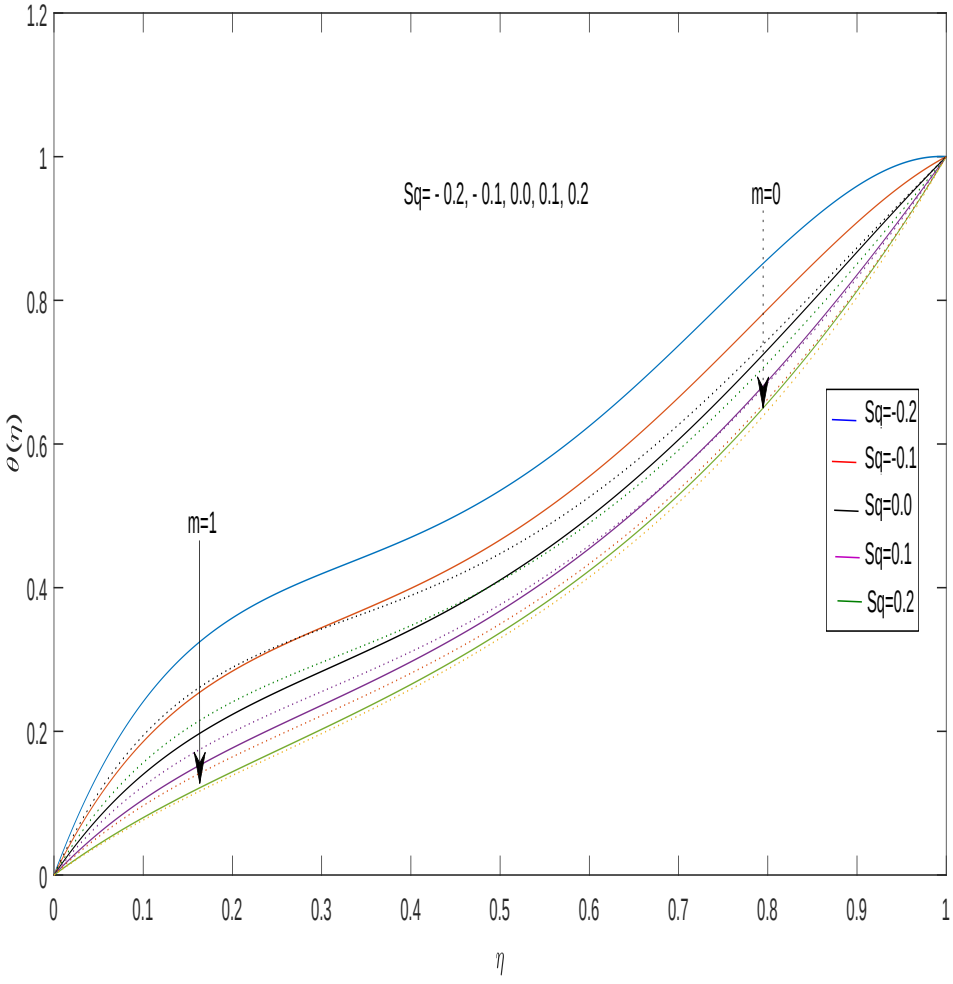

FIGURE 3.9: Influence of m and Sq on temperature when $Ec = R = 1$, $S = 0.2$, and $\lambda = 0$.

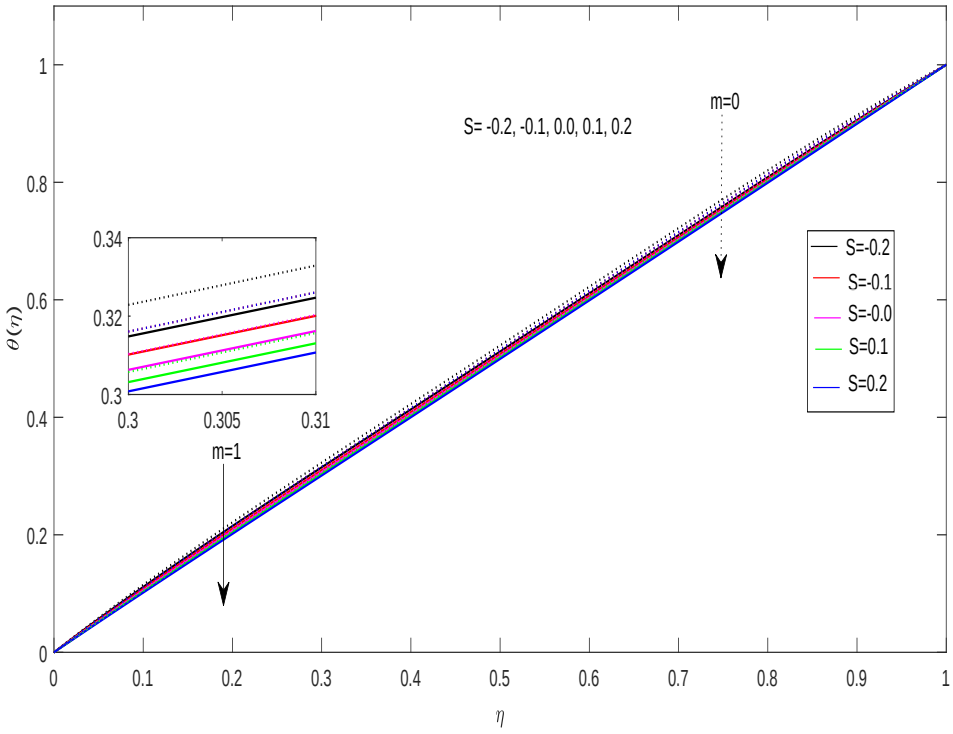

FIGURE 3.10: Influence of m and S on temperature when $Sq = Ec = R = 1$, $S = 0.2$, and $\lambda = 0$.

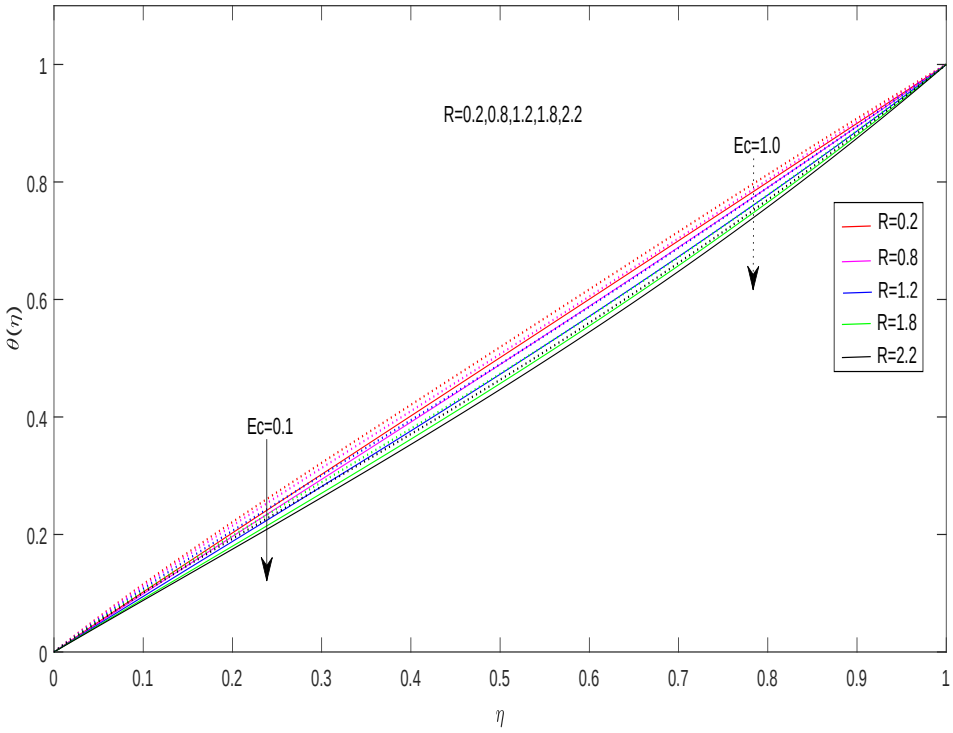

FIGURE 3.11: Influence of R and Ec on temperature when $Sq = m = 1$, $S = 0.2$, and $\lambda = 0$.

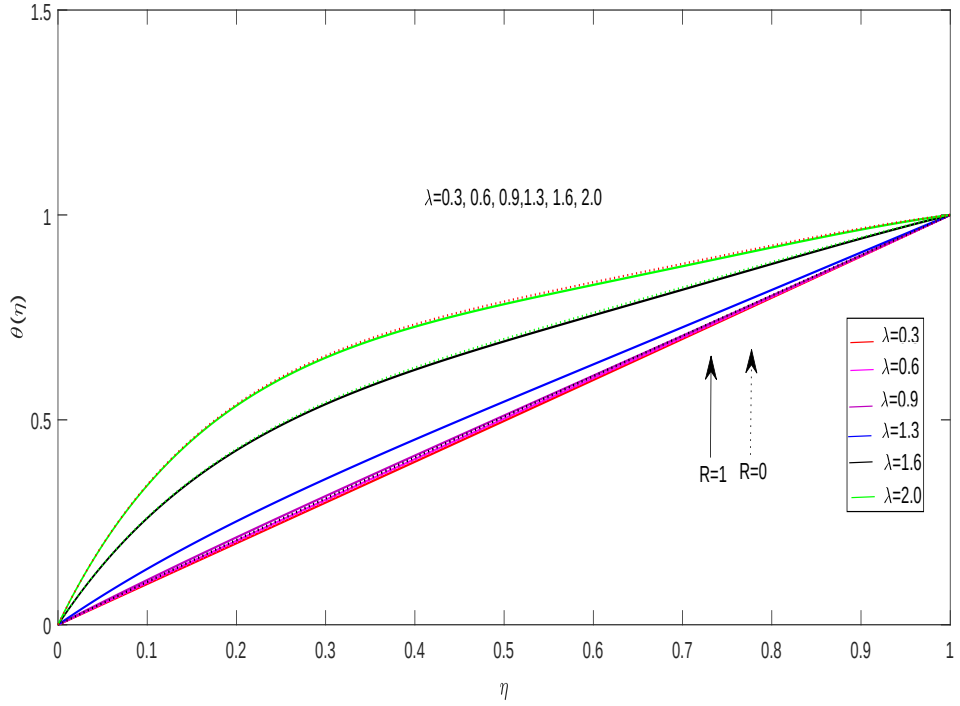

FIGURE 3.12: Influence of λ and R on temperature when $Sq = Ec = R = m = 1$, $S = 0.2$,

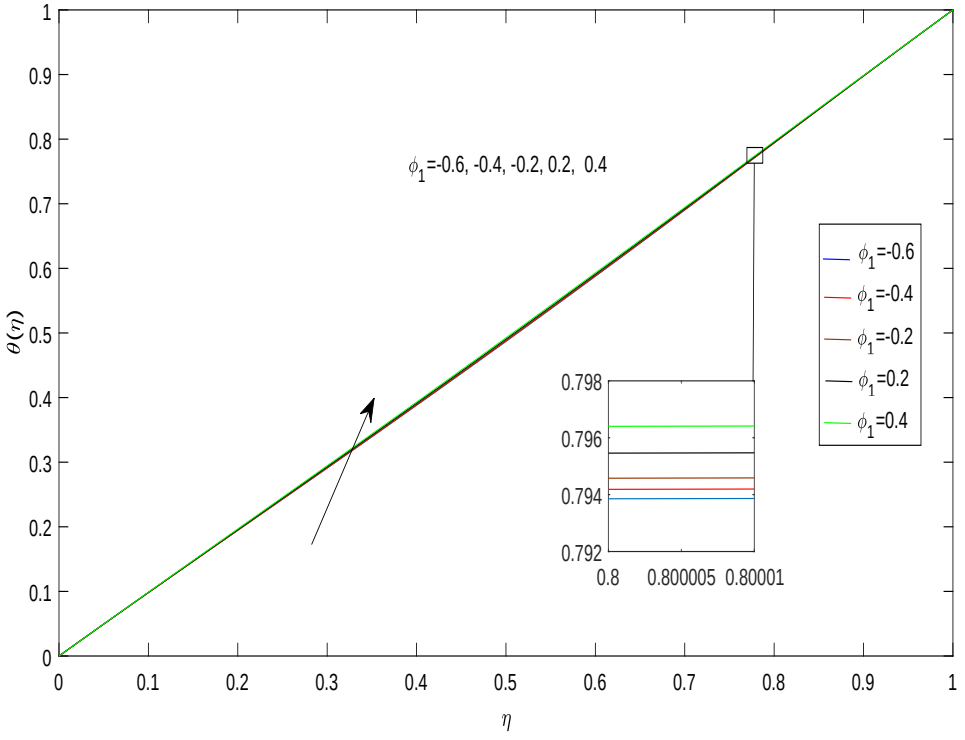

FIGURE 3.13: Influence of ϕ_1 on temperature when $S = 0.2$, $q = 1$, $\phi_2 = 0.5$, $M = 0.25$.

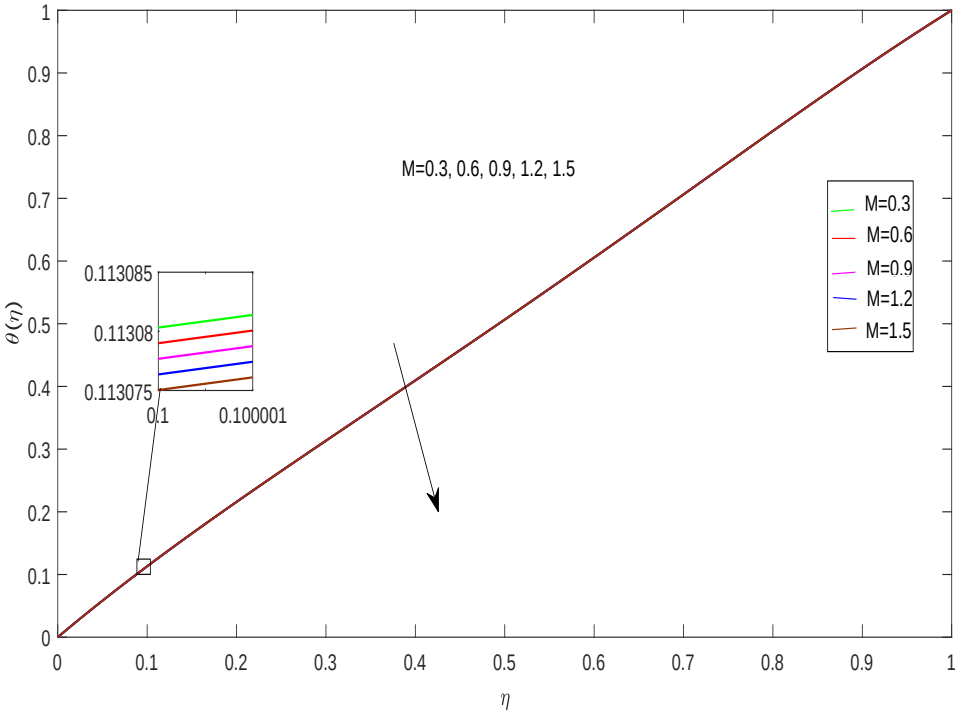

FIGURE 3.14: Variation of M and R on temperature when S=0.2, Sq=1, $\phi_1 = 0.2$, $\phi_2 = 0.5$, $Ec = 1$.

Chapter 4

Viscous Dissipattion and Thermal Radiation of Squeezing Hybrid Nanofluid Flow with Bioconvection

4.1 Introduction

This chapter establishes the extension of model discussed in **Chapter 3** [23] by incorporating the Casson fluid's effect in the momentum and energy equation. In addition, the model is further extended by considering the concentration equation. Bio convection is a natural phenomena caused by random movement of single cells or colonies of microorganisms. The model considered in Chapter 3 has been expanded by discussing microorganism motion. Taking into account of these diverse effects allows us to explore the collective impact they exert on the fluid flow over parallel plates. In this chapter, we will observe heat and mass transfer rate numerically. Using similarity transformations, the controlling nonlinear partial differential equations are converted into a system of dimensionless ODEs. The numerical solution of ODEs is found using the shooting numerical technique and results are validated by Matlab inbuilt function bvp4c.

4.2 Mathematical Modeling

Consider an incompressible, two dimensional unsteady fluid flow confined between two parallel plates, experiencing viscous dissipation and the influence of thermal radiation with motile microorganisms. The lower plate is kept fixed and is denoted by

$$v(\tilde{t}) = \frac{dh}{dt} = -\frac{\delta}{2}\sqrt{\frac{\tilde{v}_f}{\tilde{c}(1-\delta t)}},$$

while the upper plate is positioned at specified distance y given by

$$y = h(t) = \sqrt{\frac{\tilde{v}_f(1-\delta t)}{\tilde{c}}}.$$

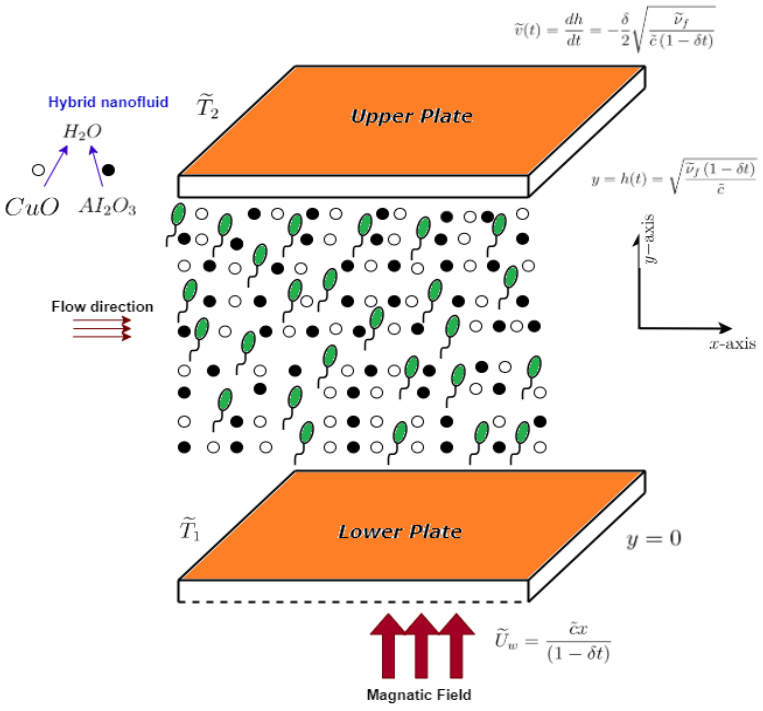

FIGURE 4.1: Geometry of the problem

Additionally, it is assumed that the lower and upper plates are maintained at fixed temperature, denoted as $\tilde{T}_1$ and $\tilde{T}_2$, respectively. Furthermore, the feasibility for suction ($\tilde{v}_o > 0$)/injection ($\tilde{v}_o < 0$) demands the incorporation of a porous lower plate characterized by a velocity

$$\tilde{v}_w = -\frac{\tilde{v}_o}{(1-\delta t)},$$

in the schematic representation, as depicted in Figure 4.1. It is noted that $\tilde{v}_o = 0$ signifies the absence of porosity. In the meantime, porous lower plate is considered to be stretchable with velocity

$$\tilde{U}_w = \frac{\tilde{c}x}{(1-\delta t)}.$$

4.3 Governing Equations

The mathematical representation of the flow model, derived from the relevant conservation principles, has been articulated by a system of partial differential equation. The governing equations for mass, momentum, energy, concentration, and motile microorganism discussed above are as follows [50].

Mass conservation equation:

$$\tilde{u}_x + \tilde{v}_y = 0. \tag{4.1}$$

Momentum equation:

$$\tilde{V}_t + \tilde{u}\tilde{V}_x + \tilde{v}\tilde{V}_y = \left(1 + \frac{1}{\tilde{\beta}}\right) \frac{1}{\tilde{\rho}_{hnf}} \left(\tilde{\mu}_{hnf}(T)\tilde{V}_y\right)_y - \frac{\tilde{\sigma}_{hnf} B(t) \tilde{V}}{\tilde{\rho}_{hnf}}. \tag{4.2}$$

Energy equation:

$$\tilde{T}_t + \tilde{u}\tilde{T}_x + \tilde{v}\tilde{T}_y = \frac{\tilde{k}_{hnf}}{(\tilde{\rho}\tilde{c}_p)_{hnf}} \tilde{T}_{yy} + \left(1 + \frac{1}{\tilde{\beta}}\right) \frac{\tilde{\mu}_{hnf}(T)}{(\tilde{\rho}\tilde{c}_p)_{hnf}} (\tilde{u}_y)^2 - \frac{1}{(\tilde{\rho}\tilde{c}_p)_{hnf}} (\tilde{q}_r)_y. \tag{4.3}$$

Concentration equation:

$$\tilde{C}_t + \tilde{u}\tilde{C}_x + \tilde{v}\tilde{C}_y = D_B \tilde{C}_{yy} + \frac{D_e k_T}{T_m} \tilde{T}_{yy} + \frac{D_T}{T_\infty} \tilde{T}_{yy} - k_o(\tilde{C} - \tilde{C}_2). \tag{4.4}$$

Motile microorganisms:

$$\tilde{\chi}_t + \tilde{u}\tilde{\chi}_x + \tilde{v}\tilde{\chi}_y + \frac{bW_c}{(\tilde{C} - \tilde{C}_2)} \left(\tilde{\chi}\tilde{C}_y\right)_y = D_m \tilde{\chi}_{yy}, \tag{4.5}$$

such that

$$\tilde{V} = \frac{\partial \tilde{v}}{\partial \tilde{x}} - \frac{\partial u}{\partial y}.$$

The associated BCs are as follows:

$$\left.\begin{aligned} &\tilde{u} = \lambda\frac{\tilde{c}x}{1-\delta t},\ \tilde{v} = -\frac{\tilde{V}_o}{1-\delta t},\ \tilde{T} = \tilde{T}_1, D_B\frac{\partial\tilde{C}}{\partial y} + \frac{D_T}{T_\infty}\frac{\partial\tilde{T}}{\partial y} = 0,\ \mathtt{N} = \mathtt{N}_1 \ at\ y = 0 \\ &\tilde{u} = 0,\ \ \tilde{v} = \frac{dh(t)}{dt},\ \tilde{T} = \tilde{T}_2,\ \tilde{C} = \tilde{C}_2,\ \mathtt{N} = \mathtt{N}_2 \ at\ y = h(t) \end{aligned}\right\}, \quad (4.6)$$

where $B(t)$ denotes the time magnetic field, D_B is the Brownian diffusion coefficient, D_T is the Thermophoresis diffusion coefficient, D_m is the molecular diffusion coefficient, b is constant, W_c is maximum swimming speed of micro-organisms in hybrid-nanofluid, k_o is the chemical reaction parameter, $\tilde{C}_2$ is ambient concentration, $\tilde{T}$ denotes the temperature of the hybrid nanofluid, and $\mathtt{N}_2$ is ambient motile microorganism. For the conversion of the mathematical model (4.1)- (4.5) into the system of ODEs, the following similarity transformation are used which are taken from Raees et al. [48, 51].

$$\tilde{u} = \frac{\tilde{c}x}{1-\delta t}\frac{\partial f}{\partial\eta},\quad \tilde{v} = -\sqrt{\frac{\tilde{c}\tilde{v}_f}{(1-\delta t)}}f(\eta),\quad \eta = y\sqrt{\frac{\tilde{c}}{\tilde{v}_f(1-\delta t)}},$$
$$\theta = \frac{\tilde{T}-\tilde{T}_2}{\tilde{T}_1-\tilde{T}_2},\quad \phi(\eta) = \frac{\tilde{C}-\tilde{C}_2}{\tilde{C}_1-\tilde{C}_2},\quad \mathtt{N}(\eta) = \frac{\tilde{\chi}-\tilde{\chi}_2}{\tilde{\chi}_1-\tilde{\chi}_2}.$$

here η indicates the similarity variable, f, θ, $\tilde{T}$, $\tilde{C}$ and $\mathtt{N}$ are dimensionless velocity, temperature, concentration and microorganism density respectively.

The identical satisfaction of (4.1) has been already discussed in chapter 3.

Momentum Equation:

Incorporating the casson fluid using the same derivatives in (4.2) and (4.3), we have the followings dimensionless momentum and energy equations respectively.

Therefore, the dimensionless form of momentum equation is

$$\begin{aligned} &(1+\frac{1}{\tilde{\beta}})\left(\frac{B_1}{B_2}\right)f^{iv} - \left(\frac{m}{B_2}\right)f'''\theta' e^{-m\theta} + f(\eta)f''' - f'f'' - \frac{Sq}{2}(3f'' + \eta f''') \\ &- \left(\frac{B_3}{B_2}\right)Mf'' = 0. \end{aligned} \quad (4.7)$$

The following dimensionless parameters are used in (4.7),

$$B_1 = \frac{\tilde{\mu}_{hnf}}{\tilde{\mu}_f},\quad B_2 = \frac{\tilde{\rho}_{hnf}}{\tilde{\rho}_f},\quad B_3 = \frac{\tilde{\sigma}_{hnf}}{\tilde{\sigma}_f},\quad M = \frac{\tilde{\sigma}_f(\tilde{\rho}\tilde{c}_p)_f}{\tilde{k}_f},\quad Sq = \frac{\delta}{\tilde{c}},\quad m = a(\tilde{T}_1 - \tilde{T}_2).$$

Now, the dimensionless form of energy equation is

$$\Rightarrow \left(\frac{B_4}{P_r B_5}\right)\theta'' + \left(\frac{E_c}{B_5}\right)\left(1+\frac{1}{\tilde{\beta}}\right)e^{-m\theta}f''^2 + f\theta' - \frac{S_q}{2}\eta\theta - \frac{R}{B_5}\theta = 0. \quad (4.8)$$

Following parameters are used in the above equations (4.8):

$$B_4 = \frac{\tilde{k}_{hnf}}{\tilde{k}_f}, \quad B_5 = \frac{(\tilde{\rho}\tilde{c}_p)_{hnf}}{(\tilde{\rho}\tilde{c}_p)_f}, \quad P_r = \frac{v_f(\tilde{\rho}\tilde{c}_p)_f}{\tilde{k}_f}, \quad R = \frac{4\tilde{\sigma}^{*2}(1-\delta t)}{\tilde{c}(\tilde{\rho}\tilde{c}_p)_f},$$
$$E_c = \frac{\tilde{U}_w^2}{(\tilde{c}_p)_f(\tilde{T}_1 - \tilde{T}_2)}, \quad S_q = \frac{\delta}{\tilde{c}}, \quad m = a(\tilde{T}_1 - \tilde{T}_2).$$

Concentration Equation:

Now, for the transformation of concentration equation (4.4), the following derivatives are required.

$$\begin{aligned}
\phi(\eta) =& \frac{\tilde{C} - \tilde{C}_2}{\tilde{C}_1 - \tilde{C}_2}, \\
\tilde{C} =& \tilde{C}_2 + (\tilde{C}_1 - \tilde{C}_2)\phi(\eta), \\
\frac{\partial \tilde{C}}{\partial x} =& 0, \\
\frac{\partial \tilde{C}}{\partial y} =& \frac{\partial}{\partial y}(\tilde{C}_1 - \tilde{C}_2)\phi(\eta), \\
\tilde{C}_y =& (\tilde{C}_1 - \tilde{C}_2)\phi' \frac{\partial \eta}{\partial y}, \\
=& (\tilde{C}_1 - \tilde{C}_2)\phi' \sqrt{\frac{\tilde{c}}{\tilde{v}_f}(1-\delta t)}, \\
\tilde{C}_{yy} =& (\tilde{C}_1 - \tilde{C}_2)\phi'' \left(\frac{\tilde{c}}{\tilde{v}_f(1-\delta t)}\right).
\end{aligned} \tag{4.9}$$

(4.10)

Now, substituting all of the above derivatives in (4.4), we get

$$\begin{aligned}
&\frac{1}{2}\frac{(\tilde{C}_1 - \tilde{C}_2)\delta\eta}{(1-\delta t)}\phi' - \frac{\tilde{c}(\tilde{C}_1 - \tilde{C}_2}{(1-\delta t)} f\phi' = D_B \frac{(\tilde{C}_1\tilde{C}_2)\tilde{c}}{\tilde{v}_f(1-\delta t)}\phi'' + \frac{D_e k_T \tilde{c}(\tilde{T}_2)\tilde{T}_o}{T_m \tilde{v}_f(1-\delta t)}\theta'' + \\
&\qquad \frac{D_T(\tilde{T}_2 - \tilde{T}_o)\tilde{c}}{T_\infty \tilde{v}_f(1-\delta t)}\theta'' - k_o(\tilde{C} - \tilde{C}_2) \\
\Rightarrow \quad & D_B \frac{(\tilde{C}_1\tilde{C}_2)\tilde{c}}{\tilde{v}_f(1-\delta t)}\phi'' + \frac{D_e k_T \tilde{c}(\tilde{T}_2)\tilde{T}_o}{T_m \tilde{v}_f(1-\delta t)}\theta'' + \frac{D_T(\tilde{T}_2 - \tilde{T}_o)\tilde{c}}{T_{infty}\tilde{v}_f(1-\delta t)}\theta'' - \\
& k_o(\tilde{C}_1 - \tilde{C}_2)\phi + \frac{\tilde{c}(\tilde{C}_1 - \tilde{C}_2}{(1-\delta t)} f\phi' - \frac{1}{2}\frac{(\tilde{C}_1 - \tilde{C}_2)\delta\eta}{(1-\delta t)}\phi' = 0,
\end{aligned}$$

$$\begin{aligned}
\Rightarrow \quad & \phi'' + \frac{D_e k_T(\tilde{T}_2 - \tilde{T}_o)\tilde{v}_f}{D_B T_m(\tilde{C}_1 - \tilde{C}_2)\tilde{v}_f}\theta'' + \frac{D_T(\tilde{T}_2 - \tilde{T}_o)\tilde{v}_f}{T_\infty D_B(\tilde{C}_1 - \tilde{C}_2)\tilde{v}_f}\theta'' - \frac{k_o \tilde{v}_f(1-\delta t)}{\tilde{c}D_B}\phi + \\
& \qquad \frac{\tilde{v}_f}{D_B} f\phi' - \frac{\delta\eta\tilde{v}_f}{D_B}\phi' = 0, \\
& \phi'' + ScSr\theta'' + \frac{Nt}{Nb}\theta'' - Sck\phi + Sc\left(f - \frac{\delta\eta}{2}\phi'\right) = 0.
\end{aligned}$$

As a result, the dimensionless form of the concentration equation has the following form:

$$\phi'' + ScSr\theta'' + \frac{Nt}{Nb}\theta'' - Sck\phi + Sc\left(f - \frac{\delta\eta}{2}\phi'\right) = 0. \tag{4.11}$$

The following dimensionless variables are incorporated in equation (4.11):

$$Sc = \frac{\tilde{v}_f}{D_B},\ Sr = \frac{D_e k_T(\tilde{T}_2 - \tilde{T}_o)}{T_m(\tilde{C}_1 - \tilde{C}_2)\tilde{v}_f},\ Nt = \frac{D_T(\tilde{T}_2 - \tilde{T}_o)}{T_\infty \tilde{v}_f},\ Nb = \frac{D_B(\tilde{C}_1 - \tilde{C}_2)}{\tilde{v}_f}$$

Motile Microorganism Equation

For the conversion of equation (4.5), the following derivatives are required.

$$\begin{aligned}
\mathtt{N}(\eta) =& \frac{\tilde{\chi} - \tilde{\chi}_2}{\tilde{\chi}_1 - \tilde{\chi}_2},\\
\tilde{\chi} =& \mathtt{N}(\tilde{\chi}_1 - \tilde{\chi}_2) + \tilde{\chi}_2,\\
\frac{\partial\tilde{\chi}}{\partial t} =& (\tilde{\chi}_1 - \tilde{\chi}_2)\mathtt{N}'\frac{\partial\eta}{\partial t},\\
\tilde{\chi}_t =& \mathtt{N}'(\tilde{\chi}_1 - \tilde{\chi}_2)\frac{\eta\delta}{2(1-\delta t)},
\end{aligned} \tag{4.12}$$

$$\begin{aligned}
\tilde{\chi}_x =& \frac{\partial}{\partial x}\left(\mathtt{N}(\tilde{\chi}_1 - \tilde{\chi}_2) + \tilde{\chi}_2\right),\\
=& \mathtt{N}'(\tilde{\chi}_1 - \tilde{\chi}_2)\frac{\partial\eta}{\partial x},\\
\tilde{\chi}_x =& 0,
\end{aligned} \tag{4.13}$$

$$\begin{aligned}
\tilde{\chi}_y =& \frac{\partial}{\partial y}\left(\mathtt{N}(\tilde{\chi}_1 - \tilde{\chi}_2) + \tilde{\chi}_2\right),\\
=& (\tilde{\chi}_1 - \tilde{\chi}_2)\mathtt{N}'\frac{\partial\eta}{\partial y},\\
\tilde{\chi}_y =& (\tilde{\chi}_1 - \tilde{\chi}_2)\mathtt{N}'\sqrt{\frac{\tilde{c}}{\tilde{v}_f(1-\delta t)}},
\end{aligned} \tag{4.14}$$

$$\tilde{\chi}_{yy} = (\chi_1 - \chi_2)\mathtt{N}''\sqrt{\frac{\tilde{c}}{\tilde{v}_f(1-\delta t)}}\frac{\partial\eta}{\partial y},$$

$$\tilde{\chi}_{yy} = (\chi_1 - \chi_2)\left(\frac{\tilde{c}}{\tilde{v}_f(1-\delta t)}\right)\mathtt{N}'', \tag{4.15}$$

$$\begin{aligned}
\tilde{\chi}\tilde{C}_y =& \left[\mathtt{N}\left(\tilde{\chi}_1 - \tilde{\chi}_2 + \tilde{\chi}_2\right)\right]\left((\tilde{C}_1 - \tilde{C}_2)\sqrt{\frac{\tilde{c}}{\tilde{v}_f(1-\delta t)}}\phi'\right),\\
(\tilde{\chi}_y)_y =& (\tilde{\chi}_1 - \tilde{\chi}_2)(\tilde{C}_1 - \tilde{C}_2)\sqrt{\frac{\tilde{c}}{\tilde{v}_f(1-\delta t)}}\mathtt{N}\phi' + \tilde{\chi}_2(\tilde{C}_1 - \tilde{C}_2)\phi'\sqrt{\frac{\tilde{c}}{\tilde{v}_f(1-\delta t)}},
\end{aligned}$$

$$(\tilde{\chi}_y)_y = (\tilde{\chi}_1 - \tilde{\chi}_2)(\tilde{C}_1 - \tilde{C}_2)\frac{\tilde{c}}{\tilde{v}_f(1-\delta t)}\left[\mathtt{N}'\phi' + \mathtt{N}\phi''\right]. \tag{4.16}$$

Substituting ((4.12)-(4.16)) in governing equation for motile equation is

$$\begin{aligned}
&\Rightarrow \ \mathtt{N}^{''}\frac{D_m(\tilde{\chi}_1-\tilde{\chi}_2)\tilde{c}}{\tilde{v}_f(1-\delta t)} = \mathtt{N}'\frac{(\tilde{\chi}_1-\tilde{\chi}_2)\delta\eta}{2(1-\delta t)} - \frac{\tilde{c}(\tilde{\chi}_1-\tilde{\chi}_2)}{(1-\delta t)}f\mathtt{N}' \\
&\quad + \frac{bW_c(\tilde{\chi}_1-\tilde{\chi}_2)\tilde{c}}{\tilde{v}_f(1-\delta t)}[\mathtt{N}'\phi' + \mathtt{N}\phi^{''}] + \frac{bW_c\tilde{c}\tilde{\chi}_2}{\tilde{v}_f(1-\delta t)}\phi^{''}, \\
&\Rightarrow \ \mathtt{N}^{''} = \frac{1}{2}\mathtt{N}'\eta\left(\frac{\tilde{v}_f}{D_m}\right)\left(\frac{\delta}{\tilde{c}}\right) - \frac{\tilde{v}_f}{D_m}f\mathtt{N}' + \frac{bW_c}{D_m}[\mathtt{N}'\phi' + \mathtt{N}\phi^{''}] + \frac{bW_c\tilde{\chi}_2}{D_m(\tilde{\chi}_1-\tilde{\chi}_2)}\phi^{''}, \\
&\Rightarrow \ \mathtt{N}^{''} = \frac{1}{2}\mathtt{N}'SqL_b\eta - L_bf\mathtt{N}' + Pe\left(\phi'\mathtt{N}' + (\omega+\mathtt{N})\phi^{''}\right), \\
&\Rightarrow \ \mathtt{N}^{''} - L_b\left(\frac{1}{2}Sq\eta\mathtt{N}'\right) + L_bf\mathtt{N}' - Pe\left(\phi'\mathtt{N}' + (\omega+\mathtt{N})\phi^{''}\right) = 0.
\end{aligned}$$

Therefore, the dimensionless form of the motile is

$$\mathtt{N}^{''} - L_b\left(\frac{1}{2}Sq\eta\mathtt{N}'\right) + L_bf\mathtt{N}' - Pe\left(\phi'\mathtt{N}' + (\omega+\mathtt{N})\phi^{''}\right) = 0. \tag{4.17}$$

The dimensionless parameters used in (4.17) are:

$$Pe = \frac{bW_c}{D_m}, \quad \omega = \frac{\tilde{\chi}_2}{\tilde{\chi}_1-\tilde{\chi}_2}, \quad L_b = \frac{\tilde{v}_f}{D_m}, \quad Sq = \frac{\delta}{\tilde{c}}$$

4.4 Dimensionless form of the BCs

The following B.C's are converted into the dimensionless form by the following procedure. $y = 0 \quad \Rightarrow \eta = 0$

$$\begin{aligned}
&\bullet \ \tilde{u} = \lambda\frac{\tilde{c}x}{(1-\delta t)}, \\
&\Rightarrow \ \frac{\tilde{c}x}{(1-\delta t)}f'(\eta) = \lambda\frac{\tilde{c}x}{(1-\delta t)}, \\
&\Rightarrow \ \frac{\tilde{c}x}{(1-\delta t)}f'(\eta) = \lambda\frac{\tilde{c}x}{(1-\delta t)}, \\
&\Rightarrow f'(0) = \lambda, \\
&\bullet \ \tilde{v} = -\frac{\tilde{V}_o}{(1-\delta t)}, \\
&\Rightarrow -\sqrt{\frac{\tilde{c}v_f}{(1-\delta t)}}f(\eta) = -\frac{\tilde{V}_o}{(1-\delta t)}, \\
&\Rightarrow \ f(\eta) = \frac{\tilde{V}_o}{(1-\delta t)}\left(\frac{1-\delta t}{\tilde{c}v_f}\right)^{\frac{1}{2}},
\end{aligned}$$

$$\Rightarrow \quad f(\eta) = \frac{\tilde{V}_o}{\sqrt{v_f(1-\delta t)\tilde{c} \times \frac{\tilde{c}}{\tilde{c}}}},$$

$$\Rightarrow \quad f(0) = \frac{\tilde{V}_o}{\sqrt{\frac{v_f(1-\delta t)\tilde{c}^2}{\tilde{c}}}},$$

$$\Rightarrow \quad f(0) = \frac{\tilde{V}_o}{\tilde{c}h},$$

$$\Rightarrow \quad f(0) = S,$$

$$\theta(\eta) = \frac{\tilde{T} - \tilde{T}_o}{\tilde{T}_2 - \tilde{T}_o},$$

$$\tilde{T} = \theta(\eta)(\tilde{T}_2 - \tilde{T}_o) + \tilde{T}_o,$$

- $\tilde{T} = \tilde{T}_1,$

$$\Rightarrow \quad \theta(\eta)(\tilde{T}_2 - \tilde{T}_o) + \tilde{T}_o = \tilde{T}_1,$$

$$\Rightarrow \quad \theta(\eta)(\tilde{T}_2 - \tilde{T}_o) = \tilde{T}_1 - \tilde{T}_o,$$

$$\Rightarrow \quad \theta(0) = \frac{\tilde{T}_1 - \tilde{T}_o}{\tilde{T}_2 - \tilde{T}_o},$$

$$\Rightarrow \quad \theta(0) = \gamma,$$

- $D_B \frac{\partial \tilde{C}}{\partial y} + \frac{D_T}{T_\infty}\frac{\partial \tilde{T}}{\partial y} = 0,$

$$\Rightarrow \quad D_B(\tilde{C}_1 - \tilde{C}_2)\sqrt{\frac{\tilde{c}}{\tilde{v}_f(1-\delta t)}}\phi' + \frac{D_T}{T_\infty}(\tilde{T}_1 - \tilde{T}_2)\sqrt{\frac{\tilde{c}}{\tilde{v}_f(1-\delta t)}}\theta' = 0,$$

$$\Rightarrow \quad D_B(\tilde{C}_1 - \tilde{C}_2)\phi' + \frac{D_T}{T_\infty}(\tilde{T}_1 - \tilde{T}_2)\theta' = 0,$$

$$\Rightarrow \quad Nb\phi' + Nt\theta' = 0,$$

$$\Rightarrow \quad \phi'(0) = -\frac{Nt}{Nb}\theta',$$

- $\tilde{\chi} = \tilde{\chi}_1,$

$$\Rightarrow \quad \mathtt{N}(\eta) = \frac{\tilde{\chi} - \tilde{\chi}_2}{\tilde{\chi}_1 - \tilde{\chi}_2},$$

$$\Rightarrow \mathtt{N}(\eta) = \frac{\tilde{\chi}_1 - \tilde{\chi}_2}{\tilde{\chi}_1 - \tilde{\chi}_2},$$

$$\Rightarrow \quad \mathtt{N}(\eta) = 1,$$

$$\Rightarrow \quad \mathtt{N}(0) = 1.$$

Choose $y = h(t) \quad \Rightarrow \eta = 1$

- $\tilde{u} = 0,$

$$\Rightarrow \frac{\tilde{c}x}{(1-\delta t)} f^{'}(\eta) = 0$$

$$\Rightarrow f^{'}(1) = 0,$$

- $\tilde{V} = \frac{dh(t)}{dt},$

$$\Rightarrow -\sqrt{\frac{\tilde{c}\tilde{v}_f}{(1-\delta t)}} f(\eta) = -\frac{\delta}{2}\sqrt{\frac{\tilde{v}_f}{\tilde{c}(1-\delta t)}},$$

$$\Rightarrow f(\eta) = \frac{\delta}{2}\frac{\sqrt{\frac{\tilde{v}_f}{\tilde{c}(1-\delta t)}}}{\sqrt{\frac{\tilde{c}\tilde{v}_f}{(1-\delta t)}}},$$

$$\Rightarrow f(\eta) = \frac{\delta}{2}\sqrt{\frac{\tilde{v}_f}{\tilde{c}(1-\delta t)}} \times \sqrt{\frac{(1-\delta t)}{\tilde{c}\tilde{v}_f}},$$

$$\Rightarrow f(1) = \frac{\delta}{2\tilde{c}},$$

$$\Rightarrow f(1) = \frac{S_q}{2}$$

- $\tilde{T} = \tilde{T}_2,$

$$\Rightarrow \theta(\eta)(\tilde{T}_2 - \tilde{T}_o) + \tilde{T}_o = \tilde{T}_2,$$

$$\Rightarrow \theta(\eta)(\tilde{T}_2 - \tilde{T}_o) = \tilde{T}_2 - \tilde{T}_o,$$

$$\Rightarrow \theta(0) = \frac{\tilde{T}_2 - \tilde{T}_o}{\tilde{T}_2 - \tilde{T}_o},$$

$$\Rightarrow \theta(1) = 1,$$

- $\tilde{C} = \tilde{C}_2,$

$$\Rightarrow \phi(\eta) = \frac{(\tilde{C} - \tilde{C}_2)}{\tilde{C}_1 - \tilde{C}_2},$$

$$\Rightarrow \phi(\eta) = \frac{(\tilde{C}_2 - \tilde{C}_2)}{\tilde{C}_1 - \tilde{C}_2},$$

$$\Rightarrow \phi(\eta) = 0,$$

$$\Rightarrow \phi(1) = 0,$$

- $\mathtt{N} = \mathtt{N}_2,$

$$\Rightarrow \mathtt{N}(\eta) = \frac{(\tilde{\chi} - \tilde{\chi}_2)}{\tilde{\chi}_1 - \tilde{\chi}_2},$$

$$\Rightarrow \mathtt{N}(\eta) = 0,$$

$$\Rightarrow \mathtt{N}(1) = 0.$$

The final form of dimensionless governing model is

$$\left.\begin{aligned}
&(1+\frac{1}{\bar{\beta}})\left(\frac{B_1}{B_2}\right)f^{iv} - \left(\frac{m}{B_2}\right)f'''\theta' e^{-m\theta} + ff''' - f'f'' \\
&\qquad - \frac{Sq}{2}(3f'' + \eta f''') - \left(\frac{B_3}{B_2}\right)Mf'' = 0, \\
&\left(\frac{B_4}{P_r B_5}\right)\theta'' + \left(\frac{E_c}{B_5}\right)e^{-m\theta}f''^2 + f\theta' - \frac{S_q}{2}\eta\theta - \frac{R}{B_5}\theta = 0, \\
&\phi'' + ScSr\theta'' + \frac{Nt}{Nb}\theta'' - Sck\phi + Sc\left(f - \frac{\delta\eta}{2}\phi'\right) = 0, \\
&\mathtt{N}^{''} - L_b\left(\frac{1}{2}Sq\eta\mathtt{N}'\right) + L_b f\mathtt{N}' - Pe\left(\phi'\mathtt{N}' + (\omega+\mathtt{N})\phi^{''}\right) = 0.
\end{aligned}\right\} \tag{4.18}$$

The dimensionless form of associated BCs (4.6) are in the form:

$$\left.\begin{aligned}
&f = S, \quad f' = \lambda, \ \theta = \gamma, \ Nt\theta' + Nb\phi^{'} = 0, \quad \mathtt{N} = 1, \ at \ \eta = 0, \\
&f = \frac{Sq}{2}, \quad f' = 0, \quad \theta = 1, \quad \phi = 0, \quad \mathtt{N} = 0, \quad at \quad \eta = 1.
\end{aligned}\right\} \tag{4.19}$$

4.5 Important Physical Parameters

Local Sherwood number is defined as:

$$Sh_x = \frac{xq_m}{D_B(\tilde{C}_1 - \tilde{C}_2)}. \tag{4.20}$$

The dimensionless form of the Sh_x is obtained through following steps:

$$\begin{aligned}
q_m &= -D_B\left(\frac{\partial\tilde{C}}{\partial y}\right)_{y=o}. \\
Sh_x &= -\frac{xD_B(\tilde{C}_1 - \tilde{C}_2)\sqrt{\frac{\tilde{c}}{\tilde{v}_f(1-\delta t)}}\phi^{'}(0)}{D_B(\tilde{C}_1 - \tilde{C}_2)} \\
&= -x\phi'(0)\sqrt{\frac{\tilde{c}}{\tilde{v}_f(1-\delta t)}} \\
&= -x\phi^{'}(0)\sqrt{\frac{\tilde{c}x}{\tilde{v}_f x(1-\delta t)}} \\
&= -\sqrt{\frac{\tilde{U}_w x}{\tilde{v}_f x}}\phi^{'}(0)
\end{aligned}$$

$$
\begin{aligned}
&= -\sqrt{\frac{\tilde{U}_w x}{\tilde{v}_f}}\phi^{'}(0) \\
&= -Re_x^{\frac{1}{2}}\phi^{'}(0) \\
\Rightarrow \quad Sh_x Re_x^{-\frac{1}{2}} &= -\phi'(0).
\end{aligned} \tag{4.21}
$$

Here, $Re_x{=}\frac{\tilde{U}_w x}{\tilde{v}_f}$ denotes the Reynolds number. Motile density number $\mathtt{N}n_x$ is defined as:

$$
\mathtt{N}n_x = \frac{x q_n}{D_m(\tilde{\chi}_1 - \tilde{\chi}_2)}. \tag{4.22}
$$

The dimensionless form of the $\mathtt{N}_x$ is obtained through following steps:

$$
\begin{aligned}
q_n &= -D_m\left(\frac{\partial \tilde{\chi}}{\partial y}\right)_{y=o}, \\
\mathtt{N}n_x &= -\frac{x D_m(\tilde{\chi}_1 - \tilde{\chi}_2)\sqrt{\frac{\tilde{c}}{\tilde{v}_f(1-\delta t)}}\mathtt{N}^{'}(0)}{D_m(\tilde{\chi}_1 - \tilde{\chi}_2)}, \\
&= -x\mathtt{N}'(0)\sqrt{\frac{\tilde{c}}{\tilde{v}_f(1-\delta t)}}, \\
&= -x\mathtt{N}^{'}(0)\sqrt{\frac{\tilde{c}x}{\tilde{v}_f x(1-\delta t)}} \\
&= -\sqrt{\frac{\tilde{U}_w x}{\tilde{v}_f x}}\mathtt{N}^{'}(0) \\
&= -\sqrt{\frac{\tilde{U}_w x}{\tilde{v}_f}}\mathtt{N}^{'}(0) \\
&= -Re_x^{\frac{1}{2}}\mathtt{N}^{'}(0) \\
\Rightarrow \quad \mathtt{N}_x Re_x^{-\frac{1}{2}} &= -\mathtt{N}^{'}(0).
\end{aligned}
$$

Here, $Re_x{=}\frac{\tilde{U}_w x}{\tilde{v}_f}$ denotes the Reynolds number.

4.6 Numerical Method for Solution

The shooting numerical technique is employed for solving systems of ordinary differential equations, subjected to specified boundary conditions. For this purpose, the following notations are utilized. The computational procedure of the shooting method, is elaborated and in Figure 4.2. To integrate the shooting method, the boundary value problem

is transformed into an initial value problem which is solved by RK-4 method. Missing initial conditions are refined by using Newton's numerical techniques.

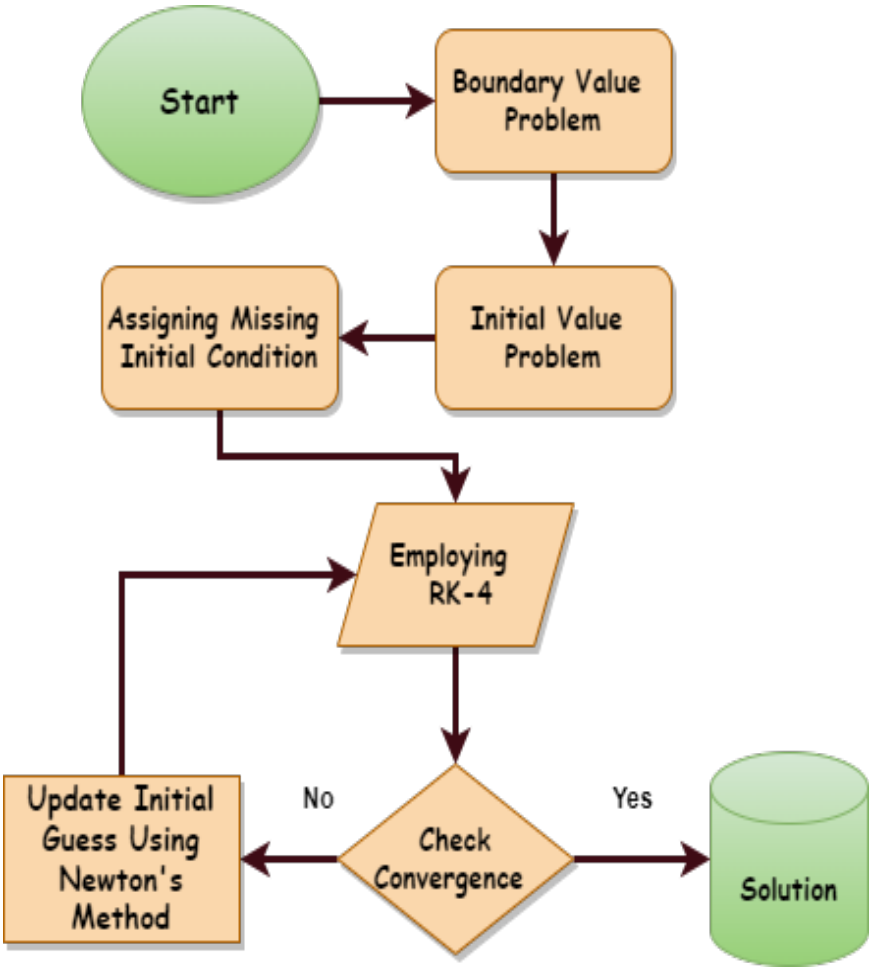

FIGURE 4.2: The shooting methods methodological framework.

The following system of ordinary differential equations (4.7) and (4.8) has been solved numerically by using the shooting technique

$$\left(1+\frac{1}{\tilde{\beta}}\right)\left(\frac{B_1}{B_2}\right)f^{iv}-\left(\frac{m}{B_2}\right)f'''\theta' e^{-m\theta}+ff'''-f'f''-\frac{Sq}{2}(3f''+\eta f''')-\frac{B_3}{B_2}Mf''=0.$$

$$\Rightarrow \frac{B_4}{P_r B_5}\theta''+\frac{E_c}{B_5}\left(1+\frac{1}{\tilde{\beta}}\right)e^{-m\theta}f''^2+f\theta'-\frac{S_q}{2}\eta\theta-\frac{R}{B_5}\theta=0.$$

The following notations have been taken:

$$f(\eta)=\tilde{Y}_1,\ f'(\eta)=\tilde{Y}_1'=\tilde{Y}_2,\ f''(\eta)=\tilde{Y}_2'=\tilde{Y}_3,$$
$$f'''(\eta)=\tilde{Y}_3'=\tilde{Y}_4,\ \theta=\tilde{Y}_5,\ \theta'(\eta)=\tilde{Y}_5'=\tilde{Y}_6.$$

The momentum and energy equation is then transformed into the system of first-order ODEs shown below.

$$\begin{aligned}
\tilde{Y}_1' &= \tilde{Y}_2, && \tilde{Y}_1(0) = S.\\
\tilde{Y}_2' &= \tilde{Y}_3, && \tilde{Y}_2(0) = \lambda.\\
\tilde{Y}_3' &= \tilde{Y}_4, && \tilde{Y}_3(0) = p.\\
\tilde{Y}_4' &= \left(\frac{\beta+1}{\beta}\right)\frac{B_2}{B_1}\left[\frac{m}{B_2}\tilde{Y}_4\tilde{Y}_6 e^{-m\tilde{Y}_5} - \tilde{Y}_1\tilde{Y}_4 + \tilde{Y}_2\tilde{Y}_3 + \frac{Sq}{2}(3\tilde{Y}_3 + \eta\tilde{Y}_4)\right.\\
&\quad \left. + \frac{B_3}{B_2}M\tilde{Y}_3\right], && \tilde{Y}_4(0) = q.\\
\tilde{Y}_5' &= \tilde{Y}_6, && \tilde{Y}_5(0) = \gamma.\\
\tilde{Y}_6' &= Pr\left(\frac{B_5}{B_4}\right)\left[\frac{Sq}{2}\eta\tilde{Y}_6 + \frac{R}{B_5}\tilde{Y}_5 - \left(\frac{\beta+1}{\beta}\right)\frac{Ec}{B_5}\tilde{Y}_3^2 e^{-m\tilde{Y}_5} - \tilde{Y}_1\tilde{Y}_6\right], && \tilde{Y}_6(0) = r,
\end{aligned}$$

where the missing initial conditions are p, q and r. Now, the Runge-Kutta method is used to solve the above mentioned IVP. It is necessary to choose the missing conditions, such as:

$$\left.\begin{aligned}
&\tilde{Y}_1(\eta_1, p, q, r) - \frac{Sq}{2} = 0,\\
&\tilde{Y}_2(\eta_1, p, q, r) = 0,\\
&\tilde{Y}_5(\eta_1, p, q, r) - 1 = 0.
\end{aligned}\right\} \tag{4.23}$$

Newton's method is used to solve the algebraic equation (4.7) and (4.8) numerically. This formula has the following iterative form:

$$\begin{bmatrix} p\\ q\\ r\end{bmatrix}_{(n+1)} = \begin{bmatrix} p\\ q\\ r\end{bmatrix}_{(n)} - \begin{bmatrix} \frac{\partial\tilde{Y}_1}{\partial p} & \frac{\partial\tilde{Y}_1}{\partial q} & \frac{\partial\tilde{Y}_1}{\partial r}\\ \frac{\partial\tilde{Y}_3}{\partial p} & \frac{\partial\tilde{Y}_3}{\partial q} & \frac{\partial\tilde{Y}_3}{\partial r}\\ \frac{\partial\tilde{Y}_5}{\partial p} & \frac{\partial\tilde{Y}_5}{\partial q} & \frac{\partial\tilde{Y}_5}{\partial r}\end{bmatrix}^{-1} \begin{bmatrix} \tilde{Y}_1 - \frac{Sq}{2}\\ \tilde{Y}_2\\ \tilde{Y}_5 - 1\end{bmatrix}_{(n)}$$

To successfully iterate the above formula we need the following derivative

$$\begin{aligned}
&\frac{\partial\tilde{Y}_1}{\partial p} = \tilde{Y}_7, \quad \frac{\partial\tilde{Y}_2}{\partial p} = \tilde{Y}_8, \quad \frac{\partial\tilde{Y}_3}{\partial p} = \tilde{Y}_9, \quad \frac{\partial\tilde{Y}_4}{\partial p} = \tilde{Y}_{10}, \quad \frac{\partial\tilde{Y}_5}{\partial p} = \tilde{Y}_{11}, \quad \frac{\partial\tilde{Y}_6}{\partial p} = \tilde{Y}_{12},\\
&\frac{\partial\tilde{Y}_1}{\partial q} = \tilde{Y}_{13}, \quad \frac{\partial\tilde{Y}_2}{\partial q} = \tilde{Y}_{14}, \quad \frac{\partial\tilde{Y}_3}{\partial q} = \tilde{Y}_{15}, \quad \frac{\partial\tilde{Y}_4}{\partial q} = \tilde{Y}_{16}, \quad \frac{\partial\tilde{Y}_5}{\partial q} = \tilde{Y}_{17}, \quad \frac{\partial\tilde{Y}_6}{\partial q} = \tilde{Y}_{18},\\
&\frac{\partial\tilde{Y}_1}{\partial r} = \tilde{Y}_{19}, \quad \frac{\partial\tilde{Y}_2}{\partial r} = \tilde{Y}_{20}, \quad \frac{\partial\tilde{Y}_3}{\partial r} = \tilde{Y}_{21}, \quad \frac{\partial\tilde{Y}_4}{\partial r} = \tilde{Y}_{22}, \quad \frac{\partial\tilde{Y}_5}{\partial r} = \tilde{Y}_{23}, \quad \frac{\partial\tilde{Y}_6}{\partial r} = \tilde{Y}_{24},
\end{aligned}$$

The Newton's iterative technique takes on the following transform as a result of these additional notations:

$$\begin{bmatrix} p \\ q \\ r \end{bmatrix}_{(n+1)} = \begin{bmatrix} p \\ q \\ r \end{bmatrix}_{(n)} - \begin{bmatrix} \tilde{Y}_7 & \tilde{Y}_{13} & \tilde{Y}_{19} \\ \tilde{Y}_9 & \tilde{Y}_{15} & \tilde{Y}_{21} \\ \tilde{Y}_{11} & \tilde{Y}_{17} & \tilde{Y}_{23} \end{bmatrix}^{-1} \begin{bmatrix} \tilde{Y}_1 - \frac{Sq}{2} \\ \tilde{Y}_2 \\ \tilde{Y}_5 - 1 \end{bmatrix}_{(n)}$$

To find the missing derivative present in the Newton formula the following equation will add up in the above initial value problem.

$$\tilde{Y}_7' = \tilde{Y}_8, \qquad \tilde{Y}_7(0) = 0.$$

$$\tilde{Y}_8' = \tilde{Y}_9, \qquad \tilde{Y}_8(0) = 0.$$

$$\tilde{Y}_9' = \tilde{Y}_{10}, \qquad \tilde{Y}_9(0) = 1.$$

$$\tilde{Y}_{10}' = \frac{B_2}{B_1}\left(\frac{\beta+1}{\beta}\right)\left[\frac{m}{B_2}\left(-\tilde{Y}_4\tilde{Y}_6 e^{-m\tilde{Y}_5} m\tilde{Y}_{11} + \tilde{Y}_{10}\tilde{Y}_6 e^{-m\tilde{Y}_5} + \tilde{Y}_4\tilde{Y}_{12} e^{-m\tilde{Y}_5}\right)\right.$$
$$\left. - \tilde{Y}_1\tilde{Y}_{10} - \tilde{Y}_7\tilde{Y}_4 + \tilde{Y}_2\tilde{Y}_9 + \tilde{Y}_8\tilde{Y}_3 + \frac{Sq}{2}(3\tilde{Y}_9 + \eta\tilde{Y}_{10}) + \frac{B_3}{B_2}M\tilde{Y}_9\right], \quad \tilde{Y}_{10}(0) = 0.$$

$$\tilde{Y}_{11}' = \tilde{Y}_{12}, \qquad \tilde{Y}_{11}(0) = 0.$$

$$\tilde{Y}_{12}' = Pr\left(\frac{B_5}{B_4}\right)\left[\left(\frac{Sq}{2}\right)\eta\tilde{Y}_{12} + \left(\frac{R}{B_5}\right)\tilde{Y}_{11} - \left(\frac{\beta+1}{\beta}\right)\frac{Ec}{B_5}\right.$$
$$\left.\left(2\tilde{Y}_3\tilde{Y}_9 e^{-m\tilde{Y}_5} - \tilde{Y}_3^2 e^{-m\tilde{Y}_5} m\tilde{Y}_{11} - \tilde{Y}_1\tilde{Y}_{12} - \tilde{Y}_7\tilde{Y}_6\right)\right] \qquad \tilde{Y}_{12}(0) = 0.$$

$$\tilde{Y}_{13}' = \tilde{Y}_{14}, \qquad \tilde{Y}_{13}(0) = 0.$$

$$\tilde{Y}_{14}' = \tilde{Y}_{15}, \qquad \tilde{Y}_{14}(0) = 0.$$

$$\tilde{Y}_{15}' = \tilde{Y}_{16}, \qquad \tilde{Y}_{15}(0) = 0.$$

$$\tilde{Y}_{16}' = \left(\frac{\beta+1}{\beta}\right)\frac{B_2}{B_1}\left[\frac{m}{B_2}(-\tilde{Y}_4\tilde{Y}_6 e^{-m\tilde{Y}_5} m\tilde{Y}_{17} + \tilde{Y}_{16}\tilde{Y}_6 e^{-m\tilde{Y}_5} + \tilde{Y}_4\tilde{Y}_{18} e^{-m\tilde{Y}_5})\right.$$
$$\left. - \tilde{Y}_1\tilde{Y}_{16} - \tilde{Y}_{13}\tilde{Y}_4 + \tilde{Y}_2\tilde{Y}_{15} + \tilde{Y}_{14}\tilde{Y}_3 + \frac{Sq}{2}(3\tilde{Y}_{15} + \eta\tilde{Y}_{16}) + \frac{B_3}{B_2}M\tilde{Y}_{15}\right], \quad \tilde{Y}_{16}(0) = 1.$$

$$\tilde{Y}_{17}' = \tilde{Y}_{18}, \qquad \tilde{Y}_{17}(0) = 0.$$

$$\tilde{Y}_{18}' = Pr\frac{B_5}{B_4}\left[\frac{Sq}{2}\eta\tilde{Y}_{18} + \frac{R}{B_5}\tilde{Y}_{17} - \left(\frac{\beta+1}{\beta}\right)\frac{Ec}{B_5}\left(2\tilde{Y}_3\tilde{Y}_{15} e^{-m\tilde{Y}_5} - \tilde{Y}_3^2 e^{-m\tilde{Y}_5} m\tilde{Y}_{17}\right)\right.$$

$$- \tilde{Y}_1\tilde{Y}_{18} - \tilde{Y}_{13}\tilde{Y}_6\Bigg] \qquad \tilde{Y}_{18}(0) = 0.$$

$$\tilde{Y}'_{19} = \tilde{Y}_{20}, \qquad \tilde{Y}_{19}(0) = 0.$$

$$\tilde{Y}'_{20} = \tilde{Y}_{21}, \qquad \tilde{Y}_{20}(0) = 0,$$

$$\tilde{Y}'_{21} = \tilde{Y}_{22}, \qquad \tilde{Y}_{21}(0) = 0.$$

$$\tilde{Y}'_{22} = \left(\frac{\beta+1}{\beta}\right)\frac{B_2}{B_1}\Bigg[\frac{m}{B_2}\left(-\tilde{Y}_4\tilde{Y}_6e^{-m\tilde{Y}_5}m\tilde{Y}_{23} + \tilde{Y}_{22}\tilde{Y}_6e^{-m\tilde{Y}_5} + \tilde{Y}_4\tilde{Y}_{24}e^{-m\tilde{Y}_5}\right)$$
$$- \tilde{Y}_1\tilde{Y}_{22} - \tilde{Y}_{19}\tilde{Y}_4 + \tilde{Y}_2\tilde{Y}_{21} + \tilde{Y}_{20}\tilde{Y}_3$$
$$+ \frac{Sq}{2}(3\tilde{Y}_{21} + \eta\tilde{Y}_{22}) + \frac{B_3}{B_2}M\tilde{Y}_{21}\Bigg], \qquad \tilde{Y}_{22}(0) = 1.$$

$$\tilde{Y}'_{23} = \tilde{Y}_{24}, \qquad \tilde{Y}_{23}(0) = 0.$$

$$\tilde{Y}'_{24} = Pr\left(\frac{B_5}{B_4}\right)\Bigg[\frac{Sq}{2}\eta\tilde{Y}_{24} + \frac{R}{B_5}\tilde{Y}_{23} - \left(\frac{\beta+1}{\beta}\right)\frac{Ec}{B_5}\left(2\tilde{Y}_3\tilde{Y}_{21}e^{-m\tilde{Y}_5} - \tilde{Y}_3^2e^{-m\tilde{Y}_5}m\tilde{Y}_{23}\right)$$
$$- \tilde{Y}_1\tilde{Y}_{24} - \tilde{Y}_{19}\tilde{Y}_6\Bigg] \qquad \tilde{Y}_{24}(0) = 1.$$

Following stopping criteria is used for Newton's method

$$\max\left\{\left|\tilde{Y}_1(\eta_1, p_n, q_n, r_n) - \frac{Sq}{2}\right|, \left|\tilde{Y}_2(\eta_1, p_n, q_n, r_n)\right|, \left|\tilde{Y}_5(\eta_1, p_n, q_n, r_n) - 1\right|\right\} < \epsilon,$$

where $\epsilon = 10^{-6}$. The system of ordinary differential equations (4.11) and (4.17) has been solved numerically by using shooting method, assuming f, f'', θ and θ' as a known functions.

$$\phi'' + ScSr\theta'' + \frac{Nt}{Nb}\theta'' - Sck\phi + Sc\left(f - \frac{\delta\eta}{2}\phi'\right) = 0. \tag{4.24}$$

$$\mathtt{N}'' - L_b\left(\frac{1}{2}Sq\eta\mathtt{N}'\right) + L_bf\mathtt{N}' - Pe\left(\phi'\mathtt{N}' + (\omega + \mathtt{N})\phi''\right) = 0. \tag{4.25}$$

For this, we utilize the following notations:

$$\phi(\eta) = Z_1, \quad \phi'(\eta) = Z_1' = Z_2, \quad \mathtt{N}(\eta) = Z_3, \quad \mathtt{N}'(\eta) = Z_3' = Z_4.$$

$$Z_1' = Z_2, \qquad Z_1(0) = F_1.$$

$$Z_2' = SckZ_1 - \left(ScSr + \frac{Nt}{Nb}\right)\Bigg[Pr\frac{B_5}{B_4}\Bigg[\frac{Sq}{2}\eta\tilde{Y}_6 + \frac{R}{B_5}\tilde{Y}_5 - \left(\frac{\beta+1}{\beta}\right)\left(\frac{Ec}{B_5}\right)$$

$$\tilde{Y}_3^2 e^{-m\tilde{Y}_5} - \tilde{Y}_1\tilde{Y}_6\Big]\Big] - Sc\left(\tilde{Y}_1 - Sq\frac{\eta}{2}\right)Z_2, \qquad Z_2(0) = -\frac{Nt}{Nb}Y_6.$$

$$Z_3' = Z_4, \qquad Z_3(0) = 1.$$

$$Z_4' = Lb\tilde{Y}_1 Z_4 + PeZ_2Z_4 + Pe(\omega + Z_3)\Bigg(SckZ_1 - \left(ScSr + \frac{Nt}{Nb}\right)$$
$$\left[Pr\frac{B_5}{B_4}\left[\frac{Sq}{2}\eta\tilde{Y}_6 + \frac{R}{B_5}\tilde{Y}_5 - \left(\frac{\beta+1}{\beta}\right)\left(\frac{Ec}{B_5}\right)\tilde{Y}_3^2 e^{-m\tilde{Y}_5} - \tilde{Y}_1\tilde{Y}_6\right]\right]$$
$$+\frac{1}{2}LbSq\eta Z_4 \qquad Z_4(0) = F_2.$$

Runge-Kutta method of order four is used to solve the above IVP. F_1 and F_2 are the missing condition which are selected in such a way that,

$$Z_1(\eta, F_1, F_2) = 0, \tag{4.26}$$

$$Z_3(\eta, F_1, F_2) = 0. \tag{4.27}$$

To solve the algebraic equations (4.26) and (4.27) simultaneously, we use the following iterative scheme given by Newton.

$$\begin{bmatrix} F_1 \\ F_2 \end{bmatrix}_{(n+1)} = \begin{bmatrix} F_1 \\ F_2 \end{bmatrix}_{(n)} - \left[\begin{pmatrix} \frac{\partial Z_1}{\partial F_1} & \frac{\partial Z_1}{\partial F_2} \\ \frac{\partial Z_3}{\partial F_1} & \frac{\partial Z_3}{\partial F_2} \end{pmatrix}^{-1}\right]_{(n)} \begin{bmatrix} Z_1 \\ Z_3 \end{bmatrix}_n$$

Following notations are used to calculate the new appeared derivatives:

$$\frac{\partial Z_1}{\partial F_1} = Z_5, \ \frac{\partial Z_2}{\partial F_1} = Z_6, \ \frac{\partial Z_3}{\partial F_1} = Z_7, \ \frac{\partial Y_4}{\partial F_1} = Z_8.$$
$$\frac{\partial Z_1}{\partial F_2} = Z_9, \ \frac{\partial Z_2}{\partial F_2} = Z_{10}. \frac{\partial Z_3}{\partial F_2} = Z_{11}, \frac{\partial Z_4}{\partial F_2} = Z_{12}.$$

As a result of these new notations, the Newton's iterative scheme gets the form:

$$\begin{bmatrix} F_1 \\ F_2 \end{bmatrix}_{(n+1)} = \begin{bmatrix} F_1 \\ F_2 \end{bmatrix}_{(n)} - \left[\begin{pmatrix} Z_5 & Z_9 \\ Z_7 & Z_{11} \end{pmatrix}^{-1}\right]_{(n)} \begin{bmatrix} Z_1 \\ Z_3 \end{bmatrix}_n$$

We get the following equations by differentiating above IVP with respect to F_1 and F_2.

$$Z_5' = Z_6, \qquad Z_5(0) = 1.$$
$$Z_6' = SckZ_5 - Sc\left(\tilde{Y}_1 - Sq\left(\frac{\eta}{2}\right)\right)Z_6, \qquad Z_6(0) = 0.$$

$$Z_7' = Z_8, \qquad Z_7(0) = 0$$

$$Z_8' = Lb\tilde{Y}_1 Z_8 + PeZ_2Y_8 + PeZ_6Z_4 + Pe(w + Z(7))Z_2' + Pe(\omega + Z_3)Z_6' + \frac{1}{2}LbSqxZ_8 \qquad Z_8(0) = 0.$$

$$Z_9' = Z_{10}, \qquad Z_9(0) = 0.$$

$$Z_{10}' = SckZ_9 - Sc\left(\tilde{Y}_1 - Sq\left(\frac{\eta}{2}\right)\right)Z_{10}, \qquad Z_{10}(0) = 0.$$

$$Z_{11}' = Z_{12}, \qquad Z_{11}(0) = 0.$$

$$Z_{12}' = Lb\tilde{Y}_1 Z_{12} + PeZ_2Z - 12 + PeZ_{10}Z_4 + Pe(w + Z_{11})Z_2' + Pe(w + Z_3)Z_{10}' + \frac{1}{2}LbSq\eta Z_{12}, \qquad Z_{12}(0) = 1$$

Following stopping criteria is used for Newton's method

$$\max\left\{\left|Z_1(\eta_1, F1_n, F2_n)\right|, \left|Z_3(\eta_1, F1_n, F2_n)\right|\right\} < \epsilon,$$

where $\epsilon = 10^{-6}$.

4.6.1 Validation

Comparison of results calculated by [23] for the Skin friction and Nusselt number.

TABLE 4.1: Results of $Re^{\frac{-1}{2}}x_1Cfx_1$, $Re^{\frac{-1}{2}}x_2Cfx_2$, $Re^{\frac{-1}{2}}x_1Nux_1$ and $Re^{\frac{-1}{2}}x_2Nux_2$ for various values of β, M.

		Present Work				**Famakinwa et al.**			
β	M	Cf_{x1}	Cf_{x2}	Nu_{x1}	Nu_{x2}	Cf_{x1}	Cf_{x2}	Nu_{x1}	Nu_{x2}
1	0.25	-2.10860	1.50379	0.95596	1.13971	-2.1691	1.4639	0.9281	1.2518
5		-2.12583	1.51151	0.95595	1.13972	-2.1748	1.4639	0.9281	1.2518
	1	-2.13447	1.51543	0.95594	1.13972	-2.1861	1.4658	0.9280	1.2518
	2	-2.09230	1.51557	0.95601	1.13967	-2.2086	1.46850	0.9280	1.2518

4.7 Results and Discussion

After converting the governing partial differential equations (PDEs) that characterize the fluid flow into a set of ordinary differential equations (ODEs), various significant parameters become apparent. A thorough investigation of the impact of these parameters on the profiles of dimensionless velocity, temperature, concentration and motile micro-organisms is examined through the graphical representation. Furthermore, an assessment of the dynamic behavior of the computed skin friction $Re_x^{\frac{1}{2}} C_{fx}$, Nusselt number $Re_x^{\frac{1}{2}} Nu_x$, Sherwood number $Re_x^{\frac{1}{2}} Sh_x$ will also be conducted. Table 4.1 and 4.2 depict the effects of casson parameter β, magnetic parameter M, squeezing parameter Sq, suction parameter S and stretching parameter λ with fixed $m = 0$ on the fluid motion for the skin friction $Re_x^{\frac{1}{2}} C_{fx}$ and Nusselt number $Re_x^{\frac{1}{2}} Nu_x$.

- For rising values of β, a diminishing trend in skin friction is observed for both the lower and upper plates. Simultaneously, there is an increasing trend in the Nusselt number for the lower plate, while a decreasing trend is noted for the upper plate.
- As the parameter M increases, a reduction in the skin friction values is evident on the lower plate, while an opposite trend is observed for the upper plate. Conversely, higher values of the M parameter trend to an augmentation in the Nusselt number for the lower plate, accompanied by a declining trend for the upper plate.
- As the Sq parameter exhibits an increasing trend, a declining trend in skin friction is evident on both lower and upper plates. While, Nusselt number demonstrates an increase behavior on the lower plate and a corresponding increase on the upper plate.
- For rising values of S and λ, results an increase in skin friction of both lower and upper plate and also showing increase trend for Nusselt number of lower plate and opposite behavior for upper plate.
- The trend of the Sherwood number $Re_x^{\frac{1}{2}} Sh_x$ and density distribution of motile micro-organisms $Re_x^{\frac{1}{2}} Nn_x$ are revealed in Tables [4.3-4.4].
- The table shows clearly that the sherwood number is decreasing for rising values of Sq in Sherwood number both for lower and upper plate. While the parameters Sc, k, Sr, Lb, Pe, ω depicts no effects in Sherwood number for rising values for

lower plate but shows decreasing trend for upper plate for rising values of Sc and k and Sr depicts an increase behavior for upper plate.

- For rising values of Nt, the Sherwood number increases on both lower and upper plates and result a decreasing trend for enhancing values of Nb parameter for both upper and lower plates. $Re_x^{\frac{1}{2}} Sh_x$ falls for the rising values of ϕ_1 for lower plate and opposite behavior for upper plate. For rising values of Sq and ω, Nb and Lb, Sherwood number shows decreasing trend for lower plate and opposite trend for upper plate.

- For rising values of Sc, Nt results an increase trend for lower plate and decrease trend for upper plate. While for the rising values of k and ϕ_2 shows increasing behavior for both upper and lower plate. The$Re_x^{\frac{1}{2}} Sh_x$ falls for rising values of Sr both for upper and lower plate.

TABLE 4.2: Results of $Re_x^{\frac{1}{2}} C_{fx}$ for various values of M, Sq, S and λ when $m = 0$.

β	M	Sq	S	λ	$Re_{x1}^{\frac{1}{2}} C_{fx1}$	$Re_{x2}^{\frac{1}{2}} C_{fx2}$
1	0.25	0.1	0.2	0.3	-2.13331	1.48091
1.5					-2.14173	1.47625
1.9					-2.14849	1.47248
	0.5				-2.13412	1.48105
	1.0				-2.13573	1.48122
		0.2			-1.83368	1.18309
		0.4			-1.23115	0.58642
			0.3		-2.75633	2.06498
			0.4		-3.38643	2.64346
				0.5	-2.95284	1.86978
				0.7	-3.77659	2.25633

TABLE 4.3: Results of $Re_x^{\frac{1}{2}} C_{fx}$ for various values of M, Sq and S when $m = 0$.

β	M	Sq	S	λ	$Re_x^{\frac{-1}{2}} Nu_{x1}$	$Re_x^{\frac{-1}{2}} Nu_{x2}$
1	0.25	0.1	0.2	0.3	1.68685	0.76933
1.5					1.87146	0.67845
1.9					2.01970	0.60632
	0.5				1.68694	0.76941
	1.0				1.68711	0.769577
		0.2			1.50051	0.89395
		0.4			1.21335	1.05850
			0.3		2.16737	0.43482
			0.4		2.77154	-0.00714
				0.5	2.38003	0.51562
				0.7	3.30457	0.19243

TABLE 4.4: Results of $Re_{x1}^{\frac{-1}{2}} Sh_{x1}$ for various values of Sq, Sc, k, Sr, Nt, Nb, Lb, Pe, ω and ϕ_2 when $m \neq 0$.

Sq	Sc	k	Sr	Nt	Nb	Lb	Pe	ω	ϕ_2	$Re_{x1}^{\frac{-1}{2}} Sh_{x1}$	$Re_{x2}^{\frac{-1}{2}} Sh_{x2}$
0.1	0.3	0.1	0.2	0.1	0.1	0.5	0.2	0.1	0.5	1.02328	1.27138
0.3										0.99117	1.26968
0.6										0.96221	1.26322
	0.6									1.02328	1.22864
	0.9									1.02328	1.18819
		0.2								1.02328	1.25365
		0.3								1.02328	1.23558
			0.4							1.02328	1.28837
			0.6							1.02328	1.30536
				0.2						2.04656	2.52577
				0.3						3.06985	3.78016
					0.2					0.51164	0.64418
					0.3					0.34109	0.43512
						1.0				1.02328	1.27138
						1.5				1.02328	1.27138
							0.4			1.02328	1.27138
							0.8			1.02328	1.27138
								0.3		1.02328	1.27138
								0.5		1.02328	1.27138
									0.7	1.00827	1.07887
									0.9	1.00179	0.98035

TABLE 4.5: Results of $Re_x^{\frac{1}{2}} C_{fx}$ for various values of M, Sq and S when $m = 0$.

Sq	Sc	k	Sr	Nt	Nb	Lb	Pe	ω	ϕ_2	$Re_{x1}^{\frac{-1}{2}} \mathtt{N}_{x1}$	$Re_{x2}^{\frac{-1}{2}} \mathtt{N}_{x2}$
0.1	0.3	0.1	0.2	0.1	0.1	0.5	0.2	0.1	0.5	1.07707	0.89513
0.3										1.07339	0.90813
0.6										1.07069	0.92649
	0.6									1.07946	0.89666
	0.9									1.081741	0.89813
		0.2								1.07817	0.89587
		0.3								1.07925	0.89659
			0.4							1.07588	0.89427
			0.6							1.07468	0.89342
				0.2						1.17387	0.79217
				0.3						1.27909	0.69763
					0.2					1.03184	0.94977
					0.3					1.01723	0.96845
						1.0				0.98295	0.95865
						1.5				0.93326	0.99492
							0.4			1.12696	0.81727
							0.8			1.33742	0.63110
								0.3		1.02668	0.92513
								0.5		1.01887	0.92718
									0.7	1.04611	0.93409
									0.9	1.05176	0.93918

4.8 Representation of Graphs

This section includes graphical representation of the numerical results. The visual depictions of velocity profiles, temperature profiles, concentration profiles and motile profiles offer an insight view into the system's behavior.

4.8.1 Velocity Profile

- Figure 4.3 illustrates the intricate influence of the Casson fluid parameter β on the velocity profile $f'(\eta)$. Notably, the behavior differs significantly in the absence $(m = 0)$ and presence $(m = 1)$ of the viscosity variation parameter. For $m = 0$, an initial decrease followed by an increase in the velocity profile is observed for varying β. Conversely, for $m = 1$, the velocity profile exhibits an initial increase and subsequent decrease. This underscores the sensitivity of the hybrid nanofluid's response to changes in the Casson fluid parameter.

- Figure 4.4 depicts the impact of the squeezing flow parameter Sq on the velocity distribution $f'(\eta)$ for $m = 0$ and $m = 1$. The velocity profile consistently increases with higher values of the squeezing parameter Sq in both cases. This finding highlights the profound influence of the squeezing flow parameter on fluid motion, independent of viscosity variation, suggesting potential applications in scenarios where controlled increases in fluid velocity are desired.

- Figure 4.5 provides insights into the influence of the suction parameter (S) on the velocity profile, both in the absence and presence of viscosity variation m. In both scenarios, an overarching trend is observed: the velocity profile decreases with an increase in the suction parameter S. This consistent behavior emphasizes the role of suction in mitigating the velocity of the hybrid nanofluid, reinforcing its significance in applications where controlled fluid deceleration is paramount.

- Figure 4.6 sheds light on the combined impact of radiation parameter R and Eckert number Ec on the velocity profile $f'(\eta)$. Notably, both parameters exhibit positive influences on fluid velocity. An increase in the radiation parameter enhances fluid velocity, aligning with expectations regarding augmented thermal energy

transfer. Similarly, a higher Eckert number corresponds to elevated fluid velocity, emphasizing the significance of kinetic energy in driving fluid motion within the squeezing flow geometry.

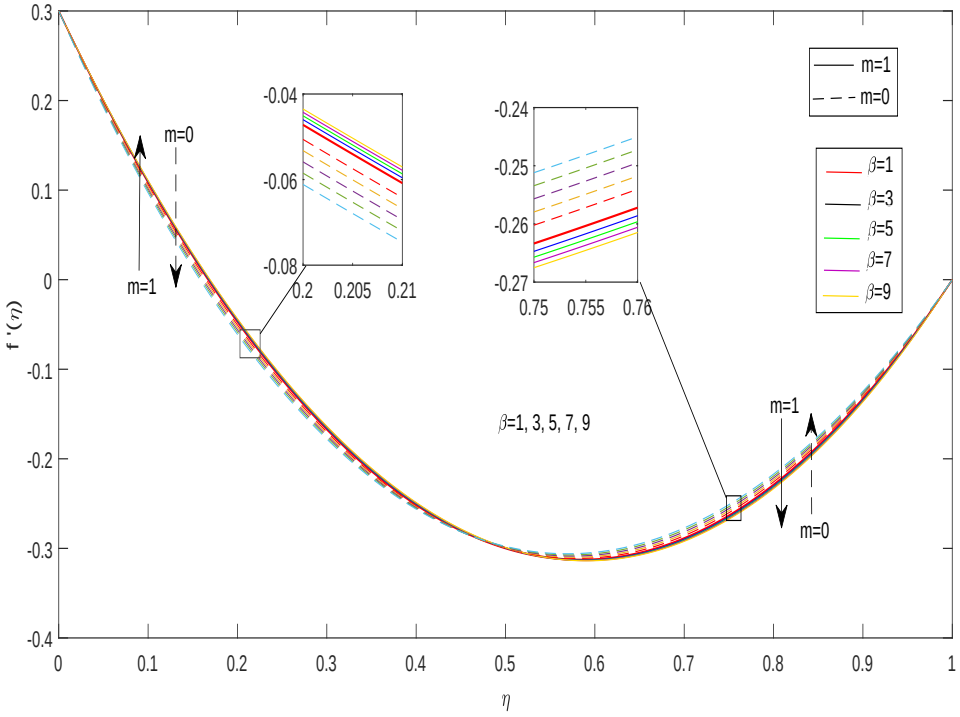

FIGURE 4.3: Influence of m and β on velocity profile

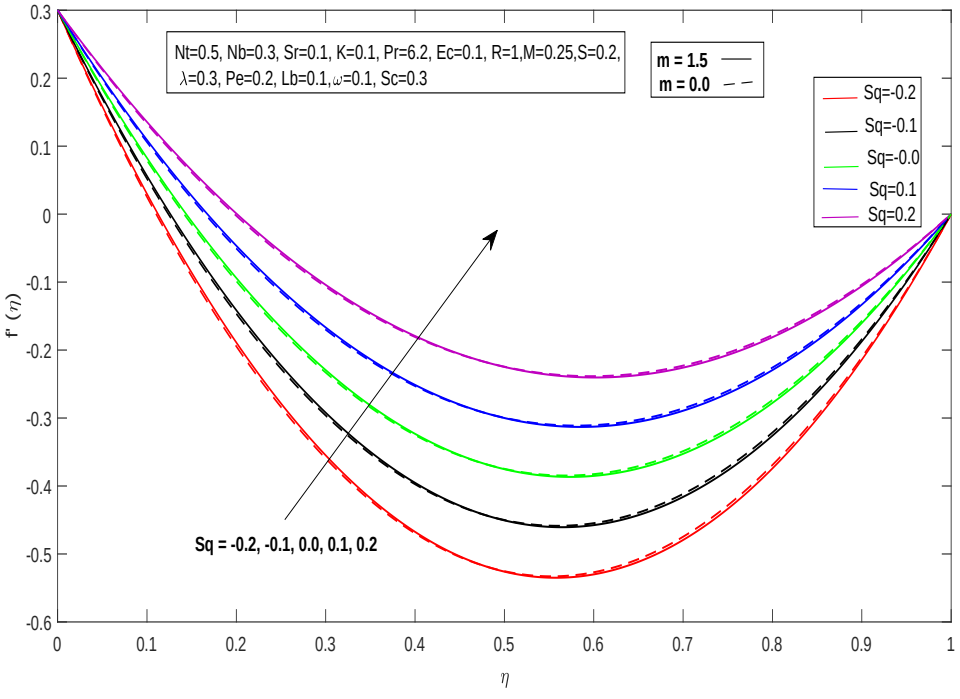

FIGURE 4.4: Influence of m and Sq on velocity profile

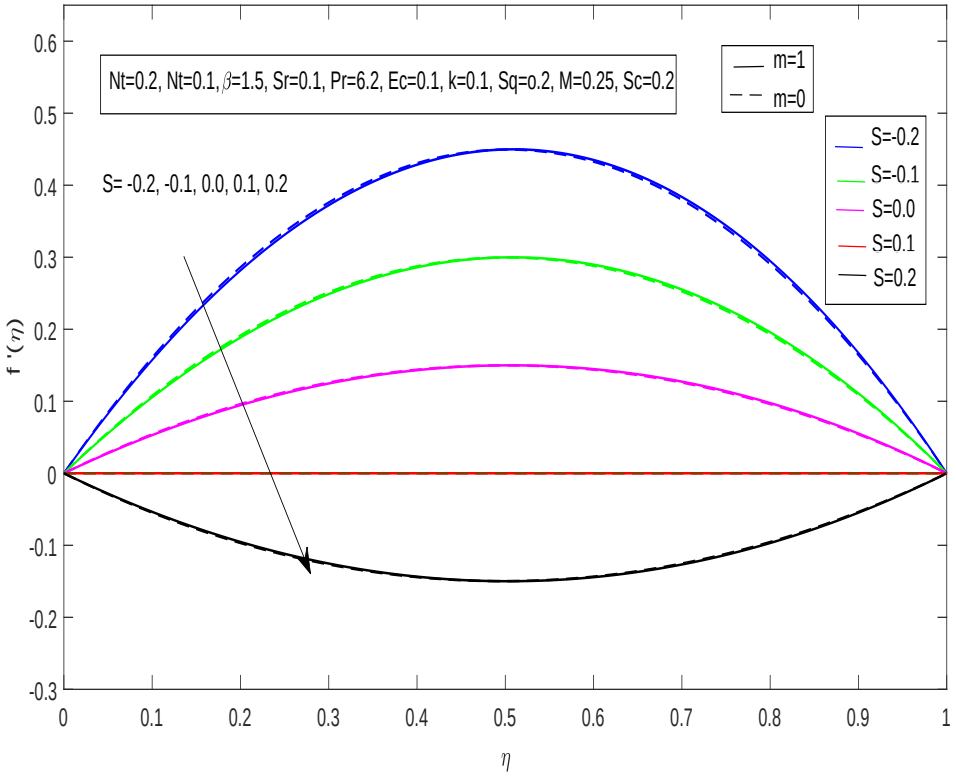

FIGURE 4.5: Influence of m and S on velocity profile.

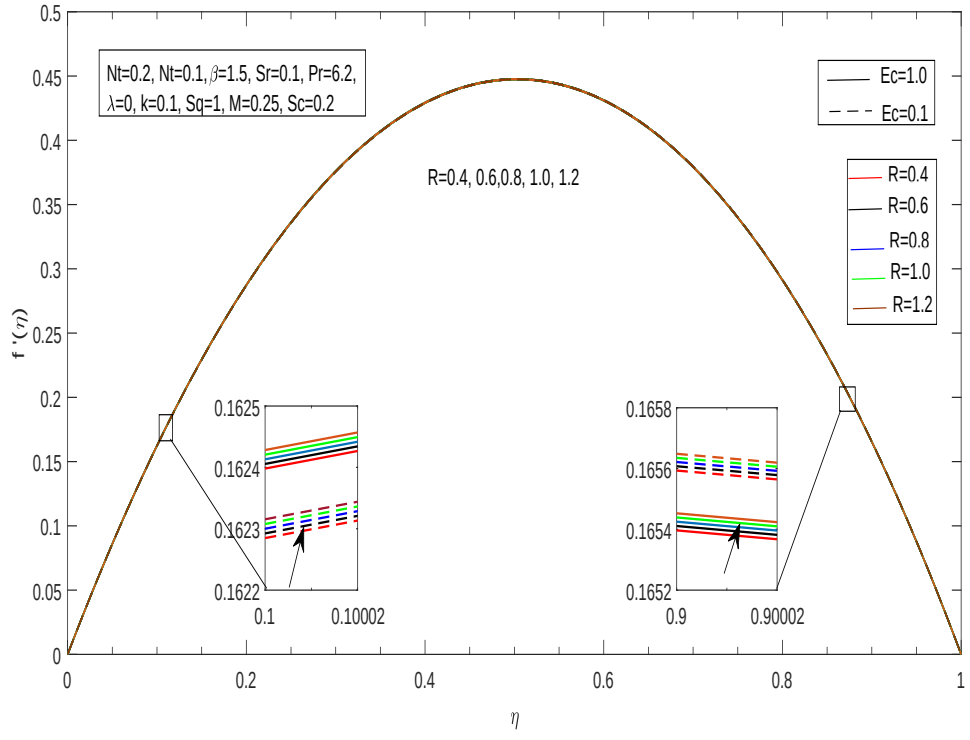

FIGURE 4.6: Influence of Ec and R on velocity profile.

4.8.2 Temperature Profile

- The temperature profile responds significantly to changes in the Casson parameter (β). As illustrated in Figure 4.7, an increase in β enhances heat transfer within the fluid and an increase in the thickness of boundary layer as β increases, resulting in a more prominent temperature profile. Notably, this enhancement is more pronounced when viscosity variation parameter (m) is absent.

- The influence of the squeezing flow parameter (Sq) on the temperature distribution is depicted in Figure 4.8. A notable observation is that an increase in Sq leads to decline in the temperature profile. This behavior holds true for both absence and presence of viscosity variation parameter (m).

- Figure 4.9 demonstrates the impact of the suction parameter (S) on the temperature profile. An increase in S results in a decrease in fluid temperature, underscoring the role of the suction parameter in enhancing heat within the fluid.

- The joint effect of the radiation parameter (R) and Eckert number (Ec) on the temperature profile is evident in Figure 4.10. An increase in R positively influences fluid velocity, decreasing the temperature profile. Moreover, for different values of Ec, the fluid temperature increases when $Ec = 0.1$ but decreases when $Ec = 1.0$.

- The stretching parameter (λ) plays a crucial role in shaping the temperature profile, as seen in Figure 4.11. An increase in λ leads to a substantial temperature increase within the fluid, emphasizing its role in promoting heat transfer.

- The effect of the Prandtl number (Pr) on the temperature profile is presented in Figure 4.12. Notably, for $Ec = 0.1$, the fluid temperature increases with higher Pr, while for $Ec = 1.0$, the temperature profile decreases. This suggests a complex interplay between Pr and Ec.

- Figure 4.13 explores the influence of the magnetic field parameter (M) on the temperature profile. The inverse effect is observed which indicates that an increase in M slightly decreases fluid temperature, highlighting the suppressing effect of the magnetic field.

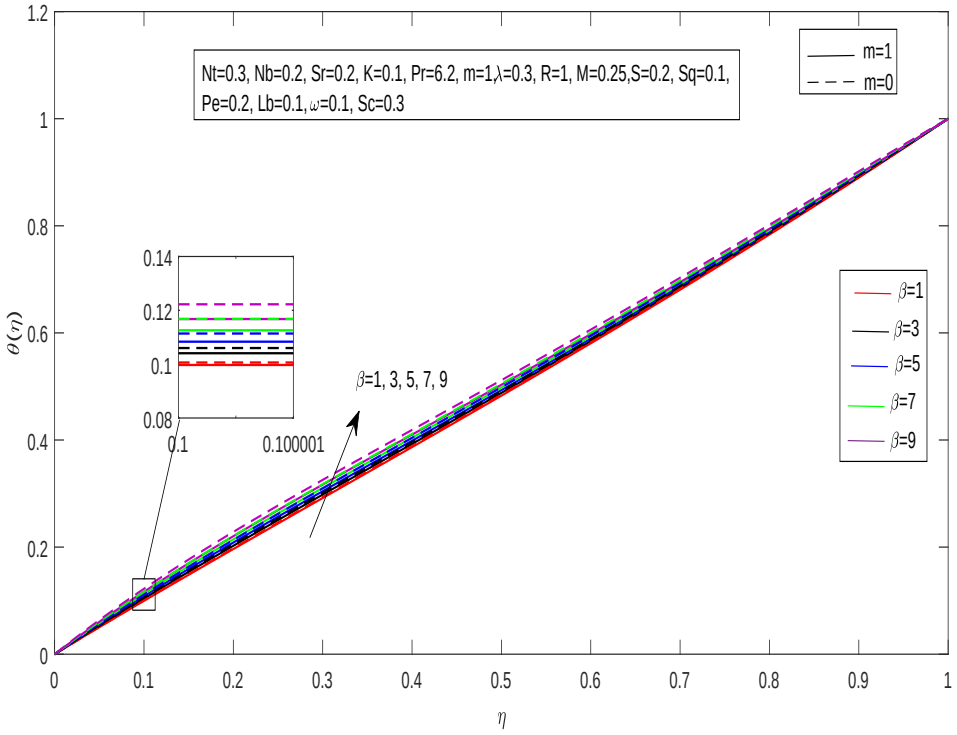

FIGURE 4.7: Influence of m and β on temperature profile.

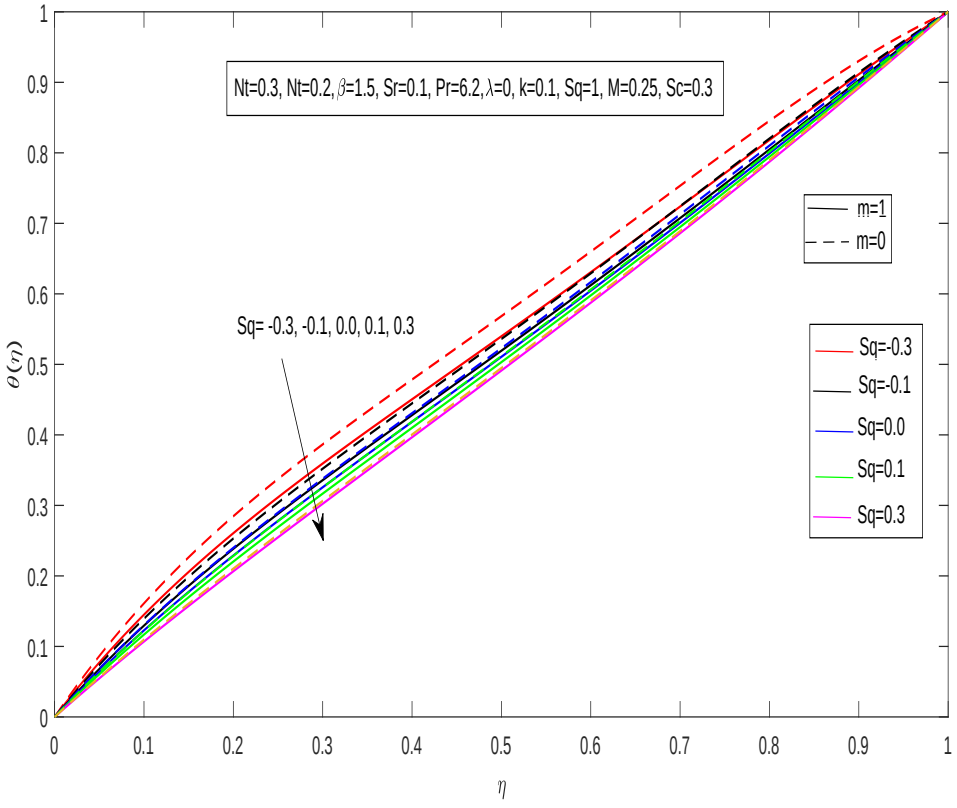

FIGURE 4.8: Influence of m and Sq on temperature profile.

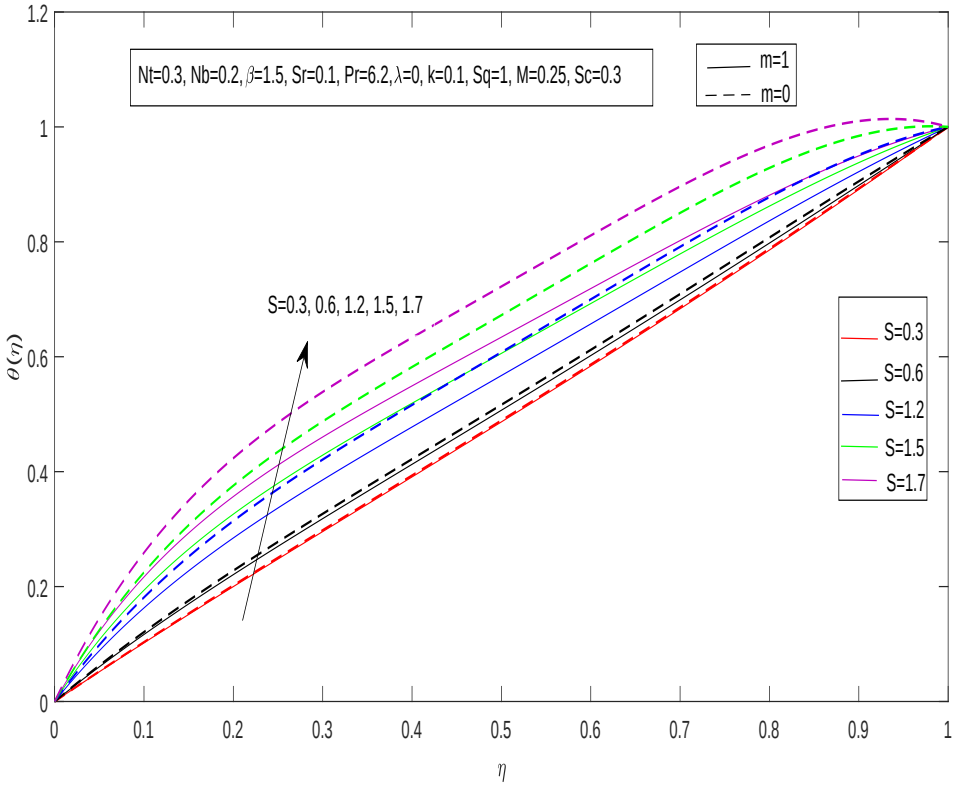

FIGURE 4.9: Influence of m and S on temperature profile.

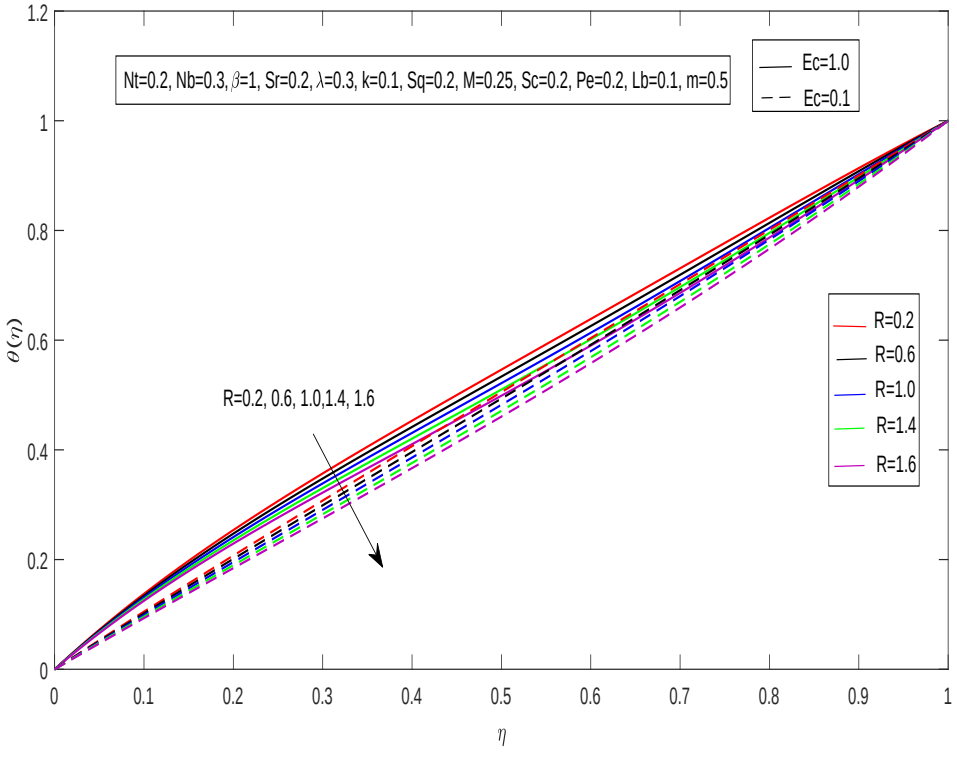

FIGURE 4.10: Influence of Ec and R on temperature profile.

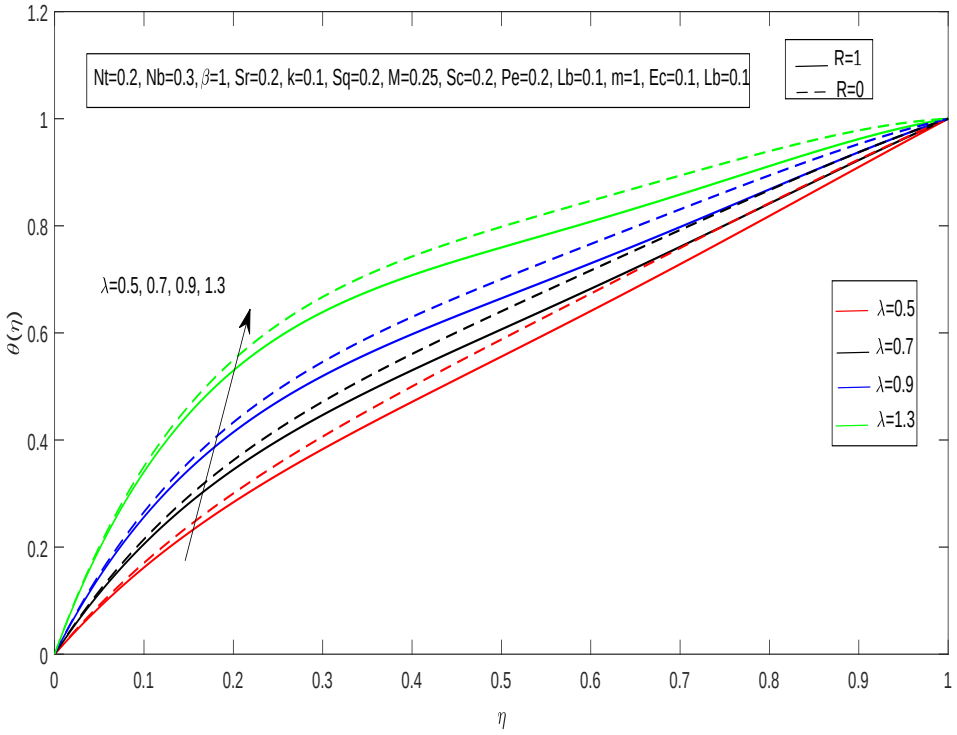

FIGURE 4.11: Influence of R and λ on temperature profile.

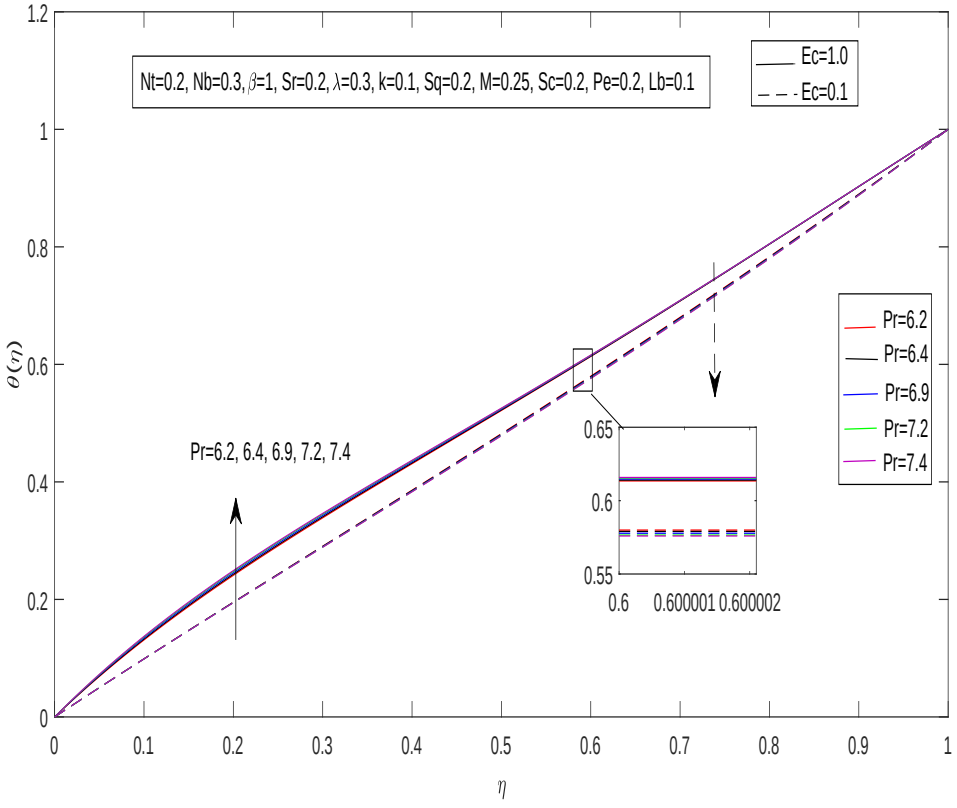

FIGURE 4.12: Influence of Ec and Pr on temperature profile.

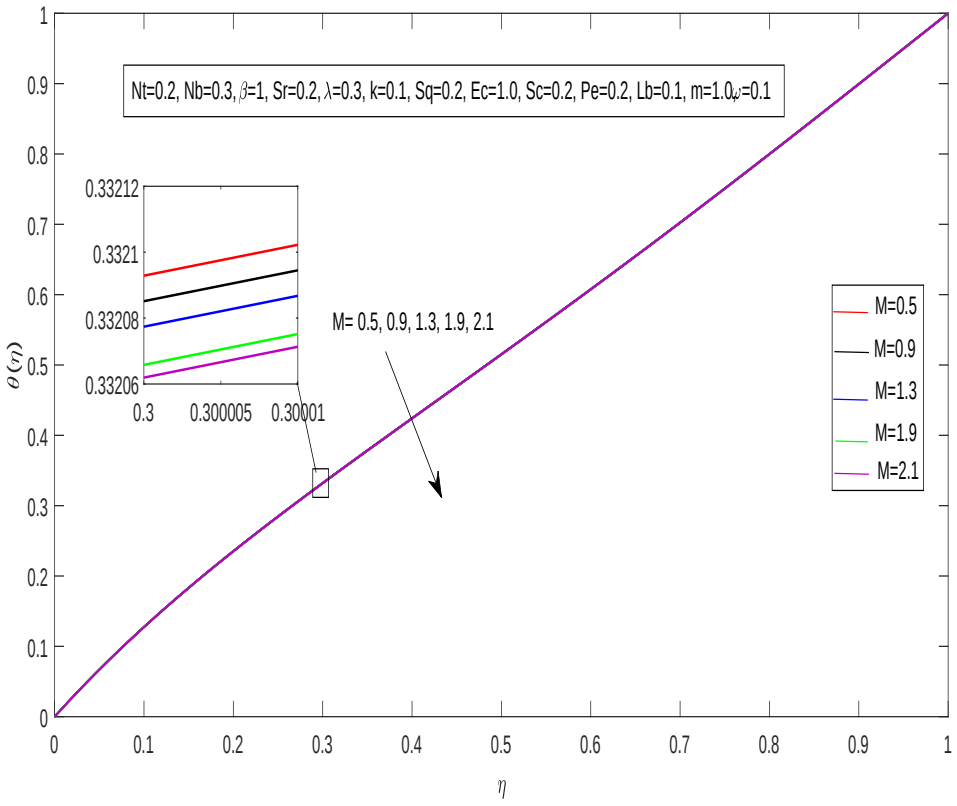

FIGURE 4.13: Influence of M on temperature profile.

4.8.3 Concentration Profile

- In Figure 4.14 the impact of the Casson parameter (β) on the concentration profile ($\phi(\eta)$) is evident. A higher Casson parameter may lead to the increase in the concentration of hybrid nanofluid. This behavior can be explained by the altered rheological characteristics affecting the dispersion and movement of nanoparticles within the fluid.

- In Figure 4.15, it is show that the concentration profile $\phi(\eta)$ is influenced by the squeezing parameter (Sq). An increase in Sq leads to a decrease in the concentration profile for both absence and presence of viscosity variation parameter (m). This indicates that squeezing flow diminishes the concentration of nanoparticles in the fluid.

- The impact of the Brownian motion parameter, in both absence and presence of thermal radiation, is observed in Figure 4.16. As the Brownian motion refers to the random movement of the particles suspended in the fluid medium. An increase

in Brownian motion parameter results in a decrease in the concentration profile, highlighting the role of Brownian diffusion in nanoparticle dispersion.

- The concentration profile $\phi(\eta)$ is influenced by the radiation parameter (R) and Eckert number (Ec) in Figure 4.17. An increase in R leads to an increase in concentration, while higher values of Ec contribute to a more pronounced concentration profile. This behavior is associated with enhanced thermal effects on nanoparticles movement.

- In Figure 4.18 the concentration profile $\phi(\eta)$ is significantly impacted by the thermophoresis parameter (Nt) in both absence and presence of thermal radiation (R). An increase in Nt parameter results in a substantial increase in the concentration of nanoparticles, demonstrating the influence of thermophoresis on particle migration.

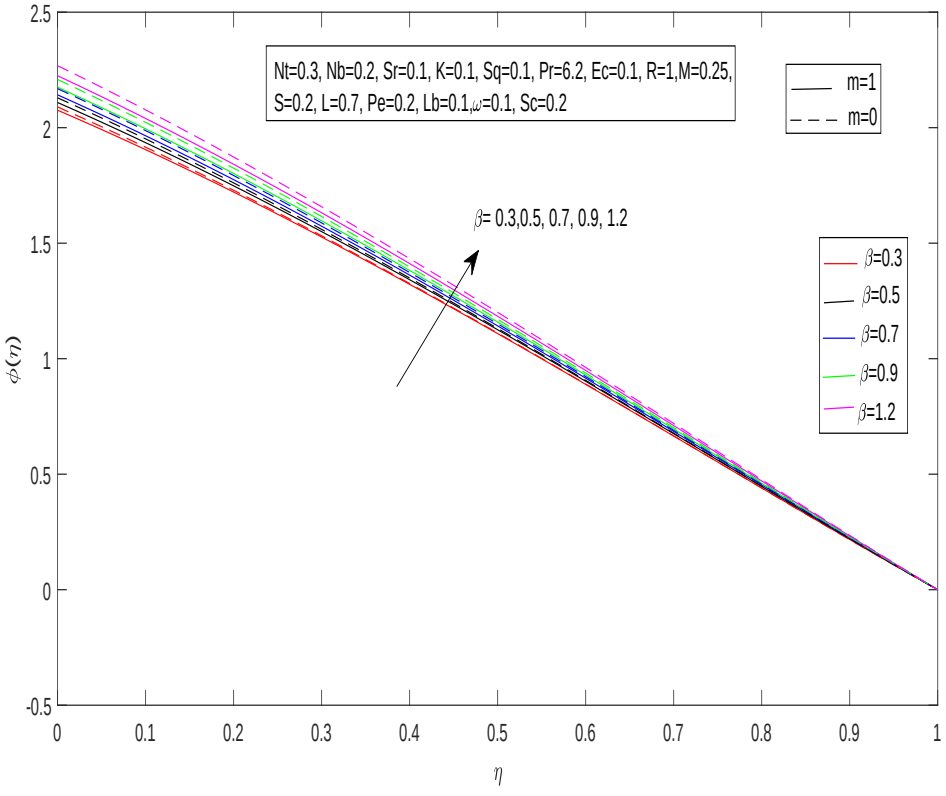

FIGURE 4.14: Influence of m and β on $\phi(\eta)$

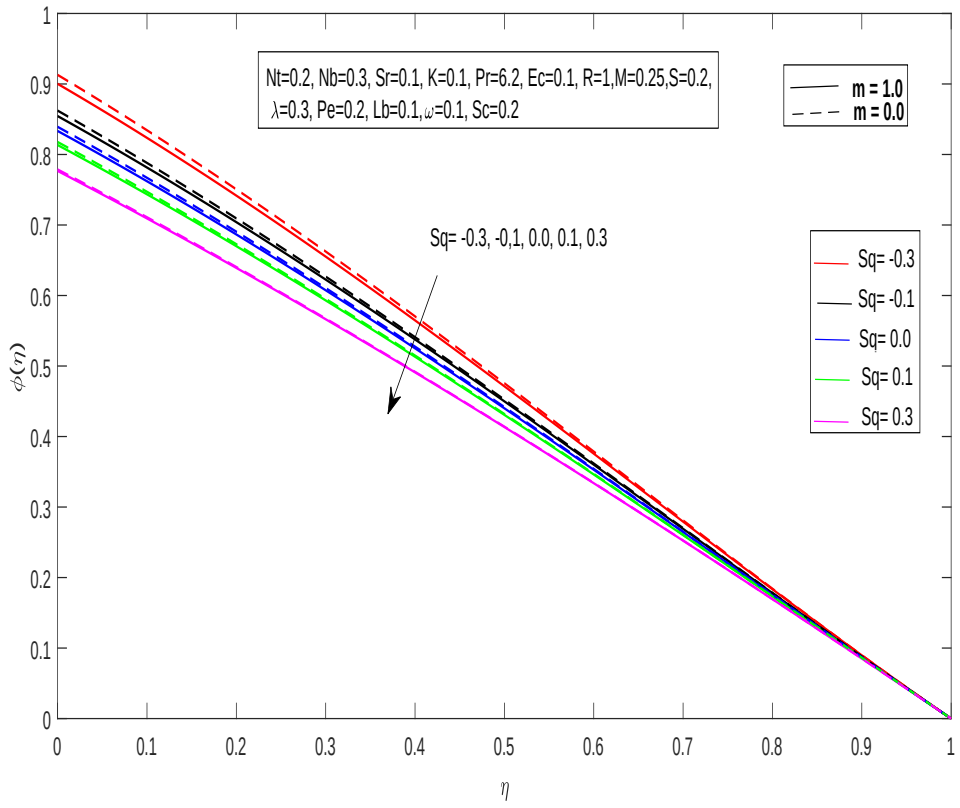

FIGURE 4.15: Influence of m and Sq on $\phi(\eta)$

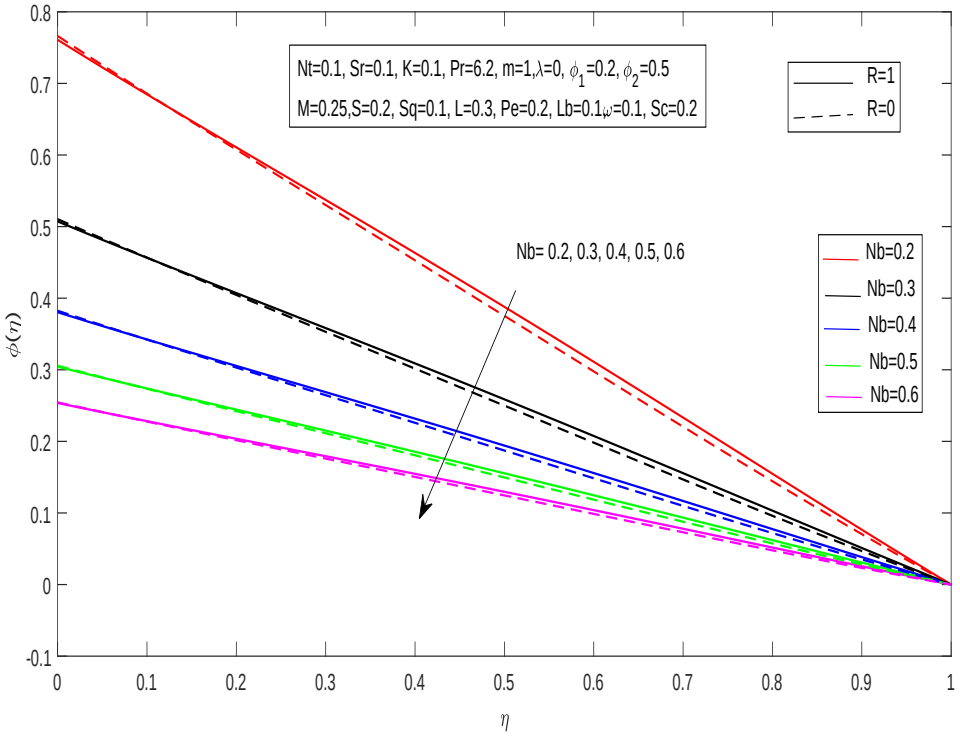

FIGURE 4.16: Influence of R and Nb on $\phi(\eta)$

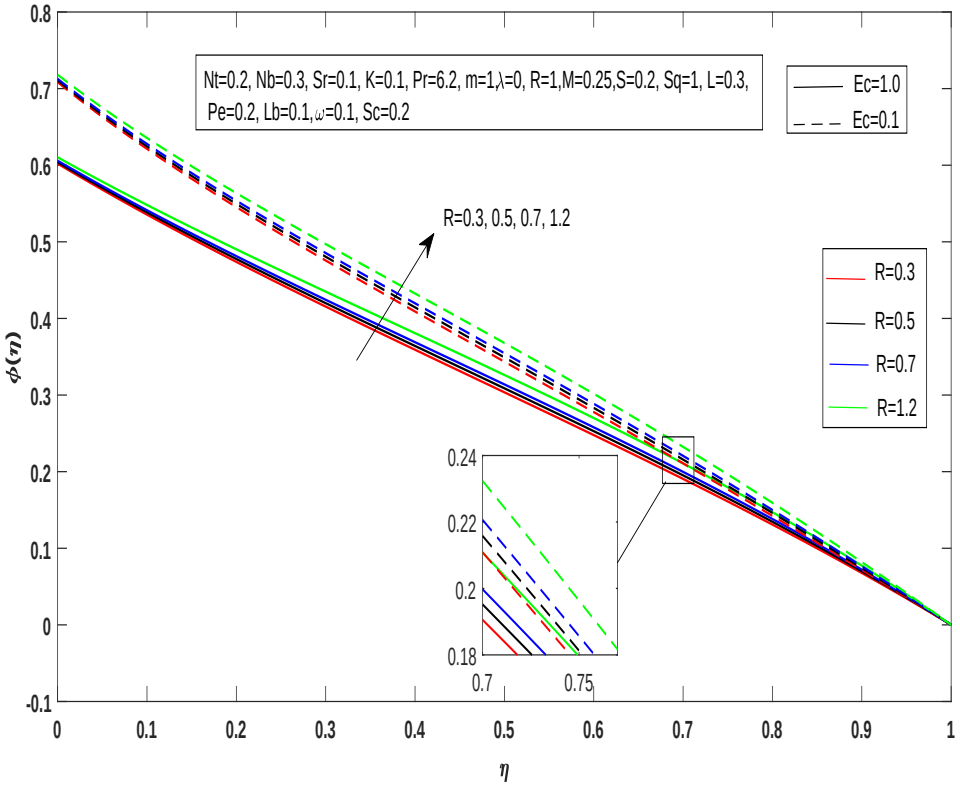

FIGURE 4.17: Influence of Ec and R on $\phi(\eta)$

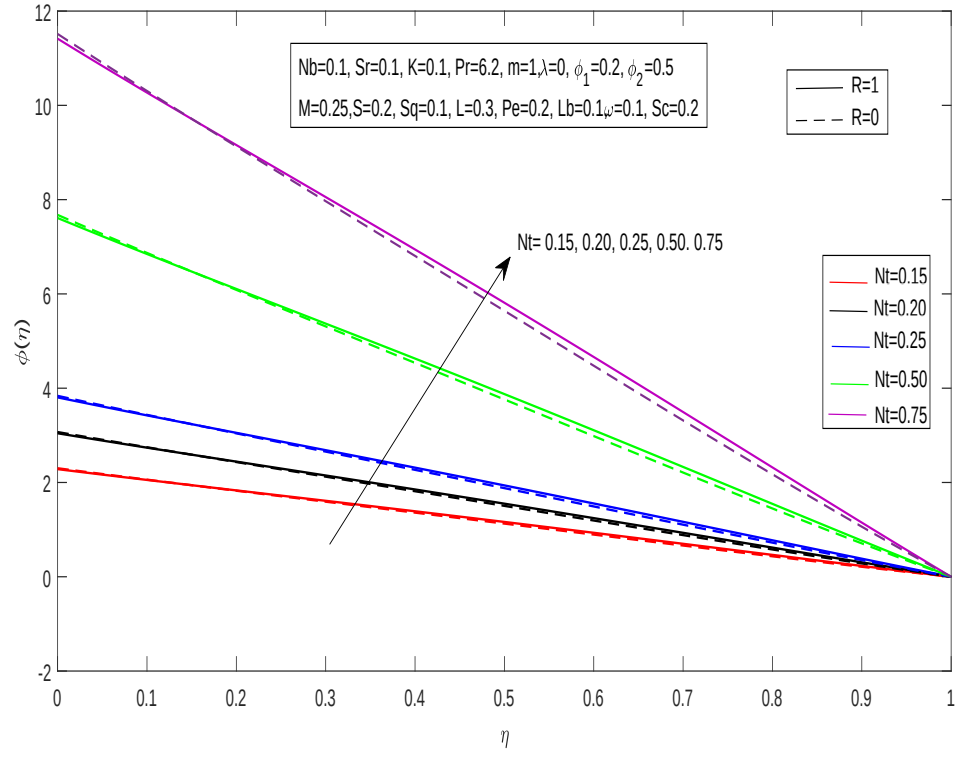

FIGURE 4.18: Influence of Nt and Ec on $\phi(\eta)$

4.8.4 Motile Profile

- In Figure 4.19, the effect of the Casson parameter (β) on the profile of motile microorganisms ($N(\eta)$) is examined for both the presence and absence of viscosity variation parameter (m). Clear observations indicate a decrease in motile microorganisms, suggesting that variations in β lead to a reduction in the distribution and concentration of microorganisms within the fluid. A decrease in profile of motile microorganisms with an increase in the Casson parameter (β) can be attributed to the rheological properties of the Casson fluid. Higher values of β imply increased yield stress, hindering the movement of microorganisms within the fluid.

- The impact of the squeezing parameter (Sq) on the profile of motile microorganisms ($N(\eta)$) is illustrated in Figure 4.20, for both the absence and presence of viscosity variation parameter (m). Interestingly, an increase in Sq results in an elevated motile microorganisms profile. This implies that squeezing flow parameters contribute to an increase in the concentration and distribution of motile microorganisms within the fluid, as depicted in Figure 4.20. The increase in motile microorganisms with higher squeezing parameter (Sq) is linked to the intensified flow due to squeezing. This dynamic enhances the dispersion of microorganisms, leading to a higher concentration and distribution within the fluid.

- In Figure 4.21 the influence of the suction parameter S on the profile of motile microorganisms profile `N` is presented in the absence and presence of thermal radiation. Figure 4.21 reveals a decrease in the motile microorganisms profile with an increase in the suction parameter S. This suggests that suction tends to reduce the concentration and distribution of motile microorganisms. The decrease in profile of motile microorganisms with the suction parameter (S) can be explained by the fluid motion induced by suction, which tends to concentrate microorganisms away from the suction region.

- In figure 4.22, an increase in bioconvection schmidth number (Lb) and radiation parameter (R) positively impacts motile microorganisms. This could be due to enhanced fluid motion and energy transfer, creating favorable conditions for the proliferation and dispersion of microorganisms.

- In figure 4.23 the influence of Peclet number (Pe) in the presence and absence of thermal radiation (R) on motile microorganisms ($N(\eta)$) is described. Peclet

number (Pe) leads to a decrease in the motile microorganisms profile, while thermal radiation parameter (R) contributes to an increase. This suggests a dynamic interplay between these parameters affecting the concentration and distribution of motile microorganisms. The decrease in motile microorganisms with higher Peclet number (Pe) might be due to increased advection dominating over diffusion, causing a lower concentration. At the same time, thermal radiation (R) enhances energy transfer, promoting microbial activity and leading to an increased motile microorganisms profile.

- in figure 4.24, the impact of radiation parameter on motile microorganisms ($N(\eta)$) for lower ($Ec = 0.1$) and higher ($Ec = 1.0$) values of Eckert number (Ec) is presented. Notably, an increase in the radiation parameter results in an increase in motile microorganisms, and this effect is more pronounced for higher values of Eckert number ($Ec = 1.0$). The increase in motile microorganisms with higher radiation parameter (R) and Eckert number (Ec) could be associated with the augmented fluid temperature and energy availability, fostering the growth and mobility of microorganisms.

- in figure 4.25 the effect of Schmidt number (Sc) under the absence and presence of viscosity variation parameter (m) is described. Interestingly, a higher value of Schmidt number (Sc) leads to a decrease in the profile motile microorganisms profile ($N(\eta)$) for both cases. The inverse effect of Schmidt number (Sc) on motile microorganisms suggests that higher Schmidt numbers hinder mass transfer, limiting the dispersion of microorganisms within the fluid.

- The illustration of the effect of the magnetic field parameter (M) on profile of motile microorganisms is presented in figure 4.26. The magnetic field is observed to decrease the motile microorganisms of the hybrid nanofluid, indicating a significant influence on the distribution and behavior of microorganisms within the fluid. The decrease in motile microorganisms with the magnetic field parameter (M) is likely due to the influence of the magnetic field on the motility and behavior of microorganisms, possibly impeding their movement within the fluid.

- In Figure **??**, the depicted trend illustrates that increasing the value of microorganism parameter ω leads to a subsequent increase in the profile of motile microorganism within the system.

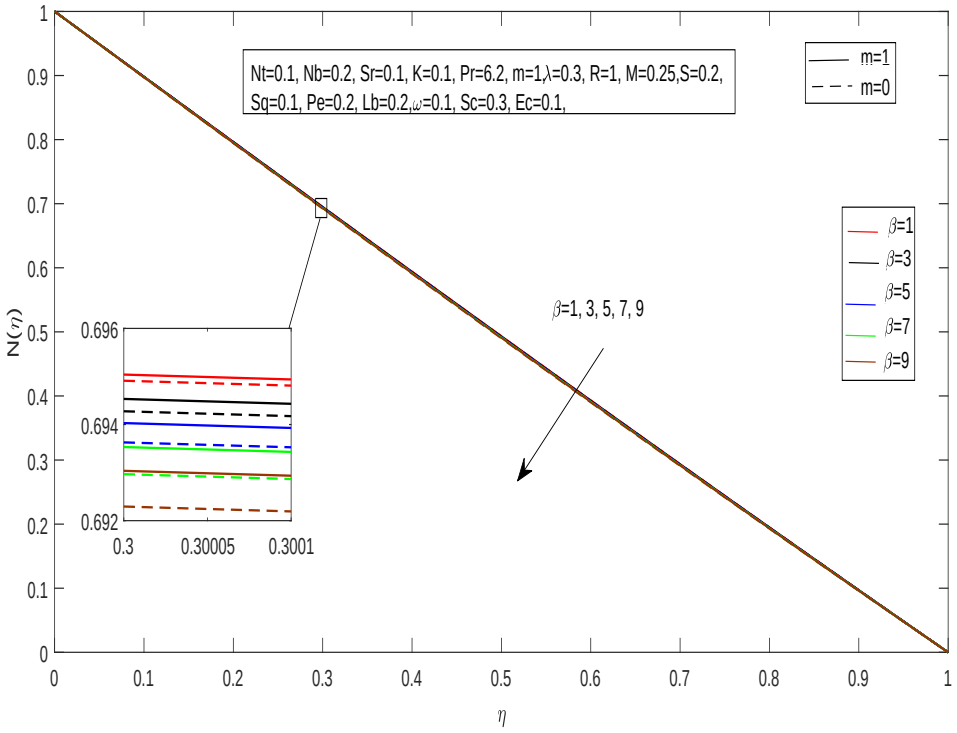

FIGURE 4.19: Influence of m and β on $\mathtt{N}(\eta)$

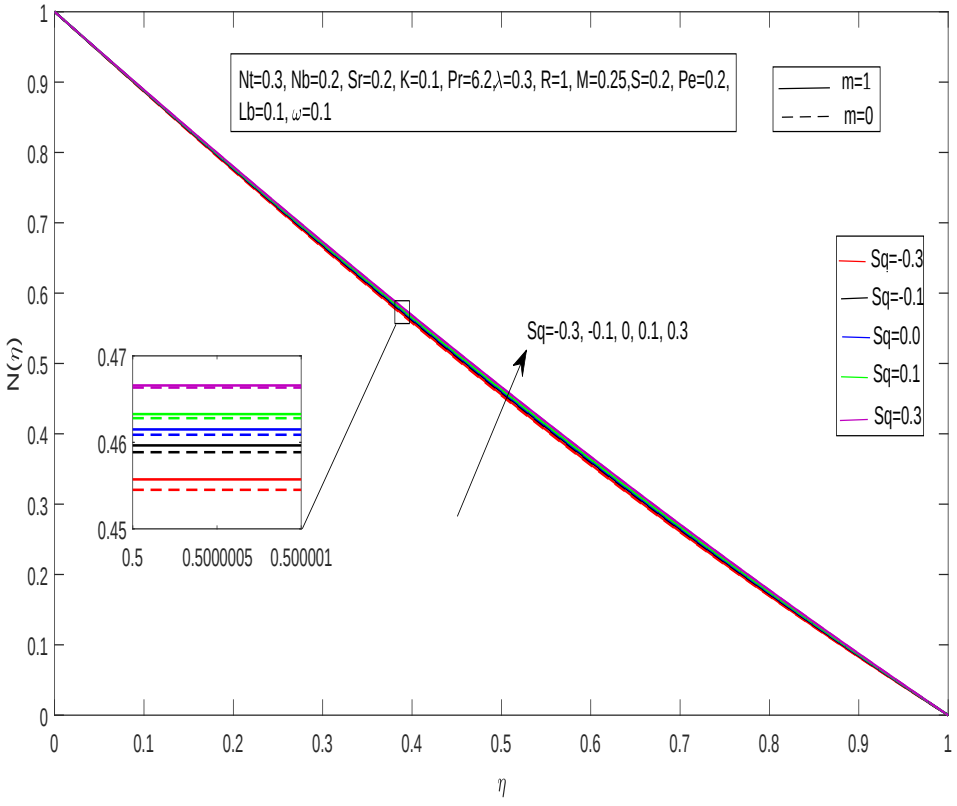

FIGURE 4.20: Influence of m and Sq on $\mathtt{N}(\eta)$

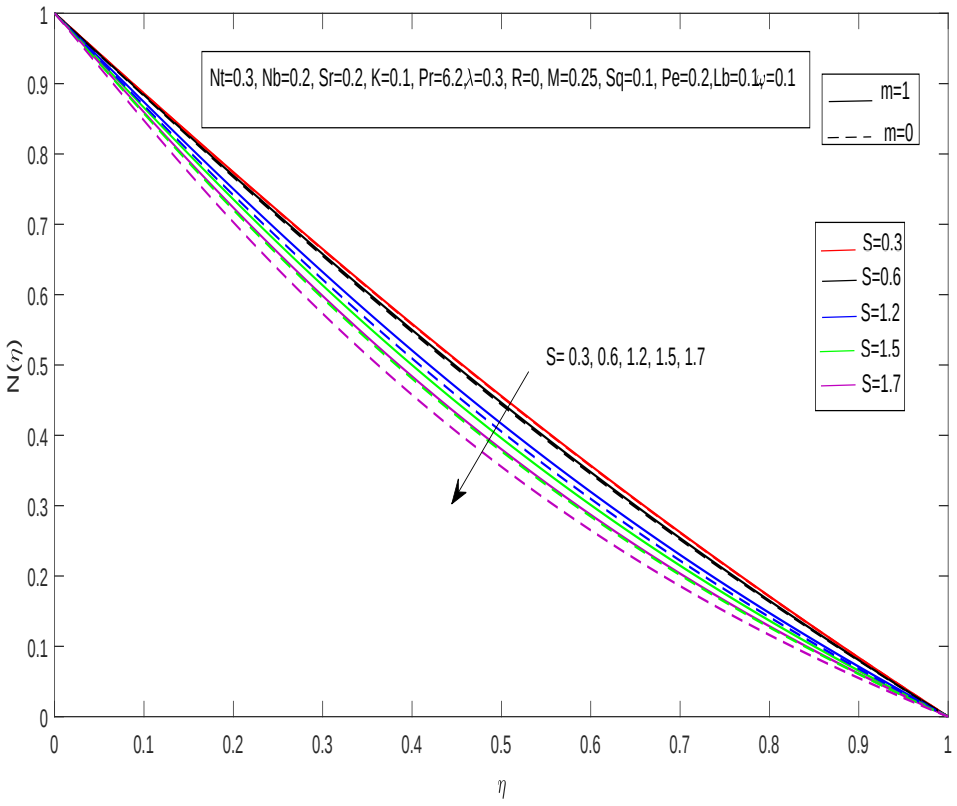

FIGURE 4.21: Influence of m and S on $\mathtt{N}(\eta)$

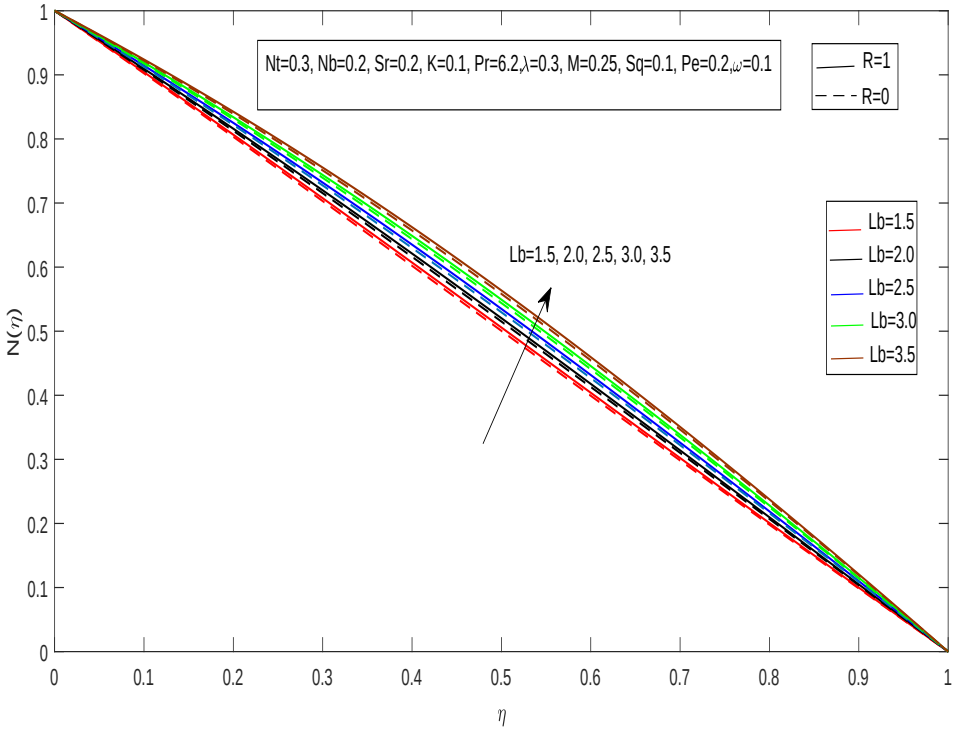

FIGURE 4.22: Influence of Lb and R on $\mathtt{N}i(\eta)$

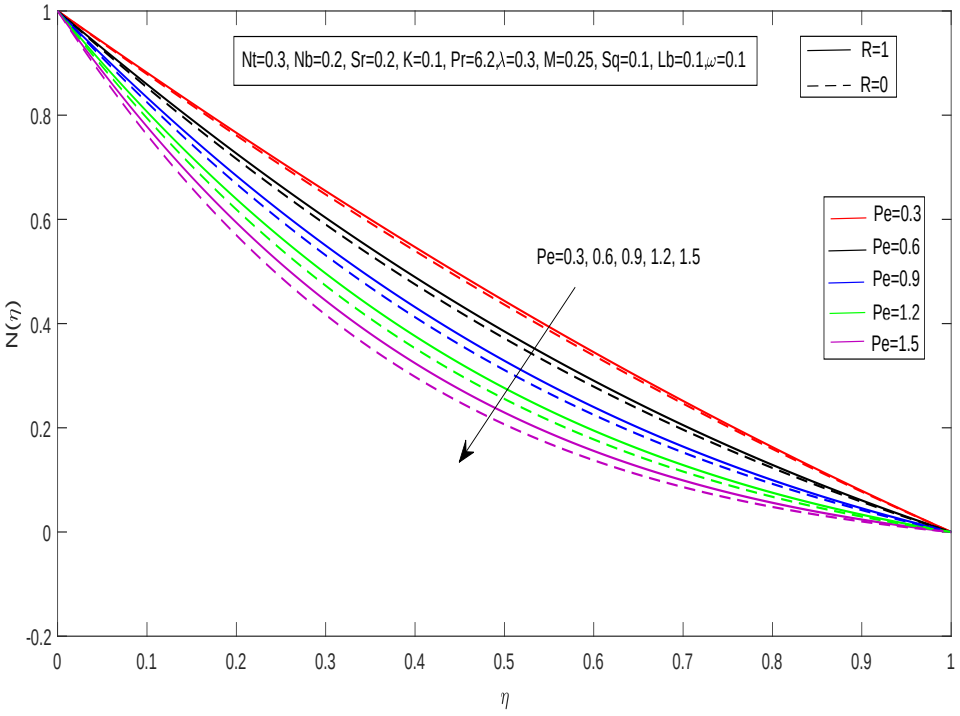

FIGURE 4.23: Influence of R and Pe on $\mathtt{N}(\eta)$

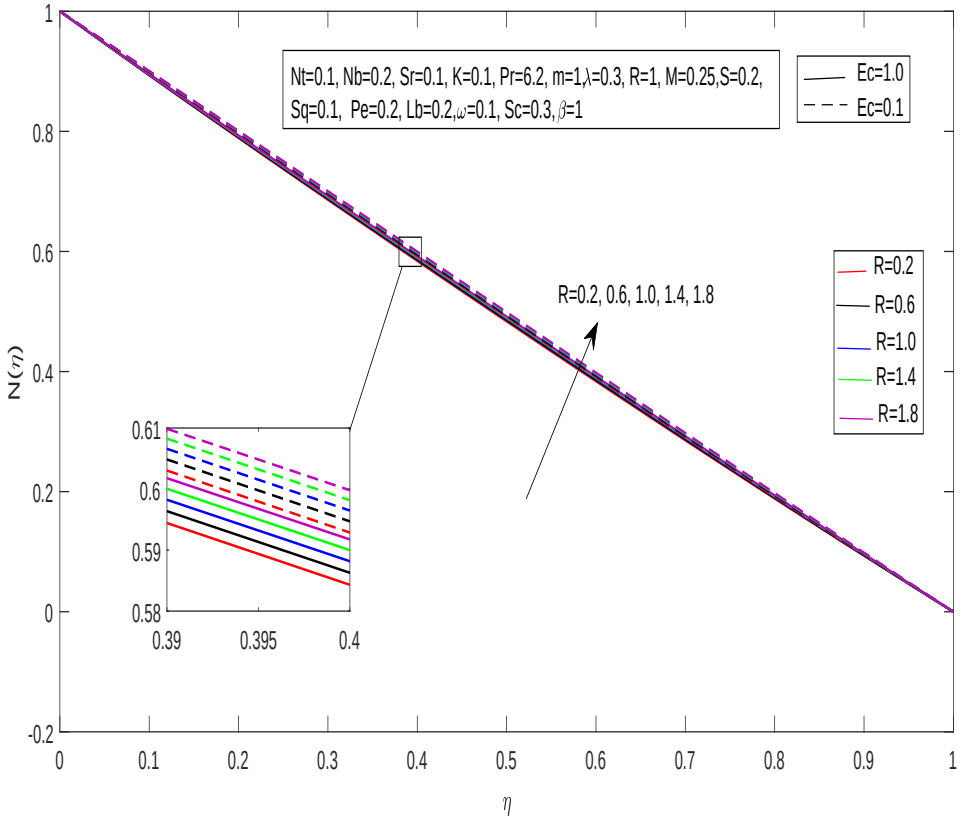

FIGURE 4.24: Influence of Ec and R on $\mathtt{N}(\eta)$

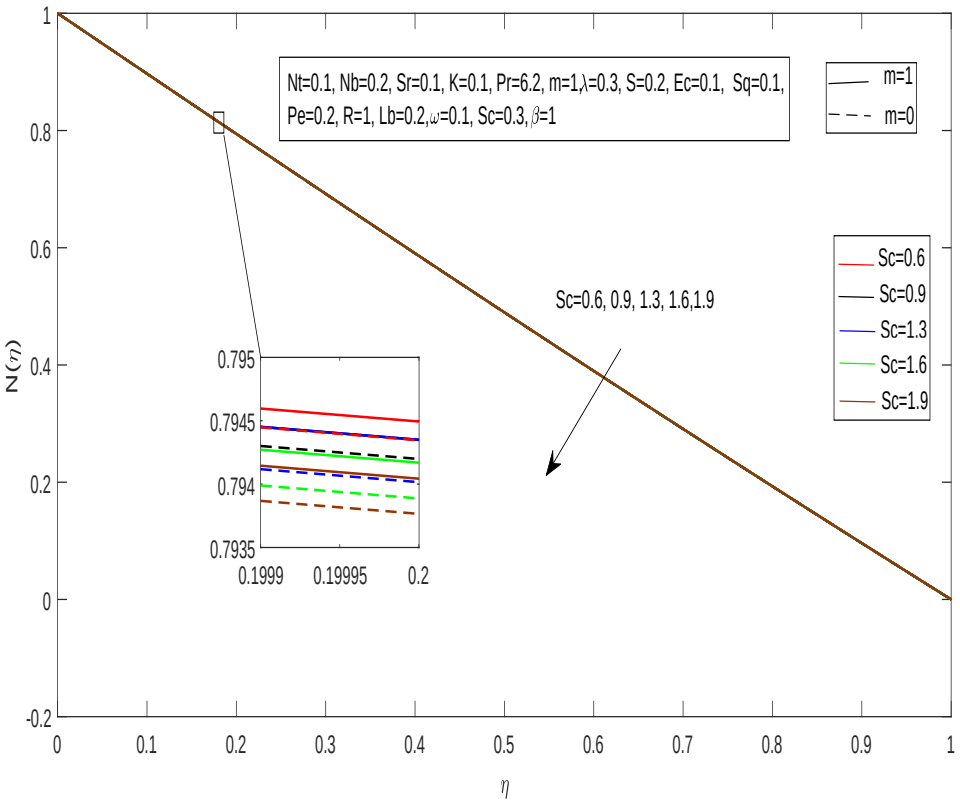

FIGURE 4.25: Influence of m and Sc on $\mathtt{N}(\eta)$

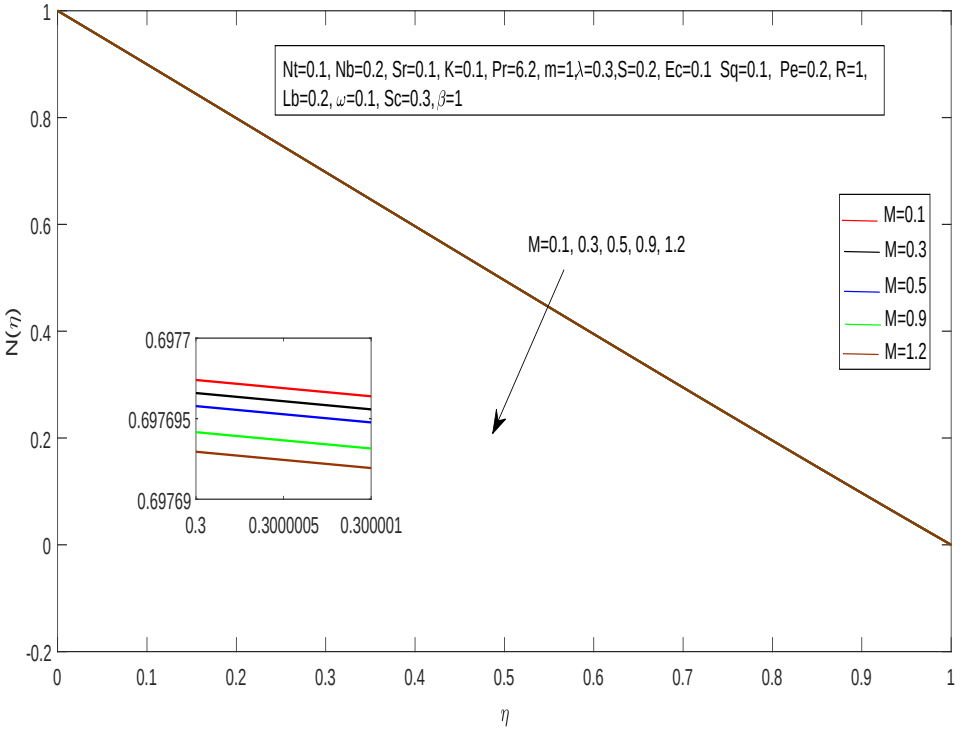

FIGURE 4.26: Influence of M on $\mathtt{N}(\eta)$

Chapter 5

Conclusion

This research examines the intricate dynamics of a time-dependent incompressible squeezing flow of CuO-Al_2O_3 /water hybrid nanofluid confined between two parallel plates. This study involves a comprehensive review and extension of the work presented by Famakinwa et al. [23] by incorporating the impact of chemical reaction, bio-convensional Lewis number, Brownian motion and Thermophoresis. The transformation of the governing equations, encompassing momentum, energy, concentration and motile microorganism equations is obtained through similarity transformation, converting them into ordinary differential equations (ODEs).The resultant transformed ODEs are subsequent solved numerically, employing the shooting technique to obtain a solution for the model under consideration. The graphical and tabular representation elucidate the impact of varoius physical parameters and effects of multiple factors on the flow and associated phenomenon. The following are some of the crucial outcomes:

- The Casson parameter (β) emerged as a key player, positively impacting heat transfer and enhancing the velocity profile.
- Squeezing parameter (Sq) intensified fluid motion, resulting in an increased velocity profile.
- A decline in the temperature profile is observed for the rising values of the Radiation parameter (R) and Eckert number (Ec) demonstrate a intricate interaction.
- An increase in β led to a decrease in the concentration of motile microorganisms, highlighting the sensitivity of biological elements to fluid rheology.

- Both absence and presence of viscosity variation parameter (m) showed that an increase in squeezing parameter (Sq) led to an increased density of motile microorganisms $N(\eta)$.

- The suction parameter (S) plays a crucial role in the temperature profile, acting as a determinant for fluid motion and nanoparticle distribution. It is observed that an increment in the temperature profile occurs for the rising values of Suction parameter (S) and examined a more organized and focused dispersion.

- Casson parameter (β) positively influences heat transfer, enhancing temperature profile, especially when viscosity variation parameter (m) is absent.

- The squeezing flow parameter positively influenced the motile profile, indicating its potential role in promoting the transport of microorganisms within the fluid.

- Schmidt number (Sc) showcases an inverse relationship with motile microorganism concentration. Higher Sc values result in a decrease in the dispersal of biological entities within the fluid.

- The augmentation of the Thermophoresis parameter (Nt) leads to an elevation in the concentration profile, whereas the opposite trend is observed for higher values of the Brownian motion parameter (Nb).

- Peclet number (Pe) regulates the dispersion of motile microorganisms within the hybrid nanofluid. A declining trend is disclosed for the rising values of Peclet number (Pe). and

Bibliography

[1] S. U. Choi and J. A. Eastman, "Enhancing thermal conductivity of fluids with nanoparticles," tech. rep., Argonne National Lab.(ANL), Argonne, IL (United States), 1995.

[2] S. Atif, S. Hussain, and M. Sagheer, "Heat and mass transfer analysis of time-dependent tangent hyperbolic nanofluid flow past a wedge," *Physics Letters A*, vol. 383, no. 11, pp. 1187–1198, 2019.

[3] P. Sreedevi, P. Sudarsana Reddy, and A. Chamkha, "Heat and mass transfer analysis of unsteady hybrid nanofluid flow over a stretching sheet with thermal radiation," *SN Applied Sciences*, vol. 2, no. 7, p. 1222, 2020.

[4] M. Jawad, Z. Khan, E. Bonyah, R. Jan, *et al.*, "Analysis of hybrid nanofluid stagnation point flow over a stretching surface with melting heat transfer," *Mathematical Problems in Engineering*, vol. 2022, 2022.

[5] A. Alhowaity, H. Hamam, M. Bilal, and A. Ali, "Numerical study of williamson hybrid nanofluid flow with thermal characteristics past over an extending surface," *Heat transfer*, vol. 51, no. 7, pp. 6641–6655, 2022.

[6] S. S. S. Sen, R. Mahato, S. Shaw, and M. Das, "Simulation of entropy and heat and mass transfer in water-eg based hybrid nanoliquid flow with mhd and nonlinear radiation," *Numerical Heat Transfer, Part A: Applications*, pp. 1–15, 2023.

[7] K. Rafique, Z. Mahmood, and U. Khan, "Mathematical analysis of mhd hybrid nanofluid flow with variable viscosity and slip conditions over a stretching surface," *Materials Today Communications*, vol. 36, p. 106692, 2023.

[8] A. S. Alnahdi and T. Gul, "Hybrid nanofluid flow over a slippery surface for thermal exploration," *Advances in Mechanical Engineering*, vol. 15, no. 8, p. 16878132231190060, 2023.

[9] H. Upreti, A. K. Pandey, N. Joshi, and O. Makinde, "Thermodynamics and heat transfer analysis of magnetized casson hybrid nanofluid flow via a riga plate with thermal radiation," *Journal of Computational Biophysics and Chemistry*, vol. 22, no. 03, pp. 321–334, 2023.

[10] M. I. Asjad, M. Zahid, M. Inc, D. Baleanu, and B. Almohsen, "Impact of activation energy and mhd on williamson fluid flow in the presence of bioconvection," *Alexandria Engineering Journal*, vol. 61, no. 11, pp. 8715–8727, 2022.

[11] A. Raje, A. A. Bhise, and A. Kulkarni, "Entropy analysis of the mhd jeffrey fluid flow in an inclined porous pipe with convective boundaries," *International Journal of Thermofluids*, vol. 17, p. 100275, 2023.

[12] N. Casson, "Flow equation for pigment-oil suspensions of the printing ink-type," *Rheology of disperse systems*, pp. 84–104, 1959.

[13] S. G. Bejawada, Y. D. Reddy, W. Jamshed, K. S. Nisar, A. N. Alharbi, and R. Chouikh, "Radiation effect on mhd casson fluid flow over an inclined non-linear surface with chemical reaction in a forchheimer porous medium," *Alexandria Engineering Journal*, vol. 61, no. 10, pp. 8207–8220, 2022.

[14] A. M. Alqahtani, M. Bilal, M. Usman, T. R. Alsenani, A. Ali, and S. R. Mahmuod, "Heat and mass transfer through mhd darcy forchheimer casson hybrid nanofluid flow across an exponential stretching sheet," *ZAMM-Journal of Applied Mathematics and Mechanics/Zeitschrift für Angewandte Mathematik und Mechanik*, p. e202200213, 2023.

[15] A. Zeeshan, M. I. Khan, R. Ellahi, and M. Marin, "Computational intelligence approach for optimising mhd casson ternary hybrid nanofluid over the shrinking sheet with the effects of radiation," *Applied Sciences*, vol. 13, no. 17, p. 9510, 2023.

[16] Y.-M. Li, I. Ullah, N. Ameer Ahammad, I. Ullah, T. Muhammad, and S. A. Asiri, "Approximation of unsteady squeezing flow through porous space with slip effect: Djm approach," *Waves in Random and Complex Media*, pp. 1–15, 2022.

[17] J. Umavathi, D. Prakasha, Y. M. Alanazi, M. M. Lashin, F. S. Al-Mubaddel, R. Kumar, and R. P. Gowda, "Magnetohydrodynamic squeezing casson nanofluid flow between parallel convectively heated disks," *International Journal of Modern Physics B*, vol. 37, no. 04, p. 2350031, 2023.

[18] M. Venkateswarlu, D. Venkata Lakshmi, and G. Darmaiah, "Influence of slip condition on radiative mhd flow of a viscous fluid in a parallel porous plate channel in presence of heat absorption and chemical reaction.," *Journal of the Korean Society for Industrial and Applied Mathematics*, vol. 20, no. 4, pp. 333–354, 2016.

[19] N. Tarakaramu and P. Satya Narayana, "Chemical reaction effects on bio-convection nanofluid flow between two parallel plates in rotating system with variable viscosity: a numerical study," *Journal of Applied and Computational Mechanics*, vol. 5, no. 4, pp. 791–803, 2019.

[20] K. Raghunath, "Study of heat and mass transfer of an unsteady magnetohydrodynamic (mhd) nanofluid flow past a vertical porous plate in the presence of chemical reaction, radiation and soret effects," *Journal of Nanofluids*, vol. 12, no. 3, pp. 767–776, 2023.

[21] J. R. Platt, "" bioconvection patterns" in cultures of free-swimming organisms," *Science*, vol. 133, no. 3466, pp. 1766–1767, 1961.

[22] P. Patil, S. Benawadi, and E. Momoniat, "Thermal analysis of bioconvective nanofluid flow over a sphere in presence of multiple diffusions and a periodic magnetic field," *Case Studies in Thermal Engineering*, vol. 51, p. 103569, 2023.

[23] O. Famakinwa, O. Koriko, and K. Adegbie, "Effects of viscous dissipation and thermal radiation on time dependent incompressible squeezing flow of $CuO - Al_2O_3$/water hybrid nanofluid between two parallel plates with variable viscosity," *Journal of Computational Mathematics and Data Science*, vol. 5, p. 100062, 2022.

[24] Y. Cengel and J. Cimbala, *Ebook: Fluid Mechanics Fundamentals and Applications (si units)*. McGraw Hill, 2013.

[25] R. Bansal, *A Textbook of Fluid Mechanics*. Laxmi Publications Pvt Limited, 2005.

[26] R. Bansal, *A Textbook of Fluid Mechanics and Hydraulic Machines*. Laxmi Publications, 2010.

[27] S. S. Molokov, R. Moreau, and H. K. Moffatt, *Magnetohydrodynamics: Historical evolution and trends*, vol. 80. Springer Science & Business Media, 2007.

[28] J. N. Reddy and D. K. Gartling, *The Finite Element Method in Heat Transfer and Fluid Dynamics*. CRC press, 2010.

[29] R. E. Collins, "Flow of fluids through porous materials," 1976.

[30] M. R. Safaei, M. Gooarzi, O. A. Akbari, M. S. Shadloo, and M. Dahari, "Performance evaluation of nanofluids in an inclined ribbed microchannel for electronic cooling applications," *Electronics cooling*, vol. 832, 2016.

[31] R. Dash, K. Mehta, and G. Jayaraman, "Casson fluid flow in a pipe filled with a homogeneous porous medium," *International Journal of Engineering Science*, vol. 34, no. 10, pp. 1145–1156, 1996.

[32] S. Som, *Introduction to Heat Transfer*. PHI Learning Pvt. Ltd., 2008.

[33] W. M. Rohsenow, J. P. Hartnett, Y. I. Cho, *et al.*, *Handbook of heat transfer*, vol. 3. Mcgraw-hill New York, 1998.

[34] C. Kothandaraman, *Fundamentals of heat and mass transfer*. New Age International, 2006.

[35] R. W. Lewis, P. Nithiarasu, and K. N. Seetharamu, *Fundamentals of the finite element method for heat and fluid flow*. John Wiley & Sons, 2004.

[36] R. W. Fox, A. McDonald, and P. Pitchard, "Introduction to fluid mechanics, 2004," 2006.

[37] M. Gad-el Hak, *Advances in fluid mechanics measurements*, vol. 45. Springer Science & Business Media, 2013.

[38] J. Kunes, *Dimensionless physical quantities in science and engineering*. Elsevier, 2012.

[39] J. Kuneš, "Thermomechanics," *Dimensionless Physical Quantities in Science and Engineering. Elsevier, Oxford*, pp. 173–283, 2012.

[40] T. Hayat, R. Sajjad, A. Alsaedi, T. Muhammad, and R. Ellahi, "On squeezed flow of couple stress nanofluid between two parallel plates," *Results in physics*, vol. 7, pp. 553–561, 2017.

[41] N. S. Khashiie, I. Waini, N. M. Arifin, and I. Pop, "Unsteady squeezing flow of cual2o3/water hybrid nanofluid in a horizontal channel with magnetic field," *Scientific reports*, vol. 11, no. 1, p. 14128, 2021.

[42] M. Massoudi and I. Christie, "Effects of variable viscosity and viscous dissipation on the flow of a third grade fluid in a pipe," *International Journal of Non-Linear Mechanics*, vol. 30, no. 5, pp. 687–699, 1995.

[43] A. C. Cogley, W. G. Vincent, and S. E. Gilles, "Differential approximation for radiative transfer in a nongrey gas near equilibrium.," *Aiaa Journal*, vol. 6, no. 3, pp. 551–553, 1968.

[44] B. Takabi and S. Salehi, "Augmentation of the heat transfer performance of a sinusoidal corrugated enclosure by employing hybrid nanofluid," *Advances in Mechanical Engineering*, vol. 6, p. 147059, 2014.

[45] M. Zubair, Z. Shah, S. Islam, W. Khan, and A. Dawar, "Study of three dimensional darcy–forchheimer squeezing nanofluid flow with cattaneo–christov heat flux based on four different types of nanoparticles through entropy generation analysis," *Advances in Mechanical Engineering*, vol. 11, no. 5, p. 1687814019851308, 2019.

[46] H. F. Oztop and E. Abu-Nada, "Numerical study of natural convection in partially heated rectangular enclosures filled with nanofluids," *International journal of heat and fluid flow*, vol. 29, no. 5, pp. 1326–1336, 2008.

[47] I. Waini, A. Ishak, and I. Pop, "Mhd flow and heat transfer of a hybrid nanofluid past a permeable stretching/shrinking wedge," *Applied Mathematics and Mechanics*, vol. 41, no. 3, pp. 507–520, 2020.

[48] A. Raees, H. Xu, and S.-J. Liao, "Unsteady mixed nano-bioconvection flow in a horizontal channel with its upper plate expanding or contracting," *International Journal of Heat and Mass Transfer*, vol. 86, pp. 174–182, 2015.

[49] N. Khashi'ie, N. Arifin, I. Pop, and R. Nazar, "Dual solutions of bioconvection hybrid nanofluid flow due to gyrotactic microorganisms towards a vertical plate," *Chinese Journal of Physics*, vol. 72, pp. 461–474, 08 2021.

[50] C. Srinivas Reddy, F. Ali, and M. F. A. F. Ahmed, "Aspects on unsteady for mhd flow of cross nanofluid having gyrotactic motile microorganism due to convectively heated sheet," *International Journal of Ambient Energy*, vol. 43, no. 1, pp. 6028–6040, 2022.

[51] S. A. A. Shah, N. A. Ahammad, E. M. T. E. Din, F. Gamaoun, A. U. Awan, and B. Ali, "Bio-convection effects on prandtl hybrid nanofluid flow with chemical reaction and motile microorganism over a stretching sheet," *Nanomaterials*, vol. 12, no. 13, p. 2174, 2022.